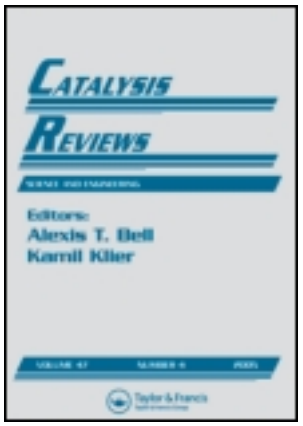

Catalysis Reviews: Science and Engineering
Publication details, including instructions for authors and subscription information:
http://www.tandfonline.com/loi/lctr20

Siting and Distribution of Framework Aluminium Atoms in Silicon-Rich Zeolites and Impact on Catalysis

J. Dědeček [a], Z. Sobalík [a] & B. Wichterlová [a]
[a] J. Heyrovský Institute of Physical Chemistry, Academy of Sciences of the Czech Republic, Prague, Czech Republic

Available online: 18 Apr 2012

To cite this article: J. Dědeček, Z. Sobalík & B. Wichterlová (2012): Siting and Distribution of Framework Aluminium Atoms in Silicon-Rich Zeolites and Impact on Catalysis, Catalysis Reviews: Science and Engineering, 54:2, 135-223

To link to this article: http://dx.doi.org/10.1080/01614940.2012.632662

Catalysis Reviews: Science and Engineering, 54:135–223, 2012

ISSN: 0161-4940 print / 1520-5703 online
DOI: 10.1080/01614940.2012.632662

Siting and Distribution of Framework Aluminium Atoms in Silicon-Rich Zeolites and Impact on Catalysis

J. Dědeček, Z. Sobalík, and B. Wichterlová

J. Heyrovský Institute of Physical Chemistry, Academy of Sciences of the Czech Republic, Prague, Czech Republic

Siting of Al atoms in the framework T sites, in zeolite rings and channel/cavity system, and the distribution of Al atoms between single Al atoms and close Al atoms in various Al-O-(Si-O)$_n$-Al sequences in Si-rich zeolites represent key parameters controlling properties of counter ion species. Framework Al siting and distribution is not random or controlled by simple rules and depends on the conditions of the zeolite synthesis. Al in Al-O-(Si-O)$_2$-Al in one 6-MR and single Al atoms predominate in Si-rich zeolites and their population can be varied to a large extent. The siting and distribution of framework Al atoms dramatically affect catalytic activity/selectivity both of protonic and transition metal ion-containing zeolite catalysts.

Keywords Si-rich zeolites, ZSM-5, Beta zeolite, Ferrierite, Mordenite, MCM-22, Al siting, Al distribution, Catalytic activity, Zeolite synthesis

1. INTRODUCTION AND HISTORY OF THE PROBLEM

Zeolites are crystalline aluminosilicates forming about 170 different tridimensional structures with inner pores and cavities of defined dimension and architecture (1). The crystalline framework bearing a negative charge provides for stabilization of well-defined protonic and/or metal ion counter species located inside the inner pore volume. These species represent active sites for acid- and redox-catalyzed reactions and they are exploited in numerous chemical processes.

Received July 20, 2011; accepted October 13, 2011.

Address correspondence to J. Dědeček, J. Heyrovský Institute of Physical Chemistry, Academy of Sciences of the Czech Republic, CZ-182 23, Prague 8, Czech Republic. E-mail: jiri.dedecek@jh-inst.cas.cz

Aluminum-rich zeolites (Si/Al 1 – 6), such as those with faujasite structure, have found broad application as catalysts for processes of catalytic cracking and fuel reforming, and zeolites of LTA topology are used as adsorbents and detergents. In recent decades, research has been focused particularly on pentasil ring silicon-rich zeolites with low concentrations of Al atoms in the framework, which provide protons with high acid strength and are industrially applied in hydrocarbon processing. Later, attention was devoted to the extraordinary redox and catalytic properties of counter cation species, not found with counter ions in Al-rich zeolites and metal oxides supported on amorphous oxides. In addition, Si-rich zeolites exhibit a wide range of pore dimensions, from small and medium sizes (~3.5–5.5 Å) up to large ones (~6.5–7.0 Å), offering shape-selective effects in reactions involving the synthesis and transformation of hydrocarbons and their derivatives of comparable kinetic diameters.

The remarkable properties and catalytic activity of protons and metal counter ion species in Si-rich zeolites stimulated analysis of their location and structure, and the consequent relationship to their catalytic activity. Prolonged effort has been devoted to analysis of the coordination of bare divalent cations (2), assumed to be charge balanced by two Al atoms, and of cations bearing extra-framework oxygen atom(s). On the other hand, only some metal-oxo structures have been supposed to be related to the presence of single Al atoms in the framework, but without any evidence (3). Much later, attempts were made to elucidate the siting and distribution of framework Al atoms (4). However, the slow progress in analysis of the positions of Al atoms in the framework T(Si,Al) sites has long prevented at least estimation of the siting and distribution of framework Al atoms.

Nevertheless, the low concentration of Al atoms corresponds to a variety of their positions and distributions in the framework T sites and of the corresponding local negative charges in the framework. This assumption has been supported by a number of laboratories which convincingly reported that the siting and distribution of Al atoms in the framework of Si–rich zeolites is not random and is not controlled by statistical rules, see, e.g., Refs. (4c-e, 5). The counter metal ions have been shown to be coordinated to specific structural rings, which are spatially distributed in the zeolite framework, see, e.g., Ref. (6). Therefore, to ensure local charge balance, the charges and locations of metal counter ion species must be related to the siting of aluminum and its distribution in the framework of Si-rich zeolites.

This implies that various local negative charges in the framework rings and in defined structural arrangements can be assumed to be decisive for the location, structure and charges on the counter ion species. Accordingly, beside the compositional Si/Al ratio, framework topology and pore dimensionality, the siting and distribution of framework Al atoms in Si-rich zeolites are important

zeolite parameters that should be included in the analysis and evaluation of the structure, properties and activity of counter ion species.

This review describes efforts and achievements in identification of the location of Al atoms in the framework T sites and their distribution in the framework of Si-rich pentasil zeolites, centered around ZSM-5 (MFI), ferrierite (FER), mordenite (MOR), the beta zeolite (BEA) and MCM-22 (MWW) structures, and the latest attempts at tuning these framework parameters by zeolite hydrothermal synthesis. In connection with the defined local negative charges of the framework, the location, structure and properties of positively charged counter ion species and the catalytic activity of H- and metallo-zeolites are discussed.

As the low Al content in Si-rich zeolites (Si/Al $>$ 8 or $>$ 12) results in the specific structure and properties of the exchanged counter-ion species, it is very important to analyze the location and distribution of the Td coordinated Al atoms in their frameworks. The literature contains sufficient support for the assumption that the negative charge of the AlO_4^- tetrahedra is not delocalized over the framework but, to the contrary, is localized at these AlO_4^- entities. Therefore, it could be suggested that the location and distribution of the framework AlO_4^- tetrahedra control the location, distribution and structure of the counter-ion species (protons, bare cations, oxo-cations or cation-ligand species in general). Although the structures of these species have been intensively studied and attempts have been made to relate these structures to their function and performance in catalytic reactions, there is a lack of analysis of the anticipated effect of the siting and distribution of framework Al atoms on the structure, properties and activity of the counter-ion species. Bare metal ions coordinated only to framework oxygen atoms and counter ion species containing extra-framework oxygen atom(s) also consisting of metal bridged structures were suggested as the active sites.

Obtaining a complete picture of the siting of Al atoms in the crystallographic distinct framework T sites in Si-rich zeolites remains a great challenge, which is difficult to reach, particularly for zeolite structures containing a large number of different T sites, like ZSM-5 and beta zeolites. Due to recent progress in ^{27}Al (3Q) MAS NMR experiments supported by density function theory (DFT) calculations the siting of framework Al atoms in ferrierite has been solved (7) and partly also in ZSM-5 zeolites (4b, 8). Moreover, it has been revealed that the distribution of Al atoms in different Al-O-(Si-O)$_n$-Al sequences in the framework is a parameter that can be accessed indirectly, without knowledge of the occupation of the individual T sites by Al atoms, by means of a combination of ^{29}Si MAS NMR and quantitative analysis of the location of defined divalent counter cations provided by suitable spectral and diffraction techniques (4d, 5a, 9).

With the conclusion that the distribution of Al atoms in the framework of Si-rich zeolites is not random and thus not controlled by statistical rules, the

question has arisen of whether the location of the Al atoms in the individual T sites and their distribution among various Al-O-$(Si-O)_n$-Al sequences can be controlled by the zeolite synthesis. In principle, the process of hydrothermal synthesis of zeolites is highly sensitive to the composition of the reaction mixture and to the synthesis conditions. The synthesis conditions have recently been shown to lead to different locations and distributions of Al atoms in the framework of Si-rich zeolites (5b, 10). Attempts have been made to control the siting of Al atoms in the framework by using various organic templates and thus location of protonic sites in different channels in the synthesis of ferrierite (7, 11). We have shown that the distribution of Al atoms in Al-O-$(Si-O)_n$-Al sequences in the framework of MFI, FER, BEA and MWW zeolite topologies can be tuned in a wide range, between Al pairs in Al-O-$(Si-O)_2$-Al sequences located in one framework ring and single Al atoms, by employing various sources of Si and Al, organic and inorganic cations, and synthesis conditions (5b, 9a, 10a).

The progress in the last 2 or 3 years in this field seems to represent a dramatic step forward, both in analysis of the siting and distribution of Al atoms in the framework and tuning of these parameters by zeolite hydrothermal synthesis. These achievements finally open the pathway to analysis of the effect of framework Al siting and distribution in the framework for catalytic properties of individual protons and metal counter ion species in Si-rich zeolites.

The review intends to draw attention to the challenges and achievements in analysis of the siting and distribution of Al atoms in the frameworks of Si-rich zeolites, to the progress in their control by zeolite synthesis, and to the studies appearing on the relationships of the structure and catalytic properties of the protons and metal counter ion species to the siting and distribution of aluminium atoms in the framework of Si-rich zeolites.

2. DEFINITION OF THE SITING AND DISTRIBUTION OF FRAMEWORK Al ATOMS IN Si-RICH ZEOLITES

The siting of Al atoms in the framework corresponds to the positions of the Al atoms in the individual framework T sites of zeolites. In Si-rich zeolites containing a low concentration of aluminum, Al atoms occur in various Al-O-$(Si-O)_n$-Al sequences. The distribution of the Al atoms in the framework is understood here to represent the mutual arrangement of at least two Al atoms.

It should be pointed out that the siting and distribution of Al atoms in Si-rich zeolites discussed here concerns only crystallographic framework T (Si,Al) positions and ideal zeolite crystals with homogeneous concentration profiles of Si and Al along the crystal axis. Homogeneous distribution of Al atoms in the framework is generally found in crystals with small dimensions (12) (from nano- up to several microns in size), such as those used in the technology

of preparation of zeolite-based catalysts. The homogeneous Al distribution along the crystal has been indicated by the close-to-surface vs. bulk composition obtained from XPS (10b) and SEM EDX analysis (13). Another type of Al in-homogeneity in the zeolite crystals, not discussed here, can appear in the severely calcined or steamed zeolites at high temperatures. Release of aluminium from the framework T positions into extra-framework sites, with possible formation of the aluminosilicate phase and aluminium enrichment in the zeolite surface layers, are found (14). Samples with these types of in-homogeneities are excluded from the analysis of the framework Al siting and its distribution.

2.1. Al Atoms in the Framework T Sites

The siting of Al atoms in the framework should be regarded as well-defined. The high number of crystallographically different $T(Si,Al)O_4$ tetrahedra units forming the frameworks in Si-rich zeolites consist of as few as four units in mordenite up to as many as 24 units in monoclinic ZSM-5. Together with the low Al content ($Si/Al > 8$), this fact leads to high variability in the siting of Al atoms, i.e., occupation of the individual framework T sites, and different populations of Al atoms in these sites. ***The siting of Al atoms in the individual framework T sites*** represents a basic parameter which governs the derived distribution of Al atoms. The parameters describing the Al siting can be suggested as:

i. ***Siting of Al atoms in the individual framework rings,*** essential for the location of protons and location and coordination of metal ions

ii. ***Siting of Al atoms with respect to the structural channel/cavity system,*** (Fig. 2-1) which thereafter controls the accessibility of charge-balancing metal ions or protons for reactants or guest molecules, and the formation of various types of reaction intermediates in the surrounding void volume of the counter ions.

2.2. Distribution of Al Atoms in the Framework

The low content of isomorphously substituted Al in the Si-rich zeolites ($Si/Al > 8$) provides a wide variety of mutual arrangements of Al atoms in the framework and thus the negatively charged AlO_4^- tetrahedra in the framework determines the distribution of the local negative charges. This implies the exchange of positively charged counter ions in the defined cationic sites bound via framework oxygen atoms neighboring to the framework T sites occupied by Al atoms. In the exchange of di- or poly-valent cations, a sufficient local negative charge balancing the charges of the cations is required. Thus the siting and distribution of Al atoms in the framework of the zeolite controls the location of

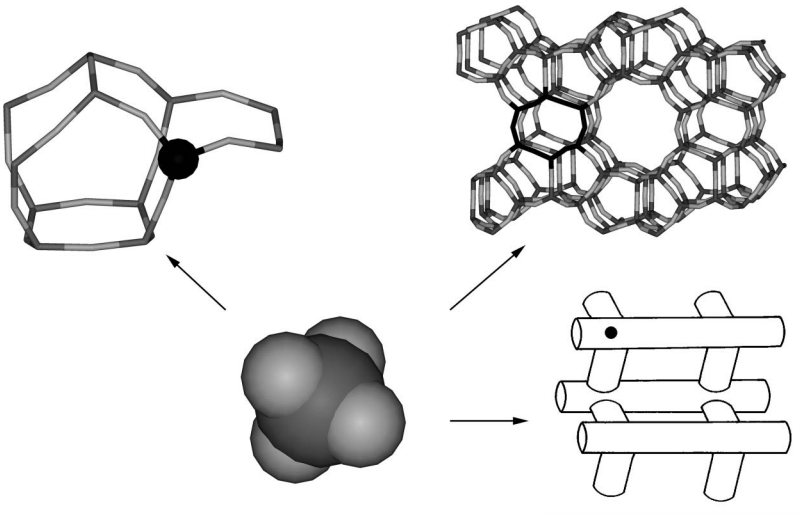

Figure 2-1: Hierarchy of the siting of the Al atom in the framework T site, zeolite ring, and zeolite channel system.

the exchanged protons and bare cations, and the structure of metal-ion complexes and their distances in the zeolite structure. This implies an essential importance of the siting and distribution of Al atoms in the zeolite framework for the catalytic properties of zeolite catalysts.

It should be stressed that ***two types of Al distribution are most important for coordination of divalent metal ions and metal-oxo species and are most populated (~97 %), i.e., Al-O-(Si-O)$_2$-Al sequences in one ring (denoted as Al pairs, Al$_{2Al}$) and single Al atoms (Al$_{1Al}$) in those Si-Al sequences able to charge balance only monovalent ions or monovalent metal-oxo complexes.*** Beside these most important and populated Si-Al sequences there are also present in the framework other types of Si-Al sequences, but they are much less populated. The selection of types of Si-Al arrangements discussed here to describe the Al distribution in the framework is based on the knowledge of the importance of specific types of distribution of Al atoms for the location and structure of the counter ion (proton or metal) species, and the methods available for analysis of the Al siting in the framework. Summary of the Si-Al sequences and their properties is given in Table 2-1.

2.2.1. Al-O-(Si-O)$_n$-Al Sequences

There is only one strict rule for the aluminum distribution in the zeolite framework, i.e., the Loewenstein rule (15) excluding sharing of an oxygen atom by two AlO_4 tetrahedra. Thus, Al-O-Al sequences are not present in the zeolite framework. The absence of other rules governing the mutual arrangement of

Table 2-1: Al sequences in zeolites, their notation and properties.

Sequence	Rings	Distance	Visibility	Notation	Balancing cations in zeolites: Hydrated	Balancing cations in zeolites: Dehydrated
Al-O-Si-O-Al[a]		Short				
Al-O-(Si-O)$_2$-Al[b]	6-MR	Short	Yes	Al pair, Al_{2Al}	$Co(H_2O)_6$	Bare Co^{2+}
Al-O-(Si-O)$_{n\geq 2}$-Al	Two	Short	Yes	unpaired Al,$Al_{UNPAIRED}$[d]	$Co(H_2O)_6$	Co-oxo
Al-O-(Si-O)$_{n>2}$-Al[b]	Two	Short	No	Single Al, Al_{1Al}	M^+	M^+
		Far	Yes	Single Al, Al_{1Al}	M^+	M^+

[a]Does not occur in ZSM-5, MCM-22 and beta zeolites with Si/Al >10 and mordenite and ferrierite with Si/Al > 8.
[b]Most populated Al atoms depending on Si/Al and synthesis conditions, see Chapter 4.

Al atoms in the framework establish conditions such that all the Al-O-(Si-O)$_n$-Al sequences are allowed in the frameworks of Si-rich zeolites (see Fig. 2-2).

The term of "close Al atoms" is introduced for Al atoms, which participate on the charge balance of the hexaquo divalent complex in hydrated zeolites. The close Al atoms are represented by Al-O-(Si-O)$_{1,2}$-Al sequences in one ring

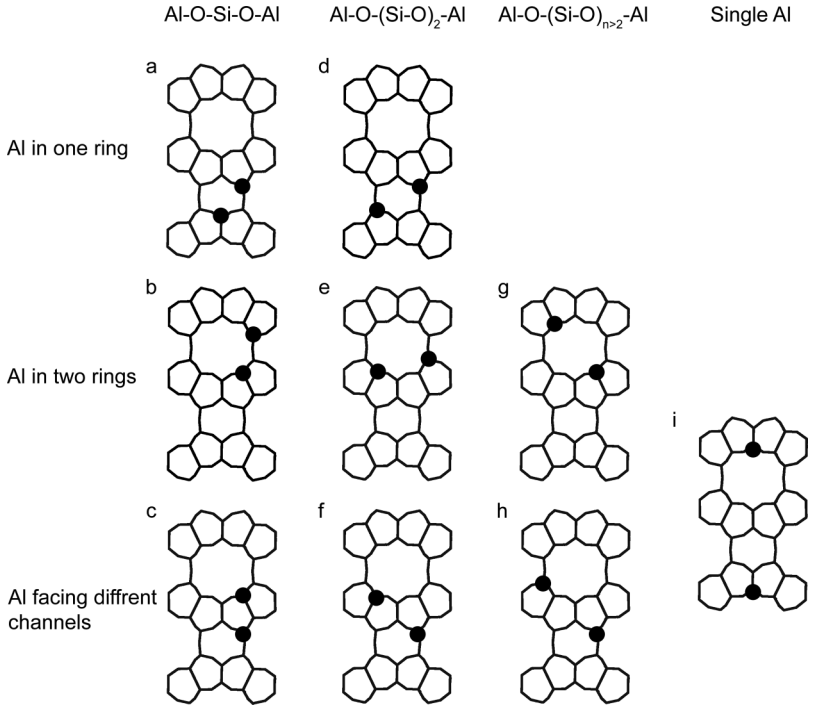

Figure 2-2: Variability of the distribution of Al atoms in the framework of Si-rich zeolite.

(and Al-O-(Si-O)$_3$-Al in mordenite), and Al-O-(Si-O)$_{1,2,3}$-Al sequences with Al atoms in different rings in close geometric distance under conditions that the heaquocomlex of the divalent ion can cooperate with both these Al atoms (see below the visible distance of Al atoms).

The closest Al atoms present in the zeolites, ***Al-O-Si-O-Al sequences,*** are well-known for Al-rich materials (e.g., LTA, FAU topologies). They can be readily detected using standard ^{29}Si MAS NMR analysis. However, these Al sequences are very rare in Si-rich frameworks (for illustration see Fig. 2-2 a,b,c, and details in Par. 4.1). On the other hand, close Al atoms of Al-O-(Si-O)$_2$-Al sequences in one ring in Si-rich zeolites represent substantial and, in some Si/Al compositions, the predominant fraction of Al atoms. The Al atoms in ***Al-O-(Si-O)$_2$-Al sequences located in one six-membered ring of cationic site (denoted further Al pairs, Al$_{2Al}$)*** are of specific importance and occur frequently (as an example see Fig. 2-2 d). The Al-O-(Si-O)$_3$-Al sequence in an 8-MR was reported only in mordenite. It would behave similarly as the Al-O-(Si-O)$_2$-Al sequences in 6-MRs and they will accordingly be discussed together. When occupied by the above sequences, the described 6- and 8-MRs represent cationic sites for bare divalent cations bound exclusively to framework oxygen atoms in dehydrated zeolites.

Al-O-(Si-O)$_n$-Al with n=2 or 3 with Al atoms ***located in different rings*** is also a possibility for Al distribution (Fig. 2-2 e,f). This is the only condition for these Al atoms, albeit there is no way of differentiating amongst the numbers of (Si-O)$_n$ groups. If close enough, the Al-O-(Si-O)$_{2.3}$-Al sequences with Al atoms in the different rings can balance the charge of the divalent hexaquo complex in hydrated zeolites, whereas they are unable to coordinate bare divalent cations in dehydrated zeolites.

2.2.2. Geometric and Visible Distance of Al Atoms

In addition to Al atoms in the Al-O-(Si-O)$_2$-Al sequence located in one ring or those in Al-O-(Si-O)$_n$-Al sequences in neighboring rings, two Al atoms separated by a high number of Si atoms in the Al-O-(Si-O)$_n$-Al chain (seemingly single Al atoms) can also exhibit rather short inter-atomic distances (Fig. 2-2 g). Nevertheless, when the two Al atoms of the Al-O-(Si-O)$_{2,3}$-Al sequence are separated by a zeolite wall consisting of a double TO$_4$ layer, despite the short distance of these Al atoms (Fig. 2-2 h), they will behave as single Al atoms unable to coordinate a divalent cation, but only monovalent species, see below in Par. 2.2.3.

The two Al atoms at a short geometric inter-atomic distance can balance divalent counter ion species only when both Al atoms face the same channel (Fig. 2-3). Similarly, the two monovalent ion centers (e.g., protons) related to two Al atoms can cooperate only if located in the same channel. On the contrary, two close Al atoms that are separated by a double layer of the wall

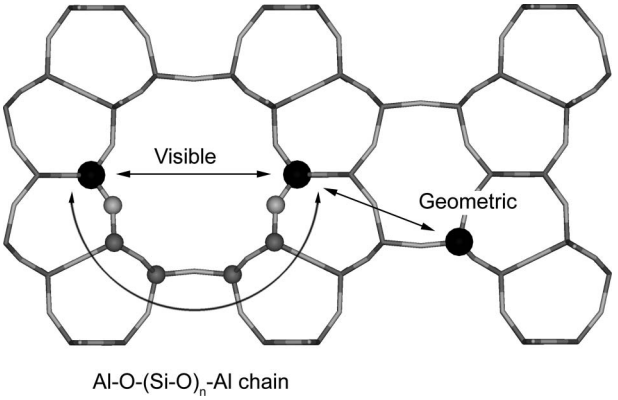

Figure 2-3: Geometric and visible distance of Al atoms in the zeolite and Al-O-(Si-O)$_n$-Al sequence.

and thus their counter ions face into different channels could not cooperate with each other. Thus, the ***visible distance of Al atoms*** is defined as a sufficiently short geometric distance (Al-O-(Si-O)$_{1,2}$-Al in one ring and Al-O-(Si-O)$_n$-Al in different rings), but excluding two close Al atoms separated by the double-layer wall. The visible distance of two Al atoms represents an important parameter, which affects the accommodation and properties of the polyvalent counter ion species, and cooperation of two close monovalent centers. These facts also suggest that this siting/distribution of Al atoms could be to some extent monitored indirectly by using the specified counter ions as probes.

Unpaired Al atoms ($Al_{UNPAIRED}$) cover two Al atoms located in different rings, close enough to balance a hexaquocomplex of divalent Co^{2+} cation, i.e., in a visible distance, but unable to accommodate bare divalent ions.

Single Al atoms represent the opposite of the close Al atoms in various Al-O-(Si-O)$_n$-Al sequences with consideration of their location in a single ring or in different rings at geometrical and visible distances (see Fig. 2-2i). Single Al atoms are understood to be two distant Al atoms (distant local charges) each exclusively balanced by monovalent cations. The distance between two single Al atoms is large or the interaction of their counter ions is geometrically restricted. A single Al atom is separated from another Al atom by a long (Si-O)$_n$ sequence with $n > 2$. However, the number of separating Si atoms differs from different points of views. Their population cannot be experimentally determined and is calculated from the balance of framework Al atoms.

2.2.3. 3-Al and 4-Al Atom Hyper-Structures

The probability of location of three Al atoms in a 6-MR in Si-rich zeolites can be excluded (see Par. 4.1). Nevertheless, in addition to the siting of

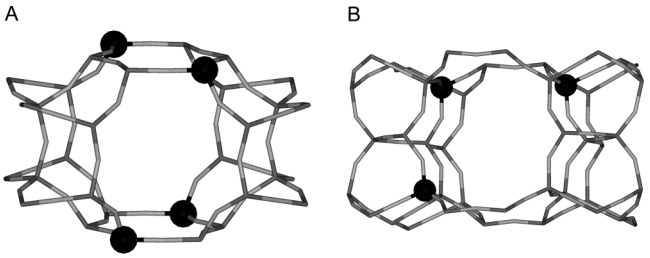

Figure 2-4: (A) 4-Al atom and (B) 3-Al atom hyper-structure in ferrierite.

Al atoms at the individual T sites or mutual arrangement of two close Al atoms, existence of more complex organization of Al atoms in the zeolite framework has to be taken into account. Two Al-O-(Si-O)$_2$-Al sequences, each located in a 6-MR of the cationic sites at the opposite sides of the channel wall, form the ***4-Al atom hyper-structure*** (Fig. 2-4). This location of four Al atoms creates the local arrangement enabling the cooperation of two divalent counter ions, e.g., participating in the catalytic reaction. Another case involves the cooperation of a divalent cation with a protonic site originating from the ***3-Al atom hyper-structure***, where a defined arrangement of three Al atoms, two of them in one ring, and the third in another nearby ring, is required.

3. METHODS FOR ANALYSIS OF THE SITING AND DISTRIBUTION OF FRAMEWORK AL ATOMS

3.1. Analysis of Distribution of Al Atoms in the Framework

3.1.1. Al-O-Si-O-Al Sequences

^{29}Si MAS NMR represents a standard method for the analysis of the Si-Al connectivity in Al-rich zeolites as reflected in the presence of Si(nAl,4-nSi) atoms with four, three, two and one neighboring Al atoms (16). The Al-O-Si-O-Al sequences yield Si(2Al,2Si) atoms with ^{29}Si chemical shift between-92 and -100 ppm, while the Si(1Al,3Si) atoms are reflected in the -97 to -107 ppm shifts (16e, f, 17). However, the application of the method developed for Al-rich frameworks with one T site on Si-rich zeolites with a high number of framework T sites results in significant limits, when analyzing Al-O-Si-O-Al sequences in Si-rich zeolites.

Si(2Al,2Si) atoms can belong to a wide variety of Si-Al connectivity with limiting cases of individual Al-O-Si-O-Al sequences and infinite -(Al-O-Si-O)- chains or rings. One Si(2Al,2Si) atom and six Si(1Al,3Si) atoms correspond to

the isolated Al-O-Si-O-Al sequence and the ratio of Al atoms in isolated Al-O-Si-O-Al sequences to the other Al atoms can be calculated using the equation:

$$Al_{Al\text{-}O\text{-}Si\text{-}O\text{-}Al}/Al_{Al\text{-}O\text{-}(Si\text{-}O)n>1\text{-}Al} = 2I_2/(I_1 - 6I_2) \qquad \text{Eq. (3-1)}$$

where I_n is the intensity of the resonance of the Si(nAl,4-nSi) atoms. On the other hand, one Si(2Al,2Si) atom and two Si(1Al,3Si) atoms correspond to one Al atom of the -(Al-O-Si-O)- ring, and the ratio of Al atoms in these rings to the remaining Al atoms is given by the equation:

$$Al_{Al\text{-}O\text{-}Si\text{-}O\text{-}Al}/Al_{Al\text{-}O\text{-}(Si\text{-}O)n>1\text{-}Al} = I_2/(I_1 - 2I_2). \qquad \text{Eq. (3-2)}$$

For illustration, if the ratio of the intensities of the resonances of the Si(2Al,2Si) and Si(1Al,3Si) atoms is 1:6, this reflects either 100% of the Al atoms in isolated Al-O-Si-O-Al sequences or only 25% of the Al atoms in the -(Al-O-Si-O)- rings/chains. The formation of -(Al-O-Si-O)- rings/chains cannot be excluded even for zeolites with Si/Al $\geq$ 8. Thus, estimation of the concentration of Al atoms in the Al-O-Si-O-Al sequences is connected with an irremovable uncertainty.

The second limitation of monitoring of Al in the Al-O-Si-O-Al sequences follows from the low intensity of the Si(2Al,2Si) signal in the spectra of Si-rich materials. 2% of the signal intensity of the Si(2Al,2Si) atoms in the entire ^{29}Si MAS NMR spectrum can reflect up to 13% of the Al-O-Si-O-Al sequences in the zeolite. Thus, highly accurate analysis of the ^{29}Si NMR spectra is essential. This is rather difficult owing to the multiple resonances of the Si(2Al,2Si) atoms in the different T sites and the overlap of the signals of the Si(2Al2Si) and Si(3Si,1OH) atoms exhibiting resonances between -90 and -100 ppm (16e, f, 17b, c, 18). Thus, the simulation of the ^{29}Si MAS NMR spectra and the attribution of the individual bands to the Si(nAl,4-nSi) and Si(3Si,1OH) atoms must be verified by using ^{29}Si CP MAS NMR, allowing identification of Si(4-nSi,nOH) atomic resonances. This should be accompanied by comparison of the framework Al content (expressed as Si/Al_{FR}), estimated using ^{29}Si MAS NMR and the Si/Al_{FR} value obtained by other methods, such as a quantitative ^{27}Al MAS NMR experiment or determination of the ion-exchange capacity of the zeolite for Na^+ or NH_4^+ ions. The Si/Al_{FR} ratio can be estimated using ^{29}Si MAS NMR according to the equation (16f, 19):

$$Si/Al_{FR} = I/\left(\sum 0.25nI_n\right) \qquad \text{Eq. (3-3)}$$

where I is the total intensity of the ^{29}Si MAS NMR spectrum. The differences between the Si/Al_{FR} values obtained from ^{29}Si MAS NMR and those determined by other methods provide clear evidence for incorrect simulation and

interpretation of the ^{29}Si MAS NMR spectrum with an unrealistically high concentration of Si(2Al,2Si) atoms. In this case, the presence of Si(2Al,2Si) atoms could be suggested for samples that are, in reality, free of Si(2Al,2Si) atoms.

3.1.2. Close Al Atoms at a Visible Distance and Single Al Atoms

Al atoms at a visible distance represent all the Al atoms which are facing the same channel and are close enough to cooperate in the accommodation of a hexaquocomplex of divalent cation. The distance between these close Al atoms is not well defined, and the accommodation of the $[Co^{2+}(H_2O)_6]^{2+}$ complex was suggested as a parameter defining these species. The zeolite exchange capacity for the divalent hexaquo-complex was suggested as an indicator of close Al atoms (9a). The Co^{2+} ion exchange into the Na-form of the zeolite from 0.05 M $Co(NO_3)_2$ solution at RT guarantees the exclusive presence of $[Co^{2+}(H_2O)_6]^{2+}$ complexes in the Co-zeolite (4d, 5a). The exclusive presence of $[Co^{2+}(H_2O)_6]^{2+}$, both in the solution and in the as-prepared hydrated zeolite, can be easy monitored by UV-Vis spectroscopy (20). Triple ion exchange with at least 50 mL of 0.05M $Co(NO_3)_2$ solution per gram of a zeolite guarantees the complete exchange of $[Co^{2+}(H_2O)_6]^{2+}$ ions (5a). The molar concentration of close visible Al atoms $[Al_{VIS}]$ can thus be estimated according to the equation:

$$[Al_{VIS}] = 2[Co] \qquad \text{Eq. (3-4)}$$

where [Co] is the molar concentration of the maximum exchanged cobalt in the zeolite. The Co^{2+} ion-exchange capacity of Si-rich zeolites never reaches 100% of the nominal capacity (Co/Al = 0.5). Nevertheless, the Co ion capacity reflects all the Al atoms which participate in accommodation of Co^{2+} ions. It should be mentioned that the Na/Al ratio was always close to 1, indicating accessibility of the Na^+ aqua-complexes for all the Al atoms, although some electrostatic repulsion might occur (5a). It can be assumed that, if all the Al atoms accommodate the larger Na^+ complexes, there is no sterical constraint for the accommodation of the smaller Co^{2+} aqua-complexes. Moreover, the electrostatic interactions result in the preferential accommodation of divalent complexes in the vicinity of two close negative charges and monovalent cations in the vicinity of single Al atoms.

The single Al atoms are those which could not accommodate the $[Co^{2+}(H_2O)_6]^{2+}$ complex (4d, 5a, 9a). Their molar concentration, $[Al_{1Al}]$, can be estimated by using the relationship:

$$[Al_{1Al}] = [Al_{FR}] - [Al_{VIS}] = [Al_{FR}] - 2[Co] \qquad \text{Eq. (3-5)}$$

where $[Al_{FR}]$ is the concentration of framework Al atoms.

3.1.3. Al-O-(Si-O)$_2$-Al Sequences in One Ring – Al Pairs

As the Al-O-Si-O-Al sequences occur in Si-rich zeolites only in exceptional cases (see Chapter 4), and Al-O-(Si-O)$_3$-Al concerns only 8-MR in mordenite, the Al-O-(Si-O)$_2$-Al in 6-MRs of cationic sites are of the main concerns.

Bare Co^{2+} ions in dehydrated zeolites (evacuated at 450°C), monitored by Vis spectroscopy, were successfully used as a probe to quantify the concentrations of two Al atoms located in one ring (4d, 5a). If the cation would be located in the ring with one Al atom and charge-balanced by a second, distant Al atom (in another ring), the bare Co^{2+} ion would be highly reactive and its presence is not probable (21). The monovalent Co-OH and Co-oxo species might be balanced by single Al atoms under these conditions. The presence of Co-OH species owing to their easy dehydroxylation above 450°C (20) is not probable and the Co-oxo species do not exhibit absorption in the Vis region (22). Thus, the d-d spectra of bare Co^{2+} ions can only be interfered by the Vis spectra of Co oxide clusters, nano- and bulk Co oxides. However, these species exhibit significantly different spectra and were never observed in Co-zeolites ion-exchanged under the conditions described in the previous paragraph. Thus, the dehydrated, fully $[Co^{2+}(H_2O)_6]^{2+}$ exchanged zeolite can be employed for quantification of the rings containing two Al atoms facing the same channel. Complete ion exchange of the zeolite by $[Co^{2+}(H_2O)_6]^{2+}$ is guaranteed under the conditions described in the previous paragraph.

The d-d spectra of bare Co^{2+} ions in the Vis region of the dehydrated zeolites are characteristic for the individual cationic sites. Three cationic sites, denoted as the α-, β- and γ-types, were distinguished for each of the mordenite, ferrierite, ZSM-5 and beta zeolites. The corresponding Co^{2+} spectral bands together with their extinction coefficients were reported elsewhere (6, 20, 23). Only the Al-O-(Si-O)$_2$-Al sequences in one ring (with the exception of the β-site in mordenite with the possible Al-O-(Si-O)$_3$-Al sequence in 8-MR) were suggested to form cationic sites in these zeolites. For details, see Par. 5.2. Quantitative analysis of the spectrum of the dehydrated maximum $[Co^{2+}(H_2O)_6]^{2+}$ exchanged zeolite by its simulation gives the concentration of the bare Co^{2+} ions in the individual cation sites, and the concentration of Al atoms in Al-O-(Si-O)$_2$-Al sequences in one ring, $[Al_{2Al}]$ is given by the equation:

$$[Al_{2Al}] = 2([Co_\alpha] + [Co_\beta] + [Co_\gamma]) \qquad \text{Eq. (3-6)}$$

where $[Co_\alpha]$, $[Co_\beta]$ and$[Co_\gamma]$ are the molar concentrations of the bareCo ions in the α-, β- and γ-type sites of mordenite, ferrierite, ZSM-5 and beta zeolites. The Co concentrations in the individual sites follow from the equation:

$$[Co_\eta] = I_\eta \varepsilon_\eta, \qquad \eta = \alpha, \beta, \gamma \qquad \text{Eq. (3-7)}$$

where I_η is the intensity of the Vis bands corresponding to the Co^{2+} ions in the individual sites and ϵ_η is the corresponding extinction coefficient. Complete dehydration of the Co-zeolite, preventing the presence of Co^{2+}-OH ions, is guaranteed at an evacuation temperature of $\geq$450°C under dynamic vacuum for 3 h, as indicated by the absence of the combination vibrational (2ν) bands of the Co-OH groups in the NIR region of UV-Vis-NIR spectra of the dehydrated sample (20).

3.1.4. Visible Al Atoms in Different Rings – Unpaired Al Atoms

There is no direct method for demonstrating the presence of the Al atoms in different rings able to balance the hexaquocomple of Co^{2+} ion. Their concentration is given by the equations:

$$[Al_{UNPAIR}] = [Al_{VIS}] - [Al_{2Al}] = 2([Co] - [Co_\alpha] + [Co_\beta] + [Co_\gamma]) \qquad \text{Eq. (3-8)}$$

where [Co] is the molar concentration in Co-zeolites, and $[Co_\alpha]$, $[Co_\beta]$ and $[Co_\gamma]$ are the molar concentrations of the bare Co^{2+} ions in the α-, β- and γ-type cationic sites of mordenite, ferrierite, ZSM-5 and beta zeolites. For the extinction coefficients of the Co sites in the individual zeolites see (6, 20, 23).

3.1.5. Statistical Approach for the Distribution of Al Atoms

For years, Monte-Carlo simulations and the configuration matrix approach were used to indicate the distribution of Al atoms, mainly the number of Al-O-Si-O-Al sequences in Si-rich zeolites. However, the experimental results obtained for ZSM-5, mordenite, ferrierite and MCM-22 clearly show that the Al distribution in the framework varies dramatically in Si-rich zeolites (4 to 84% of close Al atoms) in samples with the same topology and chemical composition, see Chapters 4 and 6 and Refs. (5a, b, 6, 9a, 10a, 24). This is because of the crucial role of the structure directing agent (SDA) (see Chapter 6) and the effect of the other synthesis parameters on the incorporation of Al atoms into the zeolite framework. Thus, the framework Al distribution is not random or controlled by statistics or other simple rules. Accordingly, none of the methods based on the statistical approach can be employed for description and prediction of the Al distribution in Si-rich zeolites.

3.1.6. Other Experimental Methods

The methods described in Par. 3.1.1–3.1.3 are the only ones that have been reported for successful monitoring of the Al distribution in Si-rich zeolites. Nevertheless, we can speculate on the capabilities of other experimental methods in this field.

EXAFS has not yet been reported for the analysis of neighboring framework Al atoms in zeolites. This method was successful in the analysis of

titanium and iron isomorphously substituted in zeolites. However, the EXAFS experiment reflects only the geometrical distances and cannot distinguish amongst the individual types of close Al atoms as Al-O-Si-O-Al and Al-O-(Si-O)$_2$-Al sequences, and close Al atoms in different rings and facing towards the same or different channels.

^{27}Al double-quantum (2Q) MAS NMR experiments were successfully used to monitor the vicinity of extra-framework Al species and framework Al atoms in dealuminated, formerly Al-rich zeolites (25). This experiment is based on the homonuclear correlation (16e, 17c). Two ^{27}Al nuclei interact when at a distance of no greater than 0.5 nm. A homonuclear correlation pulse sequence can be employed to monitor the interactions of close ^{27}Al nuclei. The presence (or absence) of a signal reflecting nuclei close enough to interact (at a distance of $\leq$0.5 nm) clearly indicates their presence (or absence). No attempt to distinguish close and single Al atoms in the framework of Si-rich zeolites using this method has been reported to date. Nevertheless, the development of pulse sequences with enhanced sensitivity (25) and the availability of ultra-high-field MAS NMR spectrometers presents the possibility of employing ^{27}Al (2Q) MAS NMR for characterization of the Al distribution in Si-rich zeolites. Extra-framework cations, such as H^+, D^+, Li^+, balancing the AlO_4 negative charge and monitored by (2Q) MAS NMR, could act as probes to monitor the presence of close Al atoms in the zeolite (26). However, the double quantum experiment reflects only the geometrical distance of the investigated nuclei and thus does not resolve Al atoms facing the same or different channels or the Al atoms located in one and two rings, see Par 3.1.1–3.1.3.

3.2. Analysis of Al Atom Siting in the Framework T Sites

3.2.1. Diffraction, XANES, EXAFS

The similar electron densities of Al and Si atoms do not allow distinguishing of these atoms in the framework by a standard diffraction experiment. The low content of framework Al atoms in Si-rich zeolites results in occupancies of the individual T sites substantially lower than 1. Thus, the observed diffraction pattern reflects a mixture of diffractions on Al and Si atoms in the same T site and, in contrast to the zeolites with Si/Al = 1, it is not possible to resolve Al and Si atoms on the basis of different bond lengths.

Recently, application of the x-ray standing-wave single-crystal experiment has been shown to represent a breakthrough in the resolution of Al and Si atoms in Al-rich zeolites (4e). Moreover, it has been suggested that this approach could be extrapolated for analysis of the Al siting in ZSM-5. However, this method is not suitable for Al analysis in the small crystallites typically employed as catalysts. Note that syntheses leading to large crystals significantly differ from those used for the preparation of small crystallites and also

result in different Al siting, see Chapter 5. Moreover, low Al content in the framework of Si-rich zeolites represents a further factor limiting the use of the x-ray standing-wave approach. XANES enables monitoring of the coordination of an Al atom. However, small deviations in the AlO_4 geometry in the individual T sites cannot be distinguished, similar to EXAFS.

3.2.2. ^{27}Al MAS NMR

High resolution ^{27}Al MAS NMR experiments allow distinguishing of Al atoms in different T sites. Successful application of ^{27}Al multi-quantum (MQ) experiments to fully hydrated zeolites for this purpose has been reported (4a, b, 7–8, 27). Nevertheless, the use of ultra-high field instruments for single-pulse ^{27}Al MAS NMR should also distinguish Al atoms in different T sites. The two-dimensional (2D) MQ MAS NMR experiment allows suppression of quadrupolar broadening in one projection and careful analysis of the spectrum yields identification of the resonances of Al atoms in the individual T sites (4a, 16e, 17c, 28). Moreover, the isotropic chemical shift of the quadrupolar nucleus, analogous to the chemical shift of non-quadrupolar nuclei, which characterizes the geometry of AlO_4 tetrahedron, can be calculated. Details of this method and its application to Si-rich zeolites have been described elsewhere (4a, b, 4d, 5c, 8, 29).

However, there are three crucial points which must be taken into account when the ^{27}Al NMR experiment is employed for analysis of the Al siting in Si-rich zeolites:

i. There is no simple correlation between the Al siting and ^{27}Al isotropic chemical shift in Si-rich zeolites. The Lippmaa correlation (30), which has been suggested for determination of the relationship between the ^{27}Al isotropic chemical shift and average T-O-T angle of the $T(Al,Si)O_4$ tetrahedron in Al-rich zeolites, cannot be used for two reasons: (1) there is no linear correlation between the AlO_4 geometry and ^{27}Al isotropic chemical shift (4b, 8, 29c, d, 31), (2) the geometry of the $T(Al,Si)O_4$ tetrahedron obtained from the diffraction experiment does not reflect the geometry of the AlO_4 tetrahedra. Note that Al atoms in the Si-rich zeolites represent typically less than 10% of the T atoms and the deformation of the AlO_4 tetrahedron due to the longer Al-O distance is thus not reflected in the T and O coordinates.

ii. A significant effect of the closeness of the second Al atom in the Al-O-$(Si-O)_{1,2}$-Al sequence, as well as the defect Al-O-Si-OH site on the ^{27}Al isotropic chemical shift, have been reported (29c, d). The change in the ^{27}Al isotropic chemical shift due to this effect reaches up to 5 ppm. Note that ^{27}Al isotropic chemical shifts in all the T sites in ZSM-5 range within

12 ppm (8). Thus, the ^{27}Al NMR experiment, without analysis of the Al-O-(Si-O)$_{1,2}$-Al sequences by ^{29}Si MAS NMR and Vis spectroscopy of Co^{2+} ions, does not even allow estimation of whether the location of the Al atoms is or is not the same in the samples. Different ^{27}Al resonances can reflect single Al atoms and Al of the Al-O-(Si-O)$_{1,2}$-Al sequences in the same T site.

iii. Dependence of the ^{27}Al isotropic chemical shift in hydrated zeolites on the type of charge-balancing cations was reported for ferrierite with Al-O-(Si-O)$_2$-Al sequences, not observed for ZSM-5 and ferrierites with the exclusive presence of single Al atoms (4d, 8, 27b, 29c). This effect can be attributed to the interaction of the framework with solvated cations located in channels/cavities with limited space for the accommodation of a larger number of solvated monovalent cations. This interaction can be minimized by transfer of the zeolite into a form where close Al atoms are balanced by small divalent cations, such as Mg^{2+} or Ca^{2+} (29c).

The isotropic chemical shifts of ^{27}Al atoms in the individual T sites (ad i) can be predicted by quantum chemical calculations. The local arrangement of the AlO_4 tetrahedra in the silicate framework must first be calculated. Note that the ^{27}Al isotropic chemical shift is highly sensitive to the Al geometry and high accuracy in the prediction of the arrangement of the Al atoms in the framework is essential. Periodic DFT (cp2k) and embedding (QM-pot) approaches were reported to be sufficiently accurate for this purpose. The ^{27}Al shielding of the Al atom in the cluster with the predicted geometry is then calculated. Finally, the ^{27}Al shielding must be converted to the ^{27}Al isotropic chemical shift. Calculation of the ^{27}Al shielding in the Si-rich chabasite or $Al(NO_3)_2$ was successfully employed for the calibration. For details of the prediction of the ^{27}Al isotropic chemical shifts in different T sites and their comparison with the experiment, see Refs. (4b, 7–8). The accuracy of the calculation of the ^{27}Al isotropic chemical shift in zeolites is approx. $\pm$0.5 ppm. Together with the accuracy of the ^{27}Al (MQ) MAS NMR experiment ($<$0.2 ppm), this represents a limiting factor for interpretation of the ^{27}Al MAS NMR spectra of ZSM-5, where several resonances were predicted within the 1 ppm range (8). Nevertheless, for zeolites with a lower number of framework T sites, such as ferrierite, analysis of the Al siting can be performed by comparison of the predicted and observed ^{27}Al isotropic chemical shifts.

The uncertainty in the analysis of the Al siting for zeolites with Al-O-(Si-O)$_{1,2}$-Al sequences can be overcome by using additional spectroscopic methods. ^{29}Si MAS NMR allows analysis of the presence of Al-O-Si-O-Al sequences and Vis spectroscopy of bare Co^{2+} ions can be used to determine the Al-O-(Si-O)$_2$-Al sequences in one ring. Moreover, bare Co^{2+} ions yield information on the rings

accommodating these sequences. Based on knowledge of the rings with Al-O-$(Si-O)_2$-Al sequences, the ^{27}Al isotropic chemical shifts of Al atoms in these sequences can be predicted by quantum chemical calculations and compared with the experimental values (7). However, this approach can be employed only for zeolites with a limited number of T sites to obtain a low, acceptable number of Al-O-$(Si-O)_2$-Al sequences, for which the ^{27}Al isotropic chemical shift must be calculated.

3.2.3. Quantum Chemical Calculations

Calculations of relative energies of Al atoms in the individual framework T sites in Si-rich zeolites initiated the discussion on the non-random Al siting in these matrices (32). However, the Al siting in the zeolite framework depends on the conditions of the zeolite synthesis (SDA, alkaline cations, Si and Al sources and products of their transformation in the synthesis gel, water molecules, pH, pressure, and temperature) and the samples of the same chemical composition with dramatic differences in Al siting can be prepared. This finding is in contradiction with the minimization of the energy of Al atoms in the framework T sites. Thus, the calculation of the relative energy of Al atoms in the individual framework T sites cannot be employed for the prediction of Al siting. Recently, Sastre et al. have involved the SDA molecule into the model for the calculation of energies of Al atoms in ITQ-7 (33). They demonstrated the crucial role of the SDA molecule in the Al atom incorporation into the D4R units of ITQ-7. The suggested Al sites in this unit have been shown to be in agreement with the vibrations of structural OH groups monitored by FTIR. Nevertheless, inclusion of the other parameters of the synthesis to the model calculations is highly desired, and the confirmation of the theoretical prediction by the experimental methods seems to be necessary.

3.2.4. Protons as Probes

H^+ ions can also be suggested as probes of the framework Al siting *via* the OH stretching vibrations of bridging SiOHAl hydroxyls monitored by the FTIR spectroscopy. Sastre et al. used it for the analysis of Al sites in the ITQ-7 zeolite (33). The observed OH stretching vibrations were compared with the predicted frequencies of OH stretching vibrations for the individual SiOHAl groups of AlO_4 tetrahedra obtained by quantum chemical calculations. Surprisingly good agreement between the predicted and observed stretching frequencies was reached. Note that the highly accurate prediction of stretching OH vibrations for the interpretation of the experimental results is essential. In contrast to ITQ-7 with only five T sites a high number of framework T sites would represent an obstacle of the successful analysis of framework Al siting in the zeolite.

3.3. Analysis of Al Siting in the Framework Rings

3.3.1. Monovalent Cations as Probes

Monovalent cations balancing the framework negative charge in dehydrated zeolites can be used as probes of Al siting. Although the Na^+, K^+, Rb^+, Cs^+ and Tl^+ ions monitored by the x-ray diffraction indicated the non-random Al siting in ZSM-5 (34), there is not a direct and simple relation between the position of the (namely large) cation and the siting of Al atom in the framework. On the one side, there is a preference for the location of the cation in the optimum distance from the charged oxygen atoms of the AlO_4 tetrahedra, as observed by EXAFS for the Co^{2+} ions in Si-rich zeolites. On the other side, the minimization of the cation potential energy by its coordination in the ring with the optimum size represents a second parameter governing the cation siting. The optimum size of the ring can be suggested to depend on the cation diameter. The x-ray data provide evidence on cation siting only in the 6-MRs or larger ones. Thus, the small cations as H^+, D^+ and Li^+ monitored by the neutron diffraction might be more appropriate probes of Al siting in zeolites (34c). Nevertheless, this approach, mainly because of the low concentration of cations, the large unit cell and a number of possible cationic sites in Si-rich zeolites, is still far from application.

Structure directing agents used in the zeolite synthesis often represent organic cations and they are generally accepted to play a crucial role in the formation of the zeolite framework as well as in the location of Al atoms in the vicinity of the positively charged part of SDA. Accordingly, the SDA might represent a probe of Al atom siting. This approach was successfully used for the analysis of Al siting in ITQ-7 by Sastre et al. (33). Nevertheless, the interaction of the SDA with the framework Al atoms might be confirmed by multinuclear MAS NMR experiment.

3.3.2. Divalent Cations as Probes of Al-O-(Si-O)$_2$-Al Sequences

Application of Vis spectroscopy of bare Co^{2+} cations for the analysis of the concentration of Al-O-(Si-O)$_2$-Al sequences in one ring of Si-rich zeolites is described in Par. 3.1.3. However, this method also provides siting of the Al-O-(Si-O)$_2$-Al sequences in the individual rings of the zeolite structure. The Vis bands of bare Co^{2+} ions in the α-, β-, and γ-type cationic sites of dehydrated zeolites reflected the corresponding rings in mordenite, ferrierite, ZSM-5 and beta zeolites (6, 20, 23). Thus, the presence of typical bands of the bare Co^{2+} ions in the α-, β-, and γ-type sites is a clear evidence that the Al-O-(Si-O)$_2$-Al sequence is present in the ring forming this site and equation Eq. (3-7) can be applied for the estimation of the concentration of Al-O-(Si-O)$_2$-Al sequences in the 6- or 8-MRs of these sites. Analysis of the siting of divalent cations in the zeolite by diffraction methods can also be applied to monitor the location

of Al-O-(Si-O)$_2$-Al sequences as follows from the satisfying agreement between the results of the analysis of Co^{2+} siting by using Co^{2+} Vis spectroscopy and synchrotron powered x-ray diffraction for Ni^{2+} and Co^{2+} ions (9b-e). However, it has to be pointed out that the confirmation of the divalent state of the x-ray monitored cation as well as exclusion of the presence of cation-ligand complex in the sample is essential for the correct analysis of Al-O-(Si-O)$_2$-Al sequences.

4. STATE OF ART OF DISTRIBUTION OF FRAMEWORK Al ATOMS IN Si-RICH ZEOLITES

There is only one rule that is generally valid for the arrangement of Al atoms in a zeolite. According the Loewenstein rule, the formation of an Al-O-Al sequence is forbidden because of its low stability (15). The Loewenstein rule was suggested as a general rule for alumosilicates and has been confirmed for zeolites with framework compositions of Si/Al 1. ^{29}Si MAS NMR yielded evidence for the exclusive presence of Si(4Al) atoms with four Al neighbors. There is no direct evidence for the validity of the Loewenstein rule for zeolites with Si/Al $>$ 1; however, it has never been shown to be violated and thus this rule is generally accepted for zeolites.

There is a limit for the incorporation of Al into the framework of Si-rich pentasil zeolites. The maximum framework Si/Al ratio for ferrierite and mordenite is 5 and the Si/Al value is 7 for mutinaite (35), the natural analogue of ZSM-5. The Dempsey rule, formulated in connection with zeolite dealumination, suggests that the stabilization energy of the Al-O-Si-O-Al sequence in Al-rich zeolites governs their occurrence (36). However, the Dempsey rule does not reflect the conditions of hydrothermal synthesis, under which the incorporation of Al into the zeolite framework occur. Thus, the reliability of the Dempsey rule has been limited ever since it was postulated. To explain these limits in the Si/Al composition, Melchior extended Dempsey's electrostatic arguments to include the Si-Al linkage in zeolites, and suggested that Al atoms are incorporated into the zeolite framework in a pattern minimizing the presence of Al-O-Si-O-Al sequences (16d, 37).

Takaishi et al. applied the configuration matrix approach to resolve the Al distribution in mordenite. They denied the Dempsey rule by demonstrating the presence of Al-O-Si-O-Al sequences in mordenite with Si/Al $\sim$ 5 by ^{29}Si MAS NMR, albeit this composition ratio would permit the energetically less demanding Al arrangement without these sequences. Therefore, Takaishi et al. postulated a new rule in addition to the Loewenstein rule (38). According to the newly postulated Takaishi and Kato rule, two Al atoms cannot be present only in 5-MRs. It follows that the Al-O-Si-O-Al sequences in mordenite can be formed in Si-rich zeolites in 6-MRs, which are generally present in pentasil ring zeolites. Nevertheless, the Takaishi and Kato rule is in contradiction with

the presence of two Al atoms in the 4-MR of A- and X-type zeolites. It seems highly improbable that the Al-O-Si-O-Al sequence in a 5-MR would be less stable than that in the 4-MR of Al-rich faujasites. However, as the Takaishi and Kato rule was derived only from ^{29}Si MAS NMR results, the presence of Si(3Si,OH) atoms surrounded by silanol groups was not included into the analysis. Consequently, the reliability of the Takaishi and Kato rule requires further verification.

It should be pointed out that the ^{29}Si resonances around 95–98 ppm reflect both the Si(2Si,2Al) and the SiOH atoms (16e, f, 17b, c, 18). Perturbation of AlO_4 tetrahedra, leading up to breaking of the Al-O bonds, and partial framework dealumination are, e.g., typical for zeolites of BEA topology (39). Therefore, the state of the framework Al and presence of Si(2Si,2OH) atoms should be taken into account. Thus, reliable conclusion on the Si(2Si,2Al) atoms can be drawn only when a ^{29}Si cross-polarization (CP) experiment and analysis of the extra-framework Al are performed.

4.1. Al-O-Si-O-Al Sequences

As follows from the previous paragraph, there is no generally valid rule for the occurrence of Al-O-Si-O-Al sequences in Si-rich zeolites or any other report dealing with this aspect. Nevertheless, ^{29}Si MAS NMR is one of the basic methods for monitoring the incorporation of Al into the silicate framework. An enormous number of ^{29}Si MAS NMR spectra of Si-rich zeolites have already been published and could be exploited to monitor the presence of Al-O-Si-O-Al sequences in the individual zeolite samples. However, it should be pointed out that the ^{29}Si MAS NMR spectra do not allow determination of the concentration of Al-O-Si-O-Al sequences in zeolites with high accuracy, but rather provide evidence for their presence and limiting concentrations (see Par. 3.1.1). The following part discusses the occurrence of Al-O-Si-O-Al sequences in zeolites of industrial importance, such as ZSM-5, beta zeolite, mordenite, ferrierite and MCM-22.

In the ZSM-5 zeolite, the Al-O-Si-O-Al sequences have never been reported for Si/Al ratios of 12–∞ (typical Al concentration range) including a large set of samples with various Si/Al ratios and synthesis conditions, see, e.g., Refs. (4b, 8, 29c). Only two reports have appeared to date on the presence of Al-O-Si-O-Al sequences in Al-rich ZSM-5 frameworks (Si/Al 8.4, and 8.3–9.0) (17b, 29c). It should be pointed out that the occurrence of extra-framework Al atoms was negligible in these samples according to ^{27}Al MAS NMR and Al-O-Si-O-Al sequences represented a substantial fraction of the Al atoms in the framework (roughly up to 60–80% of the Al atoms). This indicates that, at a framework Al content close to its limiting value for ZSM-5 (Si/Al > 7 for natural mutinaite) (35), predominantly Al-O-Si-O-Al sequences are formed. Surprisingly, while at least 80% of the Al atoms are in the Al-O-Si-O-Al

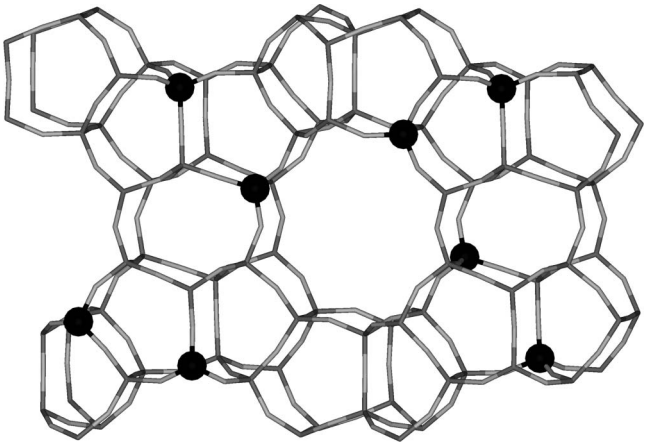

Figure 4-1: Schematic distribution and siting of Al atoms in ZSM-5 of unusual composition of Si/Al 8.5.

sequences for the zeolite with Si/Al 8.5 (about 11 Al atoms per u.c.), only 16% of the Al atoms (<2 Al per u.c.) are able to accommodate the divalent $[Co(H_2O)_6]^{2+}$ complex and, in the rest of the Al-O-Si-O-Al sequences, each Al atom faces a different channel (see Par. 2.2.2) (29c). In ZSM-5, only 5-MRs contains T atoms facing different channels; for illustration see Fig. 4-1. In contrast, all the T (Si,Al) atoms of the 6-MRs face the same channel. This indicates that at least 80% of the Al-O-Si-O-Al sequences (i.e., >8 Al per u.c.) are located in 5-MRs and, therefore, the Al distribution in ZSM-5 with high Al concentration does not obey the Takaishi and Kato rule.

The framework of ZSM-5 with Si/Al 8.5 does not require the presence of Al-O-Si-O-Al sequences for the Si/Al compositional reasons, as the Al-O-(Si-O)$_2$-Al sequences and single Al atoms would adequately meet the composition demands. This implies that the Al atoms are preferentially present in Al-O-Si-O-Al sequences in the ZSM-5 zeolite and that the formed Al-O-Si-O-Al sequences were preferentially located in 5-MRs, where each Al atom necessarily faces a different channel to minimize the electrostatic repulsion. It is anticipated that this arrangement would minimize the electrostatic repulsion of the AlO_4^- tetrahedra occurring on the channel surface, along with the required energy minimization according to the Dempsey rule.

In the wide-pore structure of the beta zeolite, the maximum framework Al content corresponds to Si/Al 3 for both natural and the reported synthesized zeolites (40). Al-O-Si-O-Al sequences occur in beta zeolites with high Al concentration and their concentration decreases with decreasing framework Al content, where beta zeolites with Si/Al > 10 are free of Al-O-Si-O-Al sequences (29a, 40a, 41). Beta zeolites with Si/Al > 12 with unperturbed framework TO_4 can be prepared if TMA (tetramethyl ammonium) is removed by calcination in a stream of ammonia (29a, 42) or the beta zeolite is synthesized in the

presence of Na^+ ions and low concentration of SDA. The absence of Al-O-Si-O-Al sequences is a typical feature of beta zeolites with Si/Al composition > 12 (9a, 43).

Mordenite, a wide pore zeolite, has a limiting Si/Al value of 5. Only mordenites with high framework Al content (Si/Al ~4–6) contain Al-O-Si-O-Al sequences (100–25% Al) depending on the Al concentration and zeolite synthesis. Their concentration decreases with decreasing Al content and it is negligible at Si/Al 8 (44), as later also confirmed for mordenites with Si/Al 5–10, prepared in fluoride and alkaline media (45). The synthesis conditions affect the occurrence of Si(2Si,2Al) atoms, as follows from less than 2.5 % Si(2Si,2Al) atoms in mordenite with Si/Al≈5 synthesized in fluoride media compared to 3.5% of the Si(2Si,2Al) atoms in mordenite with comparable Si/Al (45a), synthesized in alkaline media.

Ferrierite exhibits a limiting Si/Al ratio of 5. The Al-O-Si-O-Al sequences were not found in ferrierites with Si/Al > 8.5 (7, 46) and Si/Al > 15 (47). Nevertheless, low or negligible concentrations of Al-O-Si-O-Al sequences in ferrierites with Si/Al~8 should be tested for the individual synthesis.

The absence of Si(2Si,2Al) atoms was reported for ***ZSM-12*** with a Si/Al of l4 (48), and Al-O-Si-O-Al sequences were also not found in ***MCM-22*** (Si/Al > 10) (49) and ***MCM-49*** (Si/Al > 15) (49a). Thus, these Si-rich zeolites are free of Al-O-Si-O-Al sequences.

We summed up that the occurrence of the Al-O-Si-O-Al sequences is negligible in Si-rich zeolite frameworks with Si/Al > 12 and even at higher Al concentrations for Si/Al > 8 for ferrierites and mordenites. Above these Al contents, Al-O-Si-O-Al sequences are formed and their concentration dramatically increases with increasing Al content. However, this remarkable increase in their population compared to the other Si-Al sequences cannot be simply explained as a result of the statistical probability (38b). This is in agreement with the generally observed non-random distribution of Al atoms, whose incorporation is controlled by the synthesis procedure, see Chapter 6. For zeolites with Si/Al on the borderline between Al-rich and Si-rich pentasil zeolites (about Si/Al 10 for ZSM-5 and beta zeolites, and Si/Al 8 for mordenite and ferrierite), the concentration of Al-O-Si-O-Al sequences is probably negligible, but remains a matter of discussion. Different synthesis procedures might yield Al-O-Si-O-Al-free zeolites or zeolites with significant or even predominant concentrations of Al-O-Si-O-Al sequences.

4.2. Al-O-(Si-O)$_2$-Al Sequence in One Ring – Al Pairs, and Single Al Atoms

Al atoms in Al-O-(Si-O)$_2$-Al sequences in one ring and single Al atoms are complementary Al species and represent the majority of Al atoms in the framework of Si-rich zeolites.

Table 6-1: Maximum concentrations of Al in Al-O-(Si-O)$_2$-Al sequences in one ring (Al_{2Al}) and single Al atoms (Al_{1Al}) for selected zeolites and Si/Al molar ratios. According to Refs. (5, 9a, 10a,b, 24).

		Max. Al_{2Al}		Max. Al_{1Al}	
Zeolite	**Si/Al**	**Al_{2Al} (rel. %)**	**Al_{1Al} (rel. %)**	**Al_{2Al} (rel. %)**	**Al_{1Al} (rel. %)**
ZSM-5	12	84	16	10	90
	30	60	40	6	94
Ferrierite	10	66	34	20	80
Beta	15	65	35	39	61
MCM-22	40	68	32	18	82

With ZSM-5 it was found that zeolites with the same framework Al content can dramatically differ in the concentration of Al-O-(Si-O)$_2$-Al sequences in one ring and single Al atoms for a wide range of Si/Al compositions (4d, 5a, b, 10). The maximum populations of Al pairs and single Al atoms for various Si/Al ratios are given in Chapter 6, Table 6-1.

Although higher concentrations of Al might be expected to result in higher concentrations of Al pairs, zeolites with Si/Al from 12 to 15 might contain a predominant population of single Al atoms, up to 96%, and those with a low concentration of Al (Si/Al 30–40) can exhibit predominant concentrations of Al pairs. Typically, for one synthesis procedure (composition and conditions), the concentration of Al pairs increases, but not proportionally, with increasing Al concentration in the zeolite; nevertheless, quite the opposite effect of the Al concentration on the formation of Al-O-(Si-O)$_2$-Al sequences has also been observed (5b, 10b). Such dramatic differences in the distribution of Al atoms in the framework again clearly indicate that the Al siting in the zeolite is not random and not controlled by statistical rules. The reactivity of the synthesis mixtures is responsible for the observed Al distribution between these Al pairs and single Al atoms (for details see Chapter 6).

MCM-22 also exhibited dramatic differences in the Al distribution (Table 4-1). Similarly to ZSM-5, as the increasing concentration of Al led to an increasing population of Al pairs, the opposite effect has also been observed (24). As the synthesis of MCM-22 is carried out by using a lamellar precursor, the high variability in the Al distribution in its framework indicates that the conclusions about the framework Al distribution drawn for ZSM-5 can be supposed general for Si-rich zeolites.

Ferrierite, mordenite and the beta zeolite. Dramatic differences in the Al distribution were also observed with these zeolites structures for relatively high Al concentrations [Si/Al 12–15, see (Table 4-1)] (9a, 10a, 43b, 50). On the other hand, no variability in the Al distribution was observed for ferrierites with Si/Al >20 (7). All three ferrierite samples with Si/Al 20–30 exhibited

at least 95% single Al atoms. It should be pointed out that these differences depending on the Si/Al composition are, at least to some extent, connected with the synthesis procedure and composition of the synthesis mixture, as discussed in Chapter 6.

4.3. Close Al Atoms in Different Rings – Unpaired Al Atoms

Close Al atoms in different rings are defined as those close enough to accommodate a divalent $[Co(H_2O)_6]^{2+}$ complex, and located in different rings, but not in Al-O-Si-O-Al sequences. In contrast to well-defined Al-O-Si-O-Al and Al-O-$(Si-O)_2$-Al sequences in one ring, the distances and Al-O-$(Si-O)_n$-Al sequences in these close Al atoms are not known, and there is no direct method for their determination. This fact limits information on the population of these close framework Al atoms. So far, close Al atoms have been reported exclusively for ZSM-5, beta zeolite and MCM-22.

Beta zeolite. Close Al atoms in different rings were described for beta zeolites with Si/Al 12–16. One type of close Al atoms (close Al_I atoms) was reflected in the UV spectrum of the maximum $[Co(H_2O)_6]^{2+}$ exchanged and then dehydrated zeolite by a charge transfer (CT) band at 33 000 cm^{-1} (23b). This band was attributed to the Co peroxo, super-oxo and μ-oxo complexes. The extinction coefficient of the CT band of the Co species is at least 50 times higher than that of the d-d bands of bare Co^{2+} ions. Thus, the relatively high intensity of the CT bands corresponds to a low concentration of the related Co species, reflecting close Al_I atoms. Close Al_I atoms were observed only for some beta zeolites and their maximum concentration did not exceed 5% of total Al. Later, a significantly more populated type of close Al atoms (close Al_{II} atoms) was described (9a, 43b). This type of close Al atoms also accommodates $[Co(H_2O)_6]^{2+}$ complexes in the hydrated zeolite, but leads to Co-oxo species in dehydrated Co-samples, which cannot be recognized by any spectroscopic method. The presence of this so far spectroscopic silent Co-oxo species and thus of close Al_{II} atoms represents the difference between Co loading and the sum of the concentrations of the observed Co species (bare Co^{2+} and Co2+ balanced by Al_I atoms atoms) in the dehydrated zeolite. Location of close Al_{II} atoms at the intersection of the channels of BEA zeolites has been suggested. In contrast to close Al_I atoms, the close Al_{II} atoms accommodating spectroscopic silent Co species might represent a substantial fraction of Al atoms in the beta zeolite, at least 22% of framework Al atoms for Si/Al 12 and 16 (43b). In contrast to the latter Si/Al compositions, beta zeolites with Si/Al 12–13 exhibit a tendency towards dealumination yielding Si/Al_{FR} of 20–24, and the population of close Al_{II} atoms did not exceed 3% of the framework Al (23b).

ZSM-5. Only close Al atoms of the Al_I-type were reported for ZSM-5. Their population depends on the synthesis conditions, as follows from the presence

of Al_I-type close Al atoms only in the samples synthesized using tetraethyl orthosilicate and aluminum chloride or hydroxide (5b, 10b). Other type of syntheses did not yield these close Al_I-type atoms. These Al_I-type close Al atoms represent in ZSM-5 only a minority of the framework Al atoms (<4%). As follows from the low capacity of Al-rich ZSM-5 (Si/Al 8.5) for $[Co(H_2O)_6]^{2+}$ ions, the present Al-O-Si-O-Al sequences with Al atoms facing towards different channels do not form close Al_I atoms (5b, 10b).

MCM-22. Al_I-type close Al atoms are not present in MCM-22 or represent a minority depending on the synthesis conditions. Close Al_I–type atoms were not observed in MCM-22 prepared using aluminum nitrate for Si/Al 14; however, their concentration increased with increasing Si/Al and reached 4% of the total Al for Si/Al 38. In contrast, close Al_I-type atoms were not present in MCM-22 with Si/Al 17–40 prepared using aluminum sulfate (24).

4.4. 4-Al and 3-Al Atom Hyper-Structures

No method is available for direct demonstration of the presence of three or more close Al atoms in Si-rich zeolites. Si(1Si,3Al) atoms reflecting three Al atoms separated by one silicon were reported only for Al-rich zeolites as, e.g., faujasites. Thus, we can only speculate on the arrangement of more than two close Al atoms in Si-rich zeolites from the concentration and siting of Al-O-(Si-O)$_2$-Al sequences in one ring in zeolites with higher framework Al content or indirectly from catalytic results.

Ferrierite is the only zeolite with known Al atom hyper-structures. One unit cell of ferrierite contains 36 T atoms and one β-type 6-MR. In ferrierite with Si/Al equal to 8.5 and 52% of Al atoms in Al-O-(Si-O)$_2$-Al sequences in β-type rings, each β-type 6-MR contains an Al-O-(Si-O)$_2$-Al sequence (7, 46). For details on β-type 6-MR, see Par. 5.2. Two β-type 6-MRs each facing the ferrierite cavity and thus two Al-O-(Si-O)$_2$-Al sequences, each in one β-type 6-MR, form the 4-Al hyper-structure consisting of four Al atoms, as depicted in Fig. 2-4A. These four Al atoms mutually cooperate in the formation of two cationic sites for two corresponding divalent cations, if exchanged at these sites. In the case of ferrierite with Si/Al 10.5 and predominant single Al atoms, only 20% of the Al atoms are in Al-O-(Si-O)$_2$-Al sequences in the β-type 6-MRs (9a). Thus, the formation of 4-Al hyper-structures is not probable in this type of sample. Nevertheless, 4-Al hyper-structures are formed in this ferrierite in substantial amounts, as also follows from the high activity of these sites in N_2O decomposition over Fe-ferrierite (Si/Al 10.5). Two bare Fe^{2+} ions located in the 4-Al hyper-structure have been suggested as reaction centers (see Chapter 9.2) and N_2O decomposition might serve as a test reaction for 4-Al hyper-structures in ferrierites (46).

Formation of 4-Al hyper-structures consisting of two opposite 6-MRs is not possible in mordenite owing to its framework topology. In the beta zeolite

(Si/Al>12), the 4-Al (and 3-Al) hyper-structure is also excluded, due to the absence of Al-O-Si-O-Al sequences required for the hyper structure formation in the beta cage.

It has been suggested that the 3-Al hyper-structure with three Al atoms can also be present and that these Al atoms cooperate in zeolites (50, 51). This hyper-structure consists of an Al-O-$(Si\text{-}O)_2$-Al sequence in the 6-MR and the third Al atom is located on the opposite 6-MR of the zeolite channel (the main channel of ferrierite and sinusoidal channel in ZSM-5). For example, the Co^{2+} ions accommodated in one 6-MR of the hyper-structure, in a cooperation with the opposite protonic site balanced by a single Al atom in the opposite 6-MR (see Fig. 4-2B), act as centers for CH_4-SCR-NOx in ferrierite and ZSM-5; Ref. (52) and see Chapter 8.

On the other hand, we can speculate about the formation of 4-Al or 3-Al hyper-structures with four or three cooperating Al atoms in two opposite β-type 6-MRs of ZSM-5 or beta zeolite, as the framework topology does not exclude them. Such Al siting leading to hyper-structures can be accepted considering of the complexity of the synthesis process and diversity in its pathways.

5. STATE OF ART OF SITING OF FRAMEWORK Al ATOMS IN Si-RICH ZEOLITES

In spite of the increasing interest and numerous studies concerned with the aspect of the siting of Al atoms in the frameworks of Si-rich zeolites, some of these studies cannot be considered relevant. This is true of conclusions based exclusively on the application of calculation of the stabilization energy of Al atoms in the individual T sites not including the conditions of zeolite synthesis. Further, the interpretation of ^{27}Al MAS NMR experiments using the empirical Lippmaa correlation or omitting the presence of close Al atoms in the Al-O-$(Si\text{-}O)_2$-Al sequences in one or two neighboring rings, significantly affecting the ^{27}Al NMR resonances does not also satisfy the requirements for correct analysis of the siting and distribution of Al atoms in the framework, see Par. 3.2.2.

5.1. Al Atoms in the Framework T Sites

Ferrierite is the only zeolite for which the siting of Al atoms was completely accomplished by combining ^{27}Al and ^{29}Si MAS NMR and Vis spectroscopy of bare exchanged Co^{2+} ions, as probes for the Al-O-$(Si\text{-}O)_2$-Al sequences in one ring, and supported by quantum chemical calculations of the ^{27}Al isotropic chemical shifts of Al atoms in individual framework T sites (7). While ^{27}Al (3Q) MAS NMR is fully satisfactory for analysis of the siting of Al atoms in ferrierites containing exclusively single Al atoms, ^{29}Si MAS NMR enabled exclusion of the Al-O-Si-O-Al sequences in the ferrierite with Si/Al ≈ 9. The

characteristic d-d transitions of the Co^{2+} ions in cationic sites determined concentration Al-O-(Si-O)$_2$-Al sequences in 6-MRs. Quantum-chemical calculations showed that the Al atoms in the T1 site can exhibit two different geometries and thus the Al atom can occupy five different T sites in the ferrierite structure. The discrepancy with the X-ray data (only four T sites in ferrierite) (9b, 9d, 53) can be explained by the fact that the geometry of the T sites obtained by the diffraction patterns represents an average value reflecting mainly the geometry of the Si atoms. This can result in suppression of information on the geometry of the Al atoms. The ^{27}Al resonances observed with three Si-rich ferrierite samples (Si/Al >20) containing only single Al atoms are depicted in Fig. 5-1.

The T1$_a$ site is not occupied, while the T3 and T4 sites are occupied in all analyzed zeolites. The T1$_b$ and T2 sites are occupied in two samples. These observations provide clear evidence that the Al siting in the framework T sites is not random, and is thus not controlled by simple statistic rules or by the stabilization energy in the template-free zeolite framework. Quantitative analysis of the occupancy of the individual T sites by Al atoms (see Fig. 5-1C) shows that ferrierite with Al located predominantly in one T site can be prepared. For ferrierites with Si/Al 8.5 and 10.5 synthesized in the Na,K-form, Al(T1$_a$)-O-(Si-O)$_2$-Al(T1$_a$) and Al(T2)-O-(Si-O)$_2$-Al(T2) sequences in one 6-MR are present. The T1$_a$ site is not occupied and single Al atoms are located at the T2, T3 and T4 sites. The Al(T4)-O-(Si-O)$_2$-Al(T4) sequence in 6-MR is not present. It should be pointed out that, while the same T sites are occupied in both the analyzed ferrierites, there are significant differences in the concentrations of Al atoms at the individual T sites, cf. Fig. 5-1C. The variability of siting of the Al atoms with the synthesis conditions is in agreement with the results of Pinar et al. (11a, b) and Roman-Leshkov et al. (11c). They have reported different catalytic activities and distributions of the protonic sites in the ferrierite channel/cavity for zeolites synthesized using different amine bases as templates, for details, see Chapter 6. The results of calculations and the experiments clearly demonstrate a dramatic effect of the second Al atom in the Al-O-(Si-O)$_2$-Al sequences on the ^{27}Al isotropic shift, which is changed by up to 5.0 ppm. This is in agreement with the theoretical results on ZSM-5 and Si-rich chabasite (29c, d), see Fig. 5-2.

It should be born in mind that a single value of the ^{27}Al isotropic shift can correspond to Al atoms in two different T sites: the single Al atom at one T site and the Al atom at another T site belonging to the Al-O-(Si-O)$_2$-Al sequence. On the other hand, a single Al atom and the Al atom in the same T site, but belonging to the Al-O-(Si-O)$_2$-Al sequence, can exhibit significantly different chemical shifts. Thus, definite conclusions on the siting of the Al atoms in the individual T sites by using ^{27}Al MAS NMR can be performed only when analysis of Al-O-(Si-O)$_{1,2}$-Al sequences in one ring is performed. No conclusions

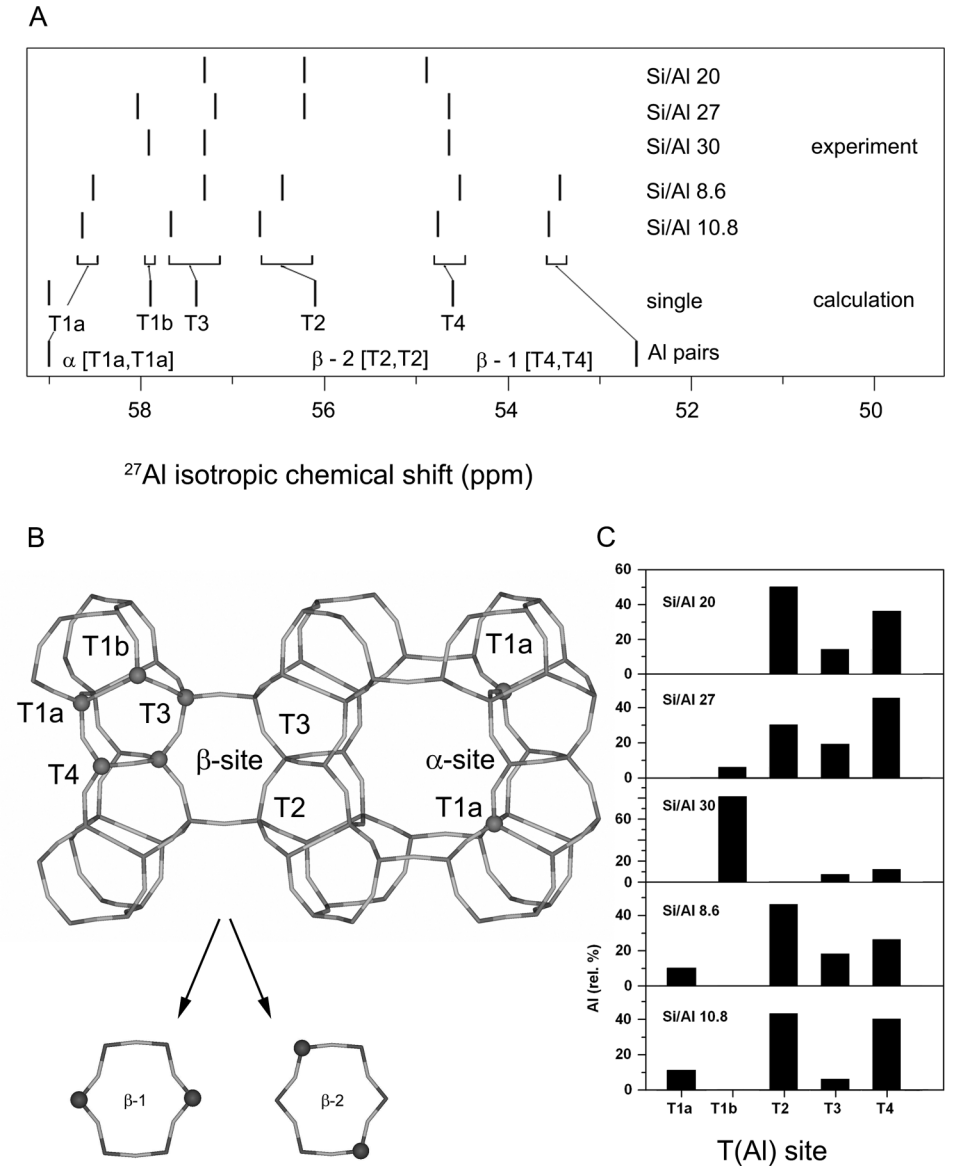

Figure 5-1: Al siting in ferrierite. (A) Notation of individual framework T sites and α- and β-type 6-MRs, (B) attribution of the observed ^{27}Al isotropic chemical shifts to those predicted for single Al atoms in the framework T sites and for Al atoms in the Al-O-(Si-O)$_2$-Al sequences in the α- and β-type 6-MRs, (C) and quantitative analysis of the Al siting in framework T sites. Adapted with permission from Ref (7). Copyright 2011 American Chemical Society.

can be drawn either on the identical or on different siting of the Al atoms in the absence of knowledge of the presence of Al-O-(Si-O)$_{1,2}$-Al sequences in the framework.

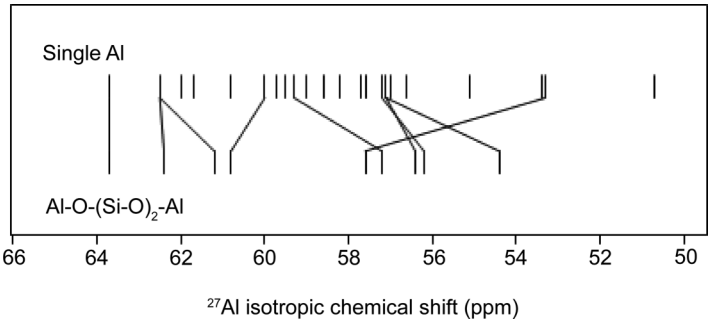

Figure 5-2: Effect of the vicinity of the second Al atom in the Al-O-(Si-O)$_2$-Al sequence on the ^{27}Al isotropic chemical shift in ZSM-5. Adapted with permission from Ref. (30c). Copyright 2009 American Chemical Society.

ZSM-22 and theta-1 are iso-structural TON topologies with the analyzed siting of Al atoms. Derewinski et al. reported different ^{27}Al (MQ) MAS NMR spectra for ZSM-22 (Si/Al 22) synthesized with 1-ethyl pyridinium bromide and theta-1 (Si/Al 77) prepared using diethanol amine as SDA (27a). Two resonances with isotropic chemical shifts at 55.1 and 57.6 ppm were observed with ZSM-22, while three resonances at 55.5, 57.6 and 58.7 ppm were reported for theta-1, indicating a non-random population of Al atoms among framework Td sites. The attribution of resonances to Al atoms in the T sites using the Lipmaa correlation (30) was recently refined by quantum chemical calculations of the AlO_4 geometries and ^{27}Al isotropic chemical shifts (29b). The splitting of T1 and T2 eight-fold sites (54) into two four-fold sites (T1$_a$ and T1$_b$, T2$_a$ and T2$_b$) was observed. Notation of T sites is given in Fig. 5-3. The resonance at 55.1–55.5 ppm corresponds to the Al atoms in the T4 sites, which predominate in both zeolites (55% Al in theta-1 and 60% in ZSM-22). The T4 site is located in the pockets at the wall of the channel and thus approx. 60% of the Al atoms are less accessible. The T1 (T1$_a$ and T1$_b$) sites are not occupied by

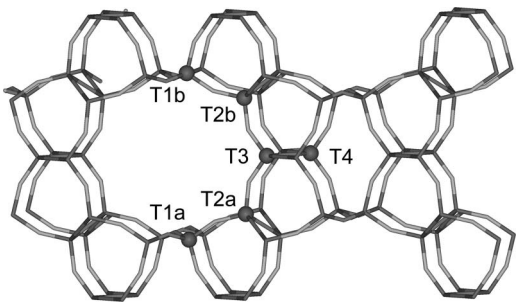

Figure 5-3: Notation of individual framework T sites in ZSM-22 and Theta-1 zeolites. According to Ref. (30b).

Al atoms. Resonance at 58.7 ppm reflecting 10% of the Al atoms in the theta-1 zeolite can be attributed to the T3 site, while the resonance at 57.6 ppm (35% in theta-1 and 40% in ZSM-22) could correspond to Al atoms in the $T2_a$ and $T2_b$ sites, for details see (29b).

ZSM-5. So far, the large number of framework T sites together with the low Al content and large unit cell size has represented an unsurpassable barrier for analysis of the Al siting in ZSM-5. However, the ^{27}Al 3Q MAS NMR study combined with theoretical calculations on a broad set of ZSM-5 zeolites with Si/Al 12.5–140 containing single Al atoms and the presence or absence of Al-O-(Si-O)$_2$-Al sequences in one ring, enabled significant conclusions to be drawn (4b, 8, 29c).

i. All 12 T sites split from the aspect of the AlO_4^- geometry and orthorhombic ZSM-5 exhibits 24 T sites available for Al atoms;

ii. Al siting in the ZSM-5 framework is neither random nor controlled by the stabilization energy of the Al atoms in the framework, but depends mainly on the conditions of the zeolite synthesis;

iii. From three to five T sites are occupied by Al atoms in the ZSM-5 sample;

iv. Seven resonances reported for ZSM-5 were attributed to the T(Al) sites. The remaining five resonances cannot be attributed to the T(Al) sites due to the high number of T(Al) sites with similar ^{27}Al isotropic shift values;

v. The presence of the second Al atom in the Al-O-(Si-O)$_{1,2}$-Al sequences can result in a significant change in the predicted ^{27}Al isotropic shift, by up to 5 ppm. This does not allow us to draw any conclusions on the Al siting in ZSM-5 with Al-O-(Si-O)$_2$-Al sequences, which occurs in ZSM-5 of Si/Al $<$20. For the observed resonances and their attribution to the T(Al) sites, and for quantitative analysis of the siting of Al atoms, see Fig. 5-4.

The above conclusions on the siting of framework Al atoms in ZSM-5 are supported by a number of additional experimental observations. The first successful attempt to monitor the siting of Al atoms in ZSM-5 was made by Sarv et al., who reported non-random Al distribution in the ZSM-5 framework based on a ^{27}Al (MQ) MAS NMR experiment (4a). The three reported resonances agree with those given above. Han et al. also suggested non-random Al distribution in ZSM-5; however, their conclusion is limited by the presence of SDA in the samples (5c). Olson et al. came to the same conclusion on the basis of the location of Cs^+ ions monitored by x-ray diffraction. They observed three types of Cs^+ ions with different site occupancy, one in the main channel and two in the sinusoidal channel (34a). A similar approach employing Tl^+ ions also led to the conclusion that the siting of framework Al atoms in ZSM-5 is

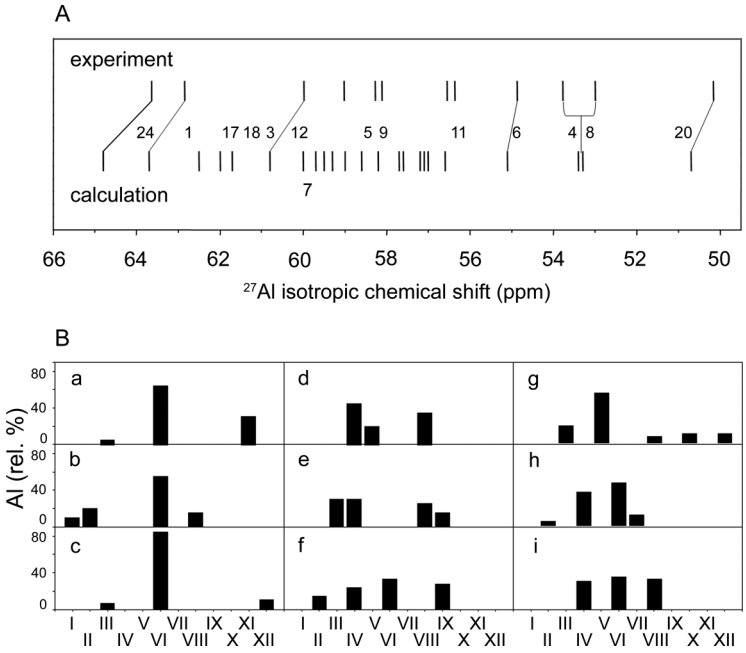

Figure 5-4: (A) Observed and predicted ^{27}Al isotropic chemical shifts in ZSM-5 with single Al atoms, (B) and the effect of synthesis conditions on Al siting. ZSM-5 synthesized using (a) TPA-OH, $Al(NO_3)_3$ and TEOS; (b) TPA-OH, Al-isopropoxide and TEOS; (c) TPA-OH, $AlCl_3$ and TEOS; (d) TPA-OH, $AlCl_3$, TEOS and Na_2CO_3; (e) TPA-Br, $Al(NO_3)_3$ and TEOS; commercial sample (f), TPA-OH, (g) $Al(NO_3)_3$ and (h) TEOS; and (i) TPA-OH, $AlCl_3$, TEOS and NaCl. Adapted according to Ref. (4b).

not random; nevertheless, 18 suggested crystallographic distinct positions represent a very excessive number, which could result from the interaction of Tl^+ ions with residues of SDA or its product, as indicated by the brownish color of the crystals (34b). Also Mentzen reported siting of monovalent cations in ZSM-5 clearly evidencing preferences in the Al siting in ZSM-5 (34c).

Beta zeolites (isomorphs A, B of BEA*) exhibit a complex ^{27}Al MAS NMR spectrum with three resonances at 55.0–56.5, 58.5–60.0 and 62.0 ppm in the tetrahedral Al region with Si/Al 9–215 (4c, 55). The resonance at 62 ppm was found only for high Si/Al > 60. The two resonances at about 56 and 59 ppm were also reported by others (43). These findings provide clear evidence for the variability of AlO_4 tetrahedra in beta zeolites and indicate non-random siting of the Al atoms. It can be speculated that three T sites are occupied by Al atoms at Si/Al > 60. However, exclusion of the Al-O-$(Si\text{-}O)_2$-Al sequences is necessary for correct ^{27}Al MAS NMR analysis. The framework of beta zeolites with Si/Al <20 is typically perturbed or partly dealuminated, and the defect vacant T site in the vicinity of the other T atom affects the ^{27}Al isotropic shift, as does the neighboring Al atom (see above).

MCM-22 exhibits two characteristic shapes of the ^{27}Al NMR spectra, the well-developed triplet of resonances at 50, 56 and 60 ppm or a band at 56 ppm with a shoulder close to 60 ppm (56). Kennedy et al. attributed these three resonances to location of Al atoms in three T sites. The presence of Al atoms in two T sites of MCM-22 was suggested by Kolodziejski et al., based on the ^{27}Al nutation experiment (57). However, the attribution of resonances to the distinct T(Al) sites in MCM-22 (Lippmaa's correlation and non-realistic AlO_4 geometries) should be reinterpreted.

ITQ-7. Corma's group suggested that 50% of the Al atoms in the framework of ITQ-7 are located in the T1 and T4 sites of the D4-MR units according to the calculated energy of Si-Al substitution in the presence of SDA and analysis of the OH vibration frequencies (33). Clear evidence was given for a non-random Al distribution in the zeolite framework, and the key role of the SDA in the siting of framework Al atoms.

The reported results for a number of structures of Si-rich zeolites obtained by numerous research groups provide unambiguous evidence that the siting of the Al atoms in the framework T sites is not random and is not controlled by simple rules or exclusively (or neither significantly) by the stabilization energy of the AlO_4 tetrahedra in the framework. Based on the synthesized zeolites prepared under different conditions and over a broad range of Si/Al compositions, with various types of organic SDA *versus* the presence of alkaline cations, the crucial role for the incorporation of Al atoms into the individual framework T sites is the nature of the cations, decisively influencing the processes of nucleation and crystallization. Dramatic differences can occur in the siting of the Al atoms as well as in the predominant occupation of one or more framework T sites by an Al atom. From three to five distinct T sites are occupied, but the number of T sites which could be occupied is significantly higher and is influenced by the synthesis procedure. The dramatic effect of the composition and reaction conditions during the hydrothermal synthesis on the resulting incorporation of Al atoms, their distribution among individual T sites and distribution with respect to the Al-O-(Si-O)$_2$-Al sequences and single Al atoms are described in Chapter 6.

5.2. Al-O-(Si-O)$_2$-Al Sequences in Zeolite Rings

Al-O-(Si-O)$_2$-Al sequences in one ring can be located in 6-MRs (or 8-MRs), and create sites for bare divalent cations. Analysis of the cationic sites containing Al-O-(Si-O)$_2$-Al was performed for mordenite, ferrierite, ZSM-5 and beta zeolites using Co^{2+} ions as probes (see Par. 3.1.3) and the notation of these cationic sites will be used to describe the location of the Al-O-(Si-O)$_2$-Al sequences in one ring. Three cationic sites of α-, β- and γ-types were suggested for mordenite, ferrierite, ZSM-5 and beta zeolites (Fig. 5-5) (6, 20, 23). For

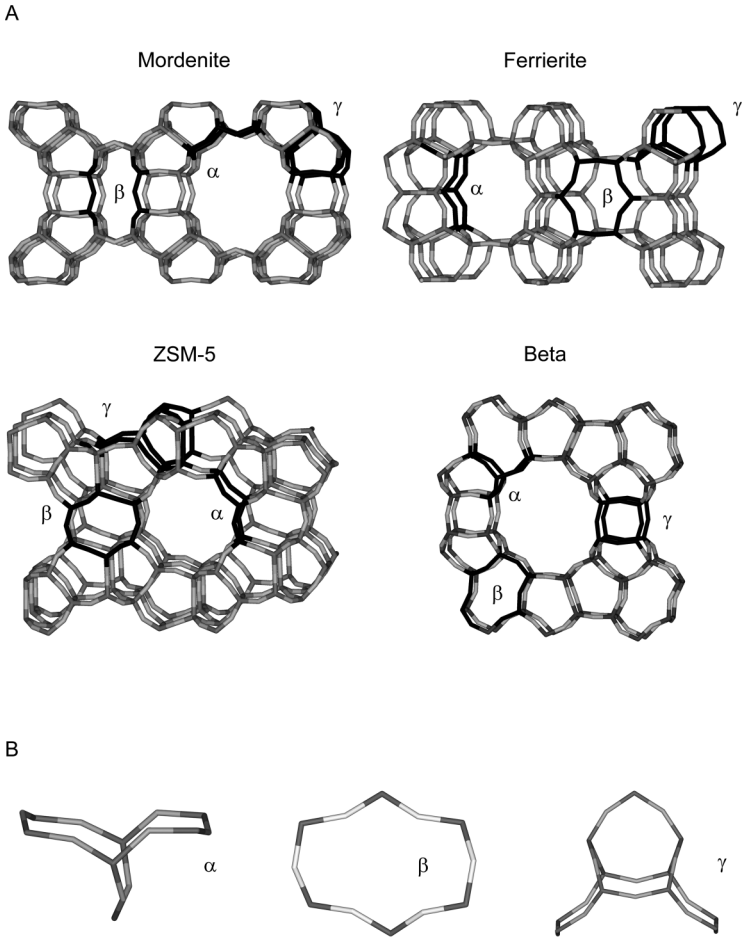

Figure 5-5: (A) The rings of the α-, β- and γ-type sites in the framework of mordenite, ferrierite, ZSM-5 and beta zeolites, and (B) detail of the α-type site in mordenite, β-type site in the beta zeolite, and γ-type site in ferrierite. According to Refs. (1, 6, 21, 24a, b).

mordenite, these sites correspond to the E, A, and C sites according to the Mortier notation (58).

The α-type 6-MR is twisted and composed of two 5-MRs and is located in the main channels of mordenite and ferrierite, in the sinusoidal channel of ZSM-5 and in the beta cage of the BEA framework. The twisted 8-MR of the mordenite pocket is arranged so as to form a planar β-type ring of six oxygen atoms. In ferrierite, a planar 6-MR of the β-type is located in the ferrierite cavity while, in ZSM-5 and beta zeolites, this planar 6-MR is located at the channel intersections of ZSM-5 and forms the beta cage in the beta zeolite. The γ-type site corresponds to a complex boat-shaped structure, composed of several 5- and 6-MRs. It is located in the mordenite pocket, in the ferrierite

cavity, in the sinusoidal channel of ZSM-5 and in the beta cage of the BEA structure. The location of the Al atoms of the Al-O-(Si-O)$_2$-Al sequence has not yet been elucidated in the γ-type rings. Most probably, the Al-O-(Si-O)$_2$-Al sequence is located in the twisted 8-MR of this site (6, 20, 23).

In ZSM-5, ferrierite, mordenite, and beta zeolites, depending on the conditions of hydrothermal synthesis, the Al-O-(Si-O)$_2$-Al sequences in the β-type 6-MR (8-MR in mordenite) predominate in these structural types and represent 60–85% of the Al-O-(Si-O)$_2$-Al sequences in these zeolites. The α-type 6-MR contains a significantly lower concentration of Al-O-(Si-O)$_2$-Al sequences, but with significant variability from 10 to 38% of the Al-O-(Si-O)$_2$-Al sequences. The concentration of the Al-O-(Si-O)$_2$-Al sequences in the γ-type rings is low and varies from 2–12% of the Al-O-(Si-O)$_2$-Al sequences (5b, 6, 9a, 10, 20, 23, 59). The distribution of the Al-O-(Si-O)$_2$-Al sequences among the α-, β- and γ-rings does not reflect the population of the corresponding rings in frameworks with different topologies. While two β-type 6-MRs correspond to one α-type 6-MR in ZSM-5, this relation is the opposite in ferrierite. Thus, it is suggested that the mechanism of synthesis and the synthesis composition and conditions control the distribution of the Al-O-(Si-O)$_2$-Al sequences in the individual rings of the cationic sites in Si-rich zeolites, for details see Chapter 6.

5.3. Al Atoms in the Zeolite Rings and the Channel/Cavity System

There is no straightforward relationship between the siting of the Al atoms in the framework T sites and the location of the Al atoms in the channels and cavities. Only the zeolites with channel walls formed by two layers of TO_4 tetrahedra (e.g., ZSM-5) yield Al atoms in the given channels. In zeolites with channel walls formed by one layer of TO_4 tetrahedra, the Al atom can belong to different channels. A similar situation occurs for Al atoms in the T sites and in framework rings. Accordingly, while the location of the counter ion in the channel (ring) unambiguously corresponds to the location of the Al atom in this channel (ring), location of the Al atom in a particular channel (ring) can result in the location of the counter ion (metal ion or proton) in different channels (rings). The location of the counter ions depends both on the siting of the Al atoms and on the energy and dynamics of the counter ions themselves. For the location of cationic sites in the mordenite, ferrierite, and ZSM-5 channel system see Fig. 5-6 (6, 20, 23).

Monovalent cations also indicate the location of the Al atoms in the individual framework rings and channels, to ensure charge balance. It follows from XRD analysis of the location of the Na^+ ions that the Al atoms are located in three characteristic 8-MRs occurring in mordenite; two of these rings are in the wall of the main channel and the third one is in the mordenite pocket (60). In ferrierite, XRD of Na-ferrierite showed that the Al atoms are located in two

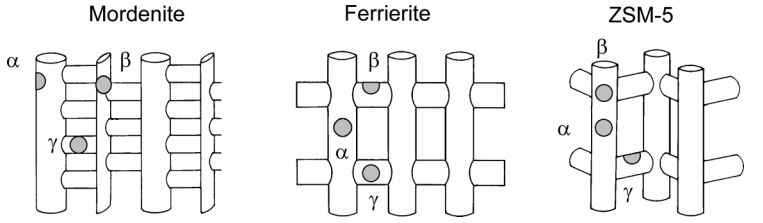

Figure 5-6: Location of the α-, β- and γ-type framework rings in the channel system of mordenite, ferrierite and ZSM-5. According to Refs. (6, 20, 23a, b).

8-MRs of the main channel (58). It should be stressed that the siting of the Al atoms obtained from the siting of the Na^+ ions is in full agreement with the more detailed analysis of the positions of the Al atoms at the individual T sites of ferrierite (7). With mordenite, the XRD results provide evidence that the Al atoms are located in the T sites of the eight rings (58). For ions with larger diameters, such as Cs^+ and Tl^+, their location is not strictly related to the siting of the Al atoms at the individual T sites because of their larger radius, see Par. 3.2.3. The position of the Cs^+ ion provides evidence only for the location of the Al atoms in the walls of the channels. Thus the location of the Cs^+ ions obtained by XRD for Cs-ZSM-5 indicates only Al atoms located in one T site of the main channels and two T sites are located in the sinusoidal channel (34a). Siting of Al atoms on the intersection of the main and sinusoidal channels results from location of Na^+, K^+, Rb^+ and Tl^+ in the ZSM-5 channel system according to the study of Mentzen et al. (34c). Moreover, siting of Al atoms in the T1 or T10, T4 or T7, and T10 was suggested using Li^+ ion as a probe monitored by neutron powder diffraction in this study. The discrepancies in the cation and Al siting in different crystallographic studies should reflect variability of Al siting in Si-rich zeolites, clearly evidenced by ^{27}Al MAS NMR studies.

6. CONTROL OF SITING AND DISTRIBUTION OF Al ATOMS IN THE FRAMEWORK BY ZEOLITE SYNTHESIS

This section does not constitute a comprehensive description and analysis of the processes of hydrothermal synthesis of Si-rich zeolites, reported in the literature and reviewed with regard to the function of organic and alkaline cations, nucleation and pre-crystallization processes of the crystal growth to nano-sized up to large single crystals (see, e.g., Ref. (61)). Broad general knowledge (particularly of the most studied synthesis of MFI topology) of the effect of the composition of the reaction mixtures, the presence of SDA and alkaline cations, and the synthesis conditions on the overall incorporation of Al atoms into the framework is extended here to the analysis and control of the

siting at the individual T sites and the distribution of framework Al atoms in the synthesis of Si-rich pentasil zeolites of MFI, FER and BEA topology. As already pointed out in Chapter 4 and thereafter in Chapters 8 and 9, the siting and distribution of framework Al atoms has naturally a decisive impact on the structure, location and void volume around the counter ion species, the catalytically active sites. Analysis of the Al siting and its distribution in the framework of synthesized zeolites, together with inspection of the local framework geometries and spatial arrangements of the framework rings given here provides deeper insight into the means of Al incorporation in the T sites facing individual zeolite pores, and the preferences for the location of Al pairs in specific framework rings, unpaired Al atoms in different rings and of the distant single Al atoms. The following parameters are of primary importance with regard to the location and structure of counter ion species and the related framework Al atoms:

i. the location of framework Al atoms at the T sites in the given rings, at the individual cationic sites and in the individual pores (for description see Par. 2.1). The siting of Al atoms in the 6- and 8-MRs (for MOR) of the α- and β-type rings, and in the complex ring (γ site) of cationic sites of Si-rich zeolites determines the local negative charge and framework environment available for the accommodation of counter ions (see Par. 5.2) The location of these rings on the walls of channels of different dimension provides accessibility and suitable geometry for reaction intermediates, and on the other hand, restrictions on the access of reactants, intermediates and products of catalytic reactions to rings containing Al atoms, and thus accommodating counter-ion species; and

ii. the distribution of framework Al atoms between Al pairs and single Al atoms (for definition see Chapter 2), the most populated Si-Al sequences, which govern the local density of the negative framework charge available for balancing the corresponding positive charges of protons or mono- and polyvalent cation complexes.

For decades, the apparent lack of intention in tuning the siting and distribution of Al atoms in the framework of Si-rich zeolites has been connected with the lack of analyses of the siting and distribution of framework Al atoms in these zeolites. Nevertheless, the ^{27}Al and ^{29}Si MAS NMR investigations of numerous samples of Si-rich zeolites of various Si/Al compositions and topologies, synthesized under various conditions in laboratories and produced by companies, indicated (4a, 5c, 27a, 29a, 33) and then unambiguously proved (4b, 4d, e, 5a, b, 7, 8, 10a, 11, 29a) that the siting and distribution of Al atoms in the framework is not random and is not controlled by statistical rules. This well-proven finding forms a base for controlling the siting and distribution of Al atoms in Si-rich zeolites by their hydrothermal synthesis.

6.1. Al Atoms in the Framework T Sites

The difficulty in placing Al atoms in the given framework T sites is consistent with the complexity and simultaneous diversity of the hydrothermal process itself corresponding to the high variability of the reactivity of reactant mixtures and conditions leading to nucleation and crystallization. This character of the synthesis is a consequence of that in all the individual steps, i.e., dissolution, nucleation and pre-crystallization. The slow progress in the field of targeted synthesis regarding the siting of Al atoms at selected T sites of Si-rich zeolites, has been also caused by the lack of complete analysis of the occupation of T sites by Al atoms. Al analysis has recently been accomplished for ferrierite by a combination of ^{27}Al MAS NMR experiments and DFT calculations (7). However, only 7 T(Al) sites have been established in the monoclinic ZSM-5 with a high number (24) of T sites (4b, 8). However, this analysis could be done only for ZSM-5 with low Al concentration, containing exclusively single Al atoms in the framework and thus the absence of close Al atoms, where the chemical shift of the Al atom is affected by the second close Al atom (29c).

First synthesis revealing the influence of a template on the siting of Al atoms in the framework was demonstrated on the isostructural theta-1 and ZSM-22 zeolites using as SDA 1-ethylpyridinium bromide and diethanolamine, respectively, and the ^{27}Al (2D) MAS NMR analysis (27a). Pioneering work in controlling the siting of the Al atoms in the T sites of the individual pores of ferrierite has been carried out in the research groups of Pinar (11a, b, 62) and Roman-Leshkov (11c). They tuned incorporation of Al atoms into the T sites of ferrierite by employing various organic bases in fluoride media in the complete absence of alkaline cations. The successful synthesis of ferrierites yielded structural OH groups prevailingly located in either the 10- or 8-MR channels (FER cavity), as detected by pyridine adsorbed on OH groups in 10-MR channels (referred to Al in the T1, T2 and T4 sites), while those in ferrierite cavity [(Al)T3 sites] were not accessible (11a, b, 62). The concentration of OH groups (at a comparable Si/Al in the product) in the 10-MR pores (T1, T2 and T4 sites) decreased in the following order when using the denoted templates: Na^+/pyrrolidine (Pyr) > tetramethylammonium (TMA)/benzylmethylpyridine > TMA/Pyr > Pyr (11a). Synthesis of ferrierite employing TMA/hexamethyleneimine (HMI) resulted in 27% of OH groups in the 8-MR channel of the FER cavity [T3(Al)], while 89 and 84% of the OH groups were located in the 8-MR FER cavity when Pyr and Pyr/TMA were used, respectively (11c). High differences in the constraint index of the synthesized ferrierites in carbonylation of dimethyl ether also corresponded to a quite different distribution of protonic sites between the 8- and 10-MR channels (63). Nevertheless, the synthesis of ferrierites (Si/Al 20–30) from alkaline media with Na^+ and K^+ ions presence also substantially changed the

concentration of Al atoms at different T sites depending on the reactant composition as indicated by the ^{27}Al MAS NMR/DFT analysis (7). These findings clearly show the dramatic effect of organic templates and Na^+ ions on the siting of Al atoms facing 10-MR and 8-MR channels of ferrierite. Although the effect of the SDA type on the location of framework Al atoms is evident, there is so far no explanation for it.

The most intriguing achievement in the synthesis of the T-site tailored directly to the zeolite application in a catalytic reaction has recently been reported by Boronat et al. (64). Based on theoretical calculations, they suggested the T3-O33 site of the mordenite pocket with 8-MR opening as the most suitable location of proton for the selective carbonylation of methanol or dimethyl ether (for details see Par. 9.1).

6.2. Distribution of Framework Al Atoms Between Al Pairs and Single Al Atoms

We reported the effect of the composition of the synthesis mixture on the populations of Al pairs and single Al atoms for the first time with ZSM-5 and MCM-22 frameworks (4d, 5b, 5d, 24). A decisive role of the reactivity of the mixture on the distribution of Al atoms in Si-rich zeolites generally has been thereafter revealed and demonstrated for MFI, FER and BEA topologies based on the analysis involving the use of various Si and Al sources with different reactivity, amorphous precipitated Si and Si-Al precursors of various degrees of networking, and the presence or absence of Na^+ ions next to the organic templates (10, 59). The broad ranges of populations of Al pairs and single Al atoms could be varied in a broad range of Si/Al compositions from 12 to 40 (or from 8 to 40 for FER) for the synthesized ZSM-5, ferrierite and the beta zeolites, which contained from 5 to 85% of the Al atoms in Al pairs (Al_{2Al}) and 15–95% of the single Al atoms (Al_{1Al}), as summarized in Table 6-1 and Refs. (10, 59, 65). Thus the preparation of frameworks of Si-rich zeolites with a broad distribution of Al atoms in Al pairs and as single Al atoms, and thus with different local negative charges, provide a platform for the variation of the density of protons and accommodation of counter ion complexes of various structures and locations. It is to be pointed out that the hydrothermal syntheses in these studies were carried out under mixing in autoclave rotation to maximize homogeneity of the zeolite products.

6.2.1. General Aspects of the Incorporation of Al Atoms into the Zeolite Framework

Owing to the complexity of the hydrothermal synthesis of Si-rich zeolites, there is no simple answer regarding the mechanism of formation of the structural units, their ordering and nuclearity in amorphous gels, and the crystal growth of various shapes and sizes (for review see, e.g., Refs (61b-i, 66).). As for

framework Al atoms, no investigations have been carried out regarding the distribution of Al atoms either in the nuclei of the amorphous phase, in the pre-crystallized gels or in the crystalline products. The attention has been focused, as far as we know, only to the degree of total Al incorporation as reviewed in Refs (61b, c). and references therein. Moreover, the nucleation and crystallization stages have mostly been studied for the Al-free silicalite-1 of MFI topology, with the exception of Ref. (5d) investigating early stages of ZSM-5 formation with a very low concentration of Al (Si/Al>38).

Small changes have been found in the enthalpy and entropy (several kcals (67),) and thus in free Gibbs energy for (Si)MFI formation. On the other hand, large changes have been recorded in the rate of nucleation and crystal growth of the zeolites depending on the synthesis conditions. The presence of aluminum can be supposed to change the energetic and kinetic contributions in formation of Al-containing zeolites. Owing to the high variability of the Si/Al in the products (Ref. (61c) and references therein) and the high variability in the framework Al distribution (5b, 10b) with the mixture compositions and synthesis conditions, the formation of Si-rich pentasil zeolites can be assumed to be controlled kinetically.

The use of different sources of Si and Al, and organic and alkaline cations for the synthesis of ZSM-5, ferrierite and beta zeolites indicated a general occurrence of the following Al-O-(Si-O)$_n$-Al sequences in the framework (for definition see Chapter 2):

i. Al pairs (Al_{2Al})in the Al-O-(Si-O)$_2$-Al sequences with two Al atoms in the ring of cationic sites,

ii. single Al atoms (Al_{1Al}) as the two most populated sequences in Si-rich zeolites,

iii. unpaired Al atoms (Al_{UNPAIR}) as two visible Al atoms in different rings in Al-O-(Si-O)$_{n\geq 2}$-Al sequence, present up to 3 rel.% Al in ZSM-5 and ferrierite, and exceptionally in the beta zeolite up to ca 25% of total Al,

iv. Al-O-Si-O-Al sequence, not present in Si-rich zeolites of usual Si/Al compositions.

The increasing electrostatic repulsion has to be considered with increasing Al concentration in both the formation and organization of an amorphous gel and the synthesized crystalline zeolite product. Under constant reactivity of the system, an increasing Al concentration would increase the population of Al pairs in the zeolite. However, this simple situation does not occur, and an increase in the population of Al pairs in various syntheses results in quite different trends in the Al distribution. The compositional and reaction conditions of the synthesis could change the order of formation of Al pairs and single

Al atoms and could even result in the completely opposite dependence of the population of Al pairs on the increasing Al concentrations (59).

The decisive role of the organic hydrophobic ions and small alkaline ions on the reactivity of the system in the formation of Si(Al)/TPA embryonic associates developed around the hydrophobic ions is generally accepted (68). The reactivity of the mixture, dynamic nucleation/dissolution, formation of the pre-crystallized units and their association during the crystal growth have been shown to depend on:

i. the large hydrophobic organic cations (TPA^+, TMA^+ etc.), which form an almost neutral environment around themselves and alkaline cations of small radius and high polarizability (Na^+), as the key parameters of the synthesis,

ii. pH and concentration of OH^- anions controlling the demineralization of the gel and related reactivity of the Si and Al components, providing highly reactive monomeric Si species and monomeric $Al(OH)_4^-$ *via* controlling the rate of dissolution of di- and polymeric species from the Na-silicate or from originally monomeric TEOS solutions, and the release of reactive small entities from the precipitated amorphous Si and Si-Al precursors with various degrees of Si-O-Si(Al) networking (65),

iii. the conditions of the synthesis (ageing, seeding, stirring, sequence of mixing) influencing the dynamic depolymerization/nucleation, reorganization of T-O-T bonds, formation of various rings and units in an amorphous phase in the pre-crystallization stage of the synthesis (10b).

6.2.2. Al Incorporation in the Assembly of Embryonic Units

Although opinions differ on the mechanism of the synthesis of Si-rich zeolites, there is straightforward evidence that the type of hydrophobic organic cations, presence of alkaline cations and the mineralizing effect of the OH^- groups play a decisive role on a degree of Al atom incorporation (61c), and on the recently revealed distribution of framework Al atoms between Al pairs and single Al atoms (5b, 10).

The pathway of nucleation in the mixtures containing TPA^+ and Na^+ ions in completely siliceous mixtures, the reorientation of T-O-T in an amorphous gel containing embryonic nuclei, and the first stages of crystallization have mostly been studied for silicalite-1. Chang and Bell elaborated the idea of Flanigen and Breck (69) on the nucleation of the synthesis gel around the TPA^+ cation, and provided a basic mechanism over Al-free (Si)MFI (68a). They suggested the rearrangement of Si-O-Si bonds around the TPA^+ ion replacing the surrounding water molecules (Fig. 6-1), while Na^+ ions were suggested to prefer attachment to the negatively charged $Si\text{-}O(OH)^-$ species. Van der Waals

interactions between the hydrophobic TPA^+ cation and the clathrate-like surrounding silicate species have been indicated at the first nucleation stage by the ^1H-^{29}Si CP MAS NMR (70) measurements, appearing well before the first long-range (XRD/IR) ordering, i.e., before the development of nuclei containing approx. 4–5 unit cells. The replacement of water molecules by Si-O species and re-orientation of Si-O-Si bonds around the TPA^+ cations to a suitable geometry of locally ordered regions (68a), formation of building units of dimeric and trimeric TPA surroundings (71) and/or crystalline nano-slabs during the pre-crystallization stage have been suggested on the basis of the results of ^{29}Si

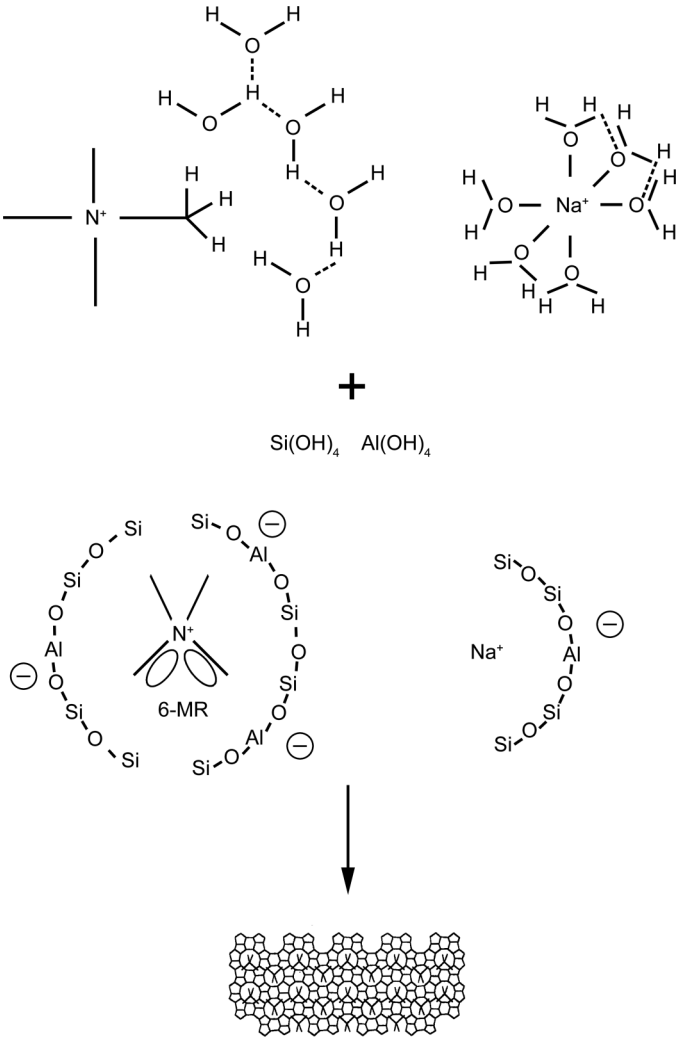

Figure 6-1: Illustration of the first stages of the synthesis of ZSM-5.

MAS NMR, FTIR of Si-O vibrations, the Raman spectra of Si-O species and in-situ X-ray scattering (72). In accordance with the mechanism suggested for the formation of embryonic Si-O nuclei around the TPA^+ ion (72d), the effective Si-H and Al-H distances measured by ^{29}Si-^{1}H and ^{27}Al-^{1}H rotational echo double resonance reflected the interaction of TPA^+ ion and its close surrounding containing Si and also Al atoms (5d).

The organic cation is assumed to have namely template function, and prefers a neutral environment on the contrary to alkaline cations of small diameter highly polarizing the Si-O surrounding. The attachment of the embryonic nuclei containing TPA^+ to the growing crystal or a mechanism that anticipates the nanoslab concept for crystal growth, or simple attachment of TPA^+ to the Si-O rings of the growing silicalite-1 crystals have been suggested (61c). The assembly process followed on a nano-scale showed that the smallest detected TPA-MFI units have the shape of nano-slabs with dimensions of $4.0 \times 4.0 \times 1.3$ nm, and then particles with a size of 2–3 nm are formed prevailingly over aggregates with a size of 5–10 nm (68c, 72f, 73). The double 5-MRs, which were originally assumed to be building blocks for the MFI structure, were not found in the amorphous gel, but appeared only in the crystallization stage (72f, 74). It is generally anticipated that Si-O in the form of dimers, trimers, and 4-, 5- 6-MRs, beside more complex rings are present in the amorphous gel. Pelster et al. has reported analysis of the early stages of nucleation and pre-crystallization at the synthesis of silicalite-1 by means of electron spray ionization mass spectrometry (ESI-MS) of the gels and dynamic light scattering (DLS) (75). A spectrum of silicate species, among them $Si_{32}O_{69}H_9^-$, prismatic hexamers and cubic octamers was observed. The increase in smaller silicate species (with prevailing prismatic hexamer) with the reaction time indicated high dynamics of the dissolution/nucleation process in the gel. Nevertheless, the occurrence of certain species in the gel cannot be directly connected with their participation in the process of crystal building and the way of Al incorporation.

The possible control of the distribution of Al atoms in the framework is demonstrated on the model synthesis of ZSM-5 carried out in dependence on the reactant composition and considering the above parameters given previously in Par. 6.2.1. The mutual reactivity of the reactants and especially the presence of TPA^+ *vs.* TPA^+/Na^+ ions and di- and polymeric Na-silicate *vs.* monomeric TEOS affect both the degree of Al incorporation into the silicate framework and the distribution of framework Al atoms between Al pairs (Al_{2Al}) and single Al atoms (Al_{1Al}), as described in detail in Ref (59). and illustrated for selected typical synthesis compositions in Table 6-2.

The high reactivity of Si source, of the typically monomeric TEOS, Si precursors of low degree of networking, and conditions dissolving fast polymeric Na-silicate yield a high degree of Al incorporation and high population of single Al atoms (65). The Na^+ ions next to TPA^+ also cause a significant increase in the degree of Al incorporation and an increase in the population of single Al

Table 6-2: Synthesis of ZSM-5 of various distribution of framework Al atoms depending on the synthesis gel composition. According to Refs. (10b, 59).

Gel	Si/Al_{gel}	Si/Al_{prod}	Al_{2Al} (%)	Al_{1Al} (%)	Al_{UNPAIR} (%)	Al_{2Al} in α (%)	Al_{2Al} in β (%)	Al_{2Al} in γ (%)	State of solutions
$Al(NO_3)_3$+TEOS	30	27	6	94	0		N.A.		Clear
$Al(OH)_3$+TEOS	22	43	37	62	1	22	72	6	2-Phase Gel
$AlCl_3$+TEOS	30	21	40	58	2	28	60	3	Sol - cond. Particles
$AlCl_3$+TEOS+NaCl	30	23	15	84	1	13	78	9	Sol - particles
$AlCl_3$+TEOS+NaOH	30	22	46	54	0	17	72	11	2-Phase Gel - Particles
$Al(NO_3)_3$+Na-SIL	30	14.5	8	92	0		N.A.		Low density gel
$AlCl_3$+Na-SIL	30	16.5	4	96	0		N.A.		Low density gel

Al_{1Al}—single Al atoms, Al_{2Al}—Al in Al-O-$(Si\text{-}O)_2$-Al in one ring, Al_{UNPAIR}—unpaired Al atoms accommodating $(Co^{2+}(H_2O)_6)^{2+}$.

atoms at the expense of Al pairs. This finding can be connected with stabilization of monomeric $Al(OH)_4^-$ in the vicinity of Na^+ ions of high polarizability. Beside that the Na^+ ions polarize the Si-O surrounding of the TPA^+ ions resulting in the increasing incorporation of Al atoms and relative concentration of single Al atoms in the 6-MRs of the clathrate-like environment. The important features are differences in composition of the starting mixtures resulting in the homogeneity or heterogeneity of solutions before their heating up for crystallization stage. The greater heterogeneity of mixtures results finally in higher population of Al pairs and *vice versa* rather homogeneous up to clear solutions lead to higher population of single Al atoms in the zeolite products (10a, 59).

Inspection of the MFI framework structure shows the occurrence of the four β-, two α- and two γ-type 6-MRs per unit cell. The composition of Si/TPA ∼ 4 (optimum for the MFI structure development (68a)) indicates four TPA^+ ions per unit cell, and therefore around one TPA^+ ion there are two 6-MRs (β-type), on the opposite side of the nitrogen atom, assembled inside a clathrate arrangement of T-O bonds forming the intersection of the straight and sinusoidal channels (see Fig. 6-2) (76). Another 6-MR is located in the wall of the straight channel (α-type); the packed boat-shaped site (γ-type) also contains a 6-MR, however combined with 5-MRs. Thus, two main types of 6-MRs [the α- and β-type, predominantly occupied by Al pairs (cf. Table 6-2)] are clearly present and each is available for accommodation of Al pair, single Al atom or only Si atoms.

The observed population of Al pairs in the rings of the cationic sites of ZSM-5 zeolites (the predominant accommodation of Al pairs in the β-sites) ranges with increasing, but still low, Al concentrations between 90–60% at the β-rings, 10–40% at the α-rings and 2–12% at the γ-rings. For a high Al concentration (Si/Al ∼ 12), the Al pairs attain values of 66% at the β-rings and 33% at the

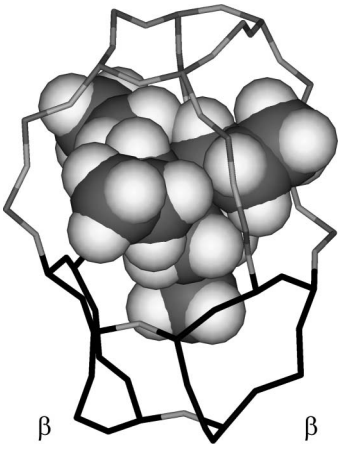

Figure 6-2: TPA-OH in the surrounding rings of ZSM-5. According to Ref. (76).

α-rings, see Table 6.1 (4d, 5a, b, 10b, 59). However, the spatial distribution of Al pairs cannot be simply connected with the occurrence of the individual rings in the MFI topology, as its unit cell contains two α-, four β- and two γ-type 6-MRs (see Fig. 5-5). This real population of Al pairs in the rings of the cationic sites, particularly of the most populated β-type rings, cannot be governed by the minimum potential energy of one of the rings, nor is it connected with the reaction kinetics of nucleation and crystallization, but depends on the location of the templating organic TPA^+ ion at the channel intersection in the structural embryonic units developing around the hydrophobic cations in the pre-crystallized stage. Thus the most populated β-type 6-MRs accommodated by Al pairs follows the "templated" geometry of the intersecting pores of MFI topology (see Fig. 6-2).

The electrostatic and van der Waals interactions of Na^+ and TPA^+ ions, respectively, within the mixtures containing Si and Al prefer the nucleation of small nuclei of negatively charged Si-O-Si(Al) around the Na^+ ion, while larger neutral Si-O-Si nuclei grow up around the large hydrophobic organic cation (61c). The preferences for the formation of Al pairs (predominantly identified in the β-type 6-MRs) in mixtures containing exclusively TPA^+ ions (Table 6-2 and Refs. (5b, 10b, 59)), in contrast to those containing both TPA^+ and Na^+ ions, yielding a higher relative population of single Al atoms, provides evidence that the Al pairs are predominantly located within the β-type 6-MRs in the Si-Al environment formed around TPA^+ (see Fig. 6-2). The incorporation of Al atoms, as revealed in Ref. (59), already in the TPA^+ ion embryonic unit containing 33–36 T sites has been supported by ^{27}Al, ^{29}Si and ^{1}H MAS NMR investigations (5d). The small radius and high polarization ability of the present Na^+ ions affects the whole system. The Na^+ ions strongly polarize the Si-O-Si groups (chains, rings) in the vicinity of TPA^+, which thus also accept single Al atoms, entering the 6-MRs in the clathrate-like TPA^+ surroundings. With an increasing concentration of Al in the initial gel and also with a increasing TPA^+/Na^+ molar ratio, the population of Al atoms in the Al pairs increases (5b, 10b, 59). The MFI topology indicates that the intersection of the channels (~9 Å diameter) contains a complex of rings containing 10-MRs at the openings of the straight and sinusoidal channels, and the two β-type 6-MRs. These 6-MRs bear some negatively charged species, either single AlO_4^- or an Al-O-(Si-O)$_2$-Al sequence. As indicated from the dependence of the population of Al pairs in the presence of TPA^+ ions (10b, 59), and as single AlO_4^- are advantageously embedded in rings attached to Na^+ ions, the 6-MRs with Al pairs are predominantly formed around the TPA^+ ion. The way of the organization of Al pairs in 6-MRs close to the nitrogen of TPA^+ ion in the opposite side cannot be at present suggested. We only can state that if Na^+ ions are not present in the mixture, a substantially higher population of Al pairs in 6-MRs is achieved, limiting to a value of 85% of the Al atoms in the β-type 6-MRs. Nevertheless, it is clear that the Al pairs or single Al atoms are incorporated in the very

initial stage of formation of first Si-O nuclei around the TPA^+ or Na^+ ions in an amorphous gel.

In addition to the occurrence of Al pairs predominating in the β-type 6-MRs, both the Al pairs and single Al atoms occur in the α-type 6-MRs in the wall of the zig-zag channel of the ZSM-5 structure. The maximum population of the α-type 6-MRs by Al pairs (∼40%) is achieved with mixtures containing only TPA^+ ions or their excess and by using highly monomeric TEOS (10b, 59).

The pH of the initial solutions and the mixtures affect the equilibrium among various silicate and aluminosilicate mono-, di- and polymeric species owing to the competition of hydrolysis and condensation reactions. Thus, both the Si sources (TEOS and Na-silicate) affect the equilibrium among monomeric, oligomeric and polymeric species of silicates and aluminosilicates (Table 6-2). The mutual "interaction" of TPA^+ and Na^+ ions and their Si-O-Si(Al) surroundings is also reflected in the dissolution/nucleation processes to such a degree that the state of the mixtures is visible to the naked eye (see Table 6-2) (59). The high positive charge of the Na^+ ions keeps the monomeric aluminate species stable and strongly polarizes the Si-O groups. These accordingly tend to accept AlO_4^- monomeric entities, resulting in the observed preferential formation of single Al atoms and an enhanced overall degree of incorporation of Al atoms in the presence of Na^+ ions. In contrast, the dynamic dissolution/nucleation of silicate and aluminosilicate species is shifted in TPA-containing solutions (rather than in Na-solutions) to more dense solutions with the formation of larger nuclei or particles. The hydrophobic TPA^+ ions surrounded by Si-O stabilize neutral Si-O units which increase in size, enabling the formation of Si-rich zeolites with very high Si/Al ratios (up to ∞) (61c), in contrast to solutions containing Na^+ ions. The TPA^+ ions attract larger polymeric "neutral" Si-O species, which do not exhibit a tendency to incorporate single AlO_4^- entities, but rather Al pairs located thereof in 6-MRs. The larger nuclei and the particles present in more dense mixtures also exhibit the "seeding" effect, leading to small regular crystallites, in contrast to the larger crystals with non-uniform size obtained from clear or less dense solutions (10b, 59). The results can be summarized as follows:

i. Both the lower tendency for the incorporation of Al atoms into the silicate framework and the higher population of Al pairs are achieved in the synthesis using TPA^+ without Na^+ ions, with various Si and Al sources, and Si and Si-Al precursors of high degree of networking. Depending on pH, these mixtures begin the crystallization from rather heterogeneous sols with condensed nuclei and/or presence of small particles;

ii. A higher tendency for the incorporation of Al atoms and simultaneously of single Al atoms is found with monomeric Si sources (TEOS, Si and Si-Al

precursors of low degree of networking or condensed Na-silicate under conditions of fast depolymerization) and the presence of Na^+ ions. The Na^+ ions stabilize monomeric $Al(OH)_4^-$ entities, and the monomeric Si species are reflected in the formation of low-density and readily depolymerized mixtures. The syntheses under these compositions start from clear solutions or low-density gels.

iii. The incorporation of Al atoms prevailingly as Al pairs or single Al atoms, affected by the TPA^+/Na^+ ions and the reactivity of the mixtures, is also connected with the formation of relatively large and small crystals. This raises a question if larger crystals compared to smaller ones of the same chemical composition might exhibit a quite different distribution of framework Al atoms.

The relationship between the tendency of Na^+ ions to form visually clear solutions presumably consisting of nano-sized nuclei or low-density gels and the readiness to incorporate Al atoms into the silicate framework are in agreement with general knowledge on the synthesis of Si-rich zeolites in the presence of Na^+ ions (61d).

By relating the increasing tendency towards incorporation of Al atoms into the framework predominantly in a form of single Al atoms, and the decreasing tendency towards building up of Al atoms with the preferred occurrence of Al pairs for most synthesis compositions, we suggest that single Al atoms surrounded by Si atoms in at least a next-next-next coordination shell to an Al atom constitute energetically and kinetically the most favorable Si-Al organization in the framework. This condition is satisfied preferentially in clear solutions and low-density gels, where monomeric-like Si species are present, and Al species are charge balanced by Na^+ ions.

7. STABILITY OF THE Al ATOMS IN THE ZEOLITE FRAMEWORK

The isomorphous substitution of the Al atom into the Td-coordinated silicate framework can be regarded as a perturbation of the T-O-T bonds owing to the longer Al-O bonds in AlO_4 tetrahedra compared to the SiO_4 tetrahedra. This perturbation is largest when AlO_4^- is charge-balanced by a proton, and mostly or completely suppressed by the presence of monovalent or divalent counter cations (10a, 29a, 39b, 42b).

Accordingly, the high-temperature treatment of Si-rich eolites in an H-form, in contrast to metal-zeolites, results in substantial perturbation of the AlO_4 site, which can lead to the opening of the Al-O bond during zeolite dehydroxylation. If the dehydroxylation is reversible, "framework" electron-acceptor Al_{FR}-Lewis sites are considered to be formed, while the irreversible

effect is connected with complete release of the Al atom from the framework T site, i.e., zeolite dealumination, see, e.g., Refs. (14, 39b, 42b, 77).

7.1. Perturbation of the Framework Al-O Bonds

Opening of the Al-O bond of the framework AlO_4 tetrahedra of H-zeolites and formation of the framework electron-acceptor Al_{FR}-Lewis site under zeolite dehydration is well known for the beta zeolites (4c, 29a, 42b, 77a, b), but also occurs to a lesser extent in ferrierite and ZSM-5 (39b, 78). The tendency towards perturbation of the AlO_4 tetrahedra depends on the stability of the Al-O bonds in the framework, which is given by the stabilization energy of the Al atom, the nature of the counter ion, and the severity of zeolite treatment.

Perturbation of the AlO_4^- tetrahedra reflected in the formation of the framework Al_{FR}-Lewis sites in ZSM-5 depends on the siting of single Al atoms in the framework. Only two T sites (with ^{27}Al isotropic shifts of 52.7 and 57.1 ppm) lead to the formation of Al_{FR}-Lewis sites, while Al in the other T sites and the presence of Al-O-(Si-O)$_2$-Al sequences in one ring did not contribute to the formation of Al_{FR}-Lewis sites. As the Al-O-Si-O-Al sequences were not present in the ZSM-5 samples (Si/Al $>$ 12), they could also not be related to the formation of these Al_{FR}-Lewis sites (79). These findings imply the stabilizing effect of Al-O-(Si-O)$_2$-Al sequences in one ring on the Al atoms. The stabilization energies of Al atoms in the individual T sites in a number of zeolites have already been reported, see, e.g., Refs. (32b, c). However, these stabilization energies calculated as single Al atoms cannot be simply correlated with the stability of Al atoms in the framework. The energy of the perturbed AlO_4 sites as well as that of Al atoms of the Al-O-(Si-O)$_2$-Al sequences in one ring must be included in the analysis of the stability of Al atoms in the framework.

7.2. Release of the Al Atoms from the Framework

The dealumination of the framework, occasionally occurring during the removal of the organic template from the as-synthesized zeolite or by its severe post-synthesis treatment, provides evidence for the presence of the least stable Al atoms in the framework. In the H-beta zeolite, dealumination is connected with specific single Al atoms (isotropic chemical shift 58.7–60.1 ppm) (4c, 55), which are preferentially released from the framework, while the Al atoms in Al-O-(Si-O)$_2$-Al sequences in 6-MR remained unperturbed (43). The contra-intuitive higher stability of Al in these Al pairs compared to the single Al atoms is in agreement with the similar resistance of Al-O-(Si-O)$_2$-Al sequences in ZSM-5 to the formation of Al_{FR}-Lewis sites. In contrast, low framework stability can be attributed to the Al atoms in the Al-O-Si-O-Al sequences in

mordenite. Their ready removal was observed for mordenite with Si/Al 6.5, similar to faujasites containing these sequences (80).

8. LOCATION, STRUCTURE AND PROPERTIES OF COUNTER ION SPECIES

8.1. Counter Protonic Sites. Framework SiOHAl Groups

The balance of the framework negative charge, originating from the individual T(Al) atoms, by protons results in the formation of structural bridging SiOHAl groups. The substantial difference in the acid strength between Al- and Si-rich zeolites is attributed to the mutual interactions of SiOHAl groups in Al-rich zeolites. This suggestion is confirmed by the calculated similar deprotonation energies of OH groups in the siliceous faujasite, ZSM-5, mordenite and ferrierite, and by the increase in the acid strength of the Al-rich zeolites like of faujasites after their dealumination. The variability in the local geometry of the AlO_4 tetrahedra reflected in the Al-O-Si angle does not significantly affect the strength of the bridging protonic sites, as is also indicated by the close deprotonation energies of protons in the Si-rich zeolites. The effect of the vicinity of the Al atoms in the Al-O-(Si-O)$_2$-Al sequence on the strength of the acid site can also be suggested to be negligible, as there is no difference in the properties of adsorbed H_2 (77 K) in ZSM-5 between the protonic sites adjacent to single Al atoms and Al-O-(Si-O)$_2$-Al sequences (81). The observed variability in the OH vibrations and ^{1}H NMR shifts of the bridging hydroxyls in the Si-rich zeolites could be connected with the different locations of the protonic sites in different pores and thus different local arrangements around the AlO_4 tetrahedra and the curvature of the zeolite channel/cavity.

8.2. Counter Metal Ion Species

In general, zeolite framework oxygen atoms neighboring the isomorpously substituted Al atom in the framework represent negatively charged ligands to counter–metal ion species exhibiting open coordination spheres (82). The individual framework rings bearing the Al atom(s) and their spatial distribution through the three-dimensional zeolite network determine the structure and coordination of the counter ion species and their corresponding spatial arrangement. While, with Al-rich zeolites (Si/Al 1–3), the high local density of the framework Al atoms provides for stabilization of up to trivalent bare cations, the Si-rich zeolites (Si/Al > 8) contain the highly predominant Al-O-(Si-O)$_2$-Al sequences in both 6-MRs or distant single Al atoms (4d, 5a, b, 9a), whose population governs the stabilization of divalent or monovalent

cation complexes. These complexes could correspond to bare cations as well as polyvalent cation-oxo complexes.

The formal ion-exchange capacity refers to the framework Al content; nevertheless, the real capacity for divalent cation exchange in Si-rich zeolites depends on the distribution of the Al atoms in the framework. In dehydrated zeolites, only rings with Al pairs accommodate bare divalent cations, while single Al atoms can be exclusively balanced by the monovalent cations (or protons) and formally monovalent complexes. Therefore, the structure of the resulting metal-ion species is determined by both these factors, the distribution of Al atoms in the framework and the metal-ion complexes formed during the ion exchange; for illustration see Fig. 8-1.

Evidence has been found for quite well-described species in metallo-zeolites, including bare divalent cations, charged metal-ligand complexes or metal-oxo species, including metal-oxo bridged species, depending on the conditions of their incorporation and calcination, see, e.g., (83). The majority of the enormous volume of literature data analyzing the structure of metal-ion species by various spectral and diffraction methods deals with the Si/Al ratio of the parent zeolite and the M(II)/Al composition of the product. Nonetheless, information on the Al distribution is mostly absent (see, e.g., (42a, 83j, k, 84)), and the possible occurrence of Al atoms in Al pairs and single Al atoms has been a subject of speculation, however, without any experimental analysis. The broad spectrum of metal-ion species (analyzed for Cu, Co and Fe species) and the diversity of the results did not provide straightforward elucidation of the structure of metallo-zeolites.

The first attempt to explain the structure of the anticipated metal-oxo bridged Fe species in ZSM-5 was based on a simplified concept assuming

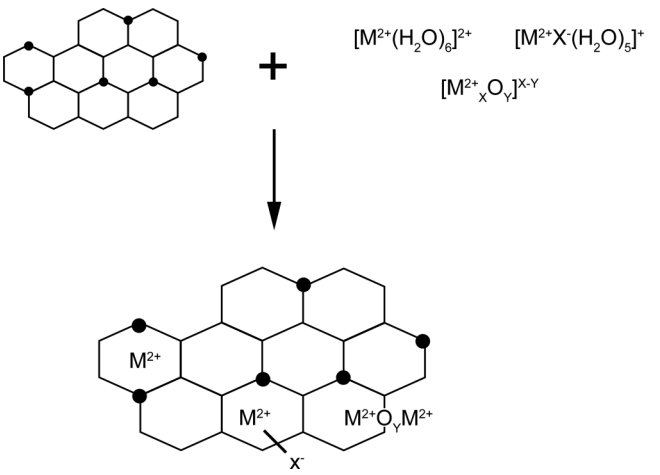

Figure 8-1: Schematic representation of the relation of Al distribution and ion exchange.

statistical distribution of the Al atoms in the framework with pre-defined metal-oxygen-metal distances through the zeolite structure (85). Other authors proposed models predicting an ion exchange capacity for the individual Fe ion species in a zeolite with a given Si/Al composition (86). However, the hypothesis related to the statistical distribution of Al atoms is generally not valid. Taking into account the real nature of the framework Al distribution in Si-rich zeolites, and the possibility of manipulating it in a broad range by hydrothermal synthesis, these predictions must be basically revised. Thus, evaluation of the capacity of the zeolite for coordination of the individual metal-ion species and their proportions must necessarily include analysis and determination of the distribution of the Al atoms in the framework.

Under the conditions of this complete analysis of both framework Al atoms and metal ions species, a clear preference has been shown at low metal concentrations for occupation of the cationic sites containing Al pairs by divalent cations, resulting in the coordination of bare cations at three typical sites (α-, β- and γ-types; for details see Pars. 5.3 and 8.2.3.1), with preferences for their occupation. The general trend with increasing metal content includes the formation of metal-oxo species, mostly adjacent to the rings containing single Al atoms. A special case consists in the presence of various metal-oxo bridges (see below) requiring optimum separation of two rings with one local negative charge (single Al atom). At high loadings (and high-temperature treatment), undefined metal oxide species also appear.

This widely accepted sequence of metal-ion species in metallo-zeolites with an increase in the metal content could not be regarded as corresponding to the statistical distribution of bare cations, metal-oxo, including metal-oxo bridged, and neutral metal oxide species; to the contrary, their occurrence is very strongly modified by the distribution of Al atoms in the zeolite framework (9a, 43, 50, 87). Thus, the structure of metal ion species is not exclusively controlled by the Si/Al ratio of the parent zeolite, as is frequently assumed in the literature, but by the distribution of framework Al atoms for a given parent zeolite.

All this implies that knowledge of the highly predominant Al atom distribution over the framework between the Al pairs and single Al atoms and their siting in the individual rings, as well as the spatial location of these rings in the crystalline network, has opened the way to a comprehensive description of metallo-zeolites as poly-ligand framework - metal ion - extra-framework ligand complexes, see Fig. 8-2.

8.2.1. Bonding of Metal Ions

The siting and distribution of monovalent cations is given by the siting of Al atoms in combination with the restrictions on pore opening and ring size. Note that the accommodation of bare cations was reported for at least 6-MRs

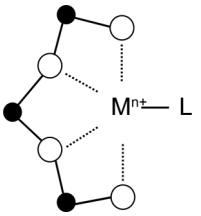

Figure 8-2: Schematic representation of the poly-ligand field of a cation in the zeolite.

(58, 60, 84a, 88). Di- and polyvalent cations require a specific arrangement of the framework Al atoms in Al pairs in the zeolite rings. Al pairs [Al-O-(Si-O)$_2$-Al sequences] in one ring and single Al atoms represent decisive local charges of the framework rings for the coordination of bare divalent ions or various metal-oxo complexes:

i. Bare divalent cations balanced by an Al pair in a 6-MR in the dehydrated zeolites;

ii. Two cooperating divalent metal ions in the 4-Al hyper-structure of two Al-O-(Si-O)$_2$-Al sequences, each located in the 6-MR situated on the opposite side of the channel/cavity (for both MFI and FER topologies; for definition see Par. 2.2.5 and Fig. 2-4A). The 3-Al hyper-structure is necessary for the cooperation of a divalent cation with a protonic site;

iii. A hexaquo divalent metal-ion complex in hydrated zeolites requires charge balance by two close Al atoms. This represents the sum of the Al pairs in 6-MRs and Al-O-(Si-O)$_{n\geq 2}$-Al in different rings (Al_{UNPAIR}) situated close enough (short visible distance) to charge-balance the divalent aquo complexes;

iv. Two close monovalent complexes balanced by two close Al atoms, i.e., those in a 6-MR and/or Al-O-(Si-O)$_{\geq 2}$-Al, in different rings establish conditions for the formation of metal-oxo bridges;

v. Exclusively monovalent cations or formally monovalent metal-ligand complexes, if the distance between two single Al atoms is too great or their cooperation of corresponding cations is geometrically restricted or all kinds of possible interaction/cooperation of their local negative charges in bonding of metal-ion species would be excluded.

8.2.2. Metal Ion Species in Hydrated Zeolites

The process of ion exchange of metal-ion species into the Si-rich zeolite framework refers to the local negative charges given by the "rigid" distribution of Al atoms between Al pairs, unpaired Al and single Al atoms in the

framework rings and, on the other hand, to the metal-ion complexes of various structures present in a given exchanging medium (e.g., aqueous solutions, vapors in a gas phase), see Fig. 8-1. Despite the possible complexity of the equilibria in the exchange medium (89), the principal features of the ion exchange will be based on the spatial restriction for accommodation of monovalent (or formally monovalent) species, and the positions for accommodation of divalent (or trivalent-ligand complexes) restricted by adequate local negative charges, given by the framework Al distribution.

Under the conditions of metal-ion exchange from aqueous metal salt solutions guaranteeing the presence of exclusively metal aquo-complexes (see, e.g., (89)), and following the zeolite dehydration, only the bare divalent cations are incorporated. However, the composition of the metal ion complexes in the solution could contain, in addition to the M^{2+} aquo complexes, also other positively charged species, e.g., soluble hydroxides or metal-anion complexes. Thus, e.g., metal chlorides and nitrates lead predominantly to the exchange of divalent cations, while the metal acetates enable also exchange of a monovalent metal-acetate complex. The composition of the metal ion species, including polynuclear species, in the solution during ion exchange is generally a function of the pH, temperature and metal-ion concentration (89). The diversity of the species in the exchange solution should be reflected in the complexity of the species accommodated in the zeolites. Thus, the outcome of the ion exchange of divalent cations or these cations in the form of complexes with negatively charged ligands (e.g., Cu^{2+} vs. $[Cu^{2+}Ac]^{+}$) in the identical parent zeolite might be dramatically different (90).

A similar situation would also apply for the introduction of metal-ion species into zeolites using volatile metal compounds, i.e., chemical vapor deposition (CVD, e.g., of chlorides). The primary product reflects the match between the local negative charges of the framework (i.e., Al distribution) and the formal charge of the volatile species (e.g., $[FeCl_2]^{+}$, $CuCl^{+}$), and possibly also their nuclearity. High formal exchange levels could be reached through this process. Nevertheless, during the final steps in the preparation, i.e., hydrolysis and calcination, the di- or trivalent cations produced would compete for the limited local negative charge, which is directly controlled by the Al distribution. Accordingly, a large number of metal-oxo species or bulk metal oxides would be regularly formed in addition to bare cations and counter metal-oxo species, see, e.g., (91). The process of solid-state ion exchange of metal chlorides actually resembles that of the CVD process and corresponds to the volatility of the metal chloride at high temperature (92). The exchange of metal oxides with H^{+} (or NH_4^{+}) ions is accompanied by the evolution of water/ammonia molecules into the gaseous phase (92, 93). Thus, e.g., relatively volatile V_2O_5, MoO_3 and Ga_2O can be exchanged as VO^{2+}, $MoO_2{}^{2+}$ (93) and Ga^{+} (94), while NiO, Fe_2O_3 (95) and Ga_2O_3 (94) do not interact with protons at all. It follows that the role of the Al distribution in directing the composition of the metal-exchanged

zeolites prepared by solid-state ion exchange would strongly depend on the formal charge of the interacting volatile species. It should also be mentioned that the solid-state ion exchange is a procedure resulting in products that also contain non-reacted bulk metal oxide in the products.

It could be summarized that the ion exchange of cations follows the existing distribution of Al atoms in the framework between the Al pairs and single Al atoms, which are further spatially distributed amongst the rings of the α-, β- and γ-type site.

The overlap of the existence of the individual metal-ion species (not much manifested for Co^{2+}, but more for Cu^{2+} ions, and dramatically for various species of Fe^{2+} ions) is decisively controlled, not by the total Si/Al ratio, but mainly by the distribution of framework Al atoms in the given zeolite, as has been repeatedly demonstrated (3a, 9a, 43, 46, 50, 52, 83d, 83g, 87, 96). Accordingly, preparation of a metallo-zeolite containing exclusively one type of metal-ion species is limited by the particular nature of the cation, beside the distribution of framework Al atoms. Nevertheless, the high population of Al pairs or single or unpaired Al atoms and their specific locations, which might be achieved by zeolite synthesis, provide for substantial enrichment in either bare cations or in various types of metal-oxo species, depending on the distances between the framework Al atoms (see below).

8.2.3. Metal Ion Species in Dehydrated Zeolites

The releasing of water molecules and other ligands of solvated metal-ion complexes through dehydration results in the coordination of metal-ion species to the framework oxygen atoms as bare cations, metal-oxo species or metal-oxo bridged structures, balancing the individual local negative framework charges. Nevertheless, the formation of neutral metal oxide species not related to the framework negative charge cannot be excluded in cases of charge unbalance formed in the dehydrated zeolite.

The relative rigidity of the zeolite framework, together with the coordination of bare cations only to framework oxygen atoms, results in unusual coordination, typically with an open coordination sphere of the metal ion (82). This results in specific properties of the ion-exchanged bare metal cations. The electronic structure of the metal ions by the interaction with the negatively charged framework is significantly altered compared to the metal ions in the bulk metal oxides or metal oxides supported on carriers.

Monovalent cations balance all the Al atoms, regardless of their location as Al pairs or single or unpaired Al atoms. The only restriction lies in the sizes of the cation and of the Al-containing ring. This is demonstrated on mordenite and ferrierite, where Na^+ ions preferably occupy 8-MRs (58, 88g). Deformed 6-MRs in mordenite and ferrierite (note that the C_{3v} symmetry of 6-MRs does not occur in Si-rich zeolites) are occupied only when the Al atom does not belong to

the 8-MRs (58). Bare divalent cations of significantly smaller diameter prefer in all pentasil ring zeolites siting in the 6-MRs (9b-e, 58, 88h), but the key parameter for their location is the presence of two Al atoms (Al pair) in the ring. A bare divalent cation in a ring containing a single Al atom is highly reactive and unstable. Bare trivalent cations do not occur in Si-rich zeolites (SiAl > 8), as the absence of Al-O-Si-O-Al sequences excludes the presence of three Al atoms in the 6- or 8-MRs.

Mono- and divalent metal-oxo species can occur as balanced by single Al atom or Al pairs in one and unpaired Al atoms in two rings. Metal-oxo bridged species, depending on their total positive charge, require two rings containing Al pairs or two Al atoms in one or two rings. These Al atoms must be located at an acceptable distance for the metal-oxygen bond and geometry allowing the formation of the metal-oxo bridging structure.

Summing up, the distribution of framework Al atoms represents a key parameter controlling the accommodation of bare cations, metal-oxo and metal-oxo bridges in Si-rich zeolites. The distribution of Al atoms in the framework T sites in Al pairs and single Al atoms controls the siting of the bare cations and metal-oxo species, and is a decisive parameter for the formation of bridging metal-oxo species.

8.2.3.1 Bare divalent cations. The Al-O-(Si-O)$_2$-Al sequences were reported to be located in the mordenite, ferrierite, ZSM-5 and beta zeolites, accommodating the divalent cations in the cationic sites of the α–, β- and γ-type rings, cf. Figs. 5–5 and 5-6 (6, 20, 23). The α-type 6-MR cationic site is composed of two 5-MRs forming the elongated 6-MR with the Al-O-(Si-O)$_2$-Al sequence on the wall of the main channel of mordenite (E site according to Mortier's notation (58, 88g)) and ferrierite, the straight channel of ZSM-5 and in the beta-cage of the beta zeolite. The divalent cations in these sites exhibit very unusual coordination at the top of the pyramid with a base of four oxygen atoms and are accessible only from the side of one channel. The β-type 6-MR cationic site is formed by approximately planar elongated 6-MR with Al-O-(Si-O)$_2$-Al sequences in the ferrierite cavity, in the crossing of the straight and sinusoidal channel of ZSM-5 and in the beta cage of the beta zeolite. In mordenite, this site is formed by six framework oxygen atoms of the twisted 8-MR at the bottom of the mordenite pocket (A-site according to Mortier (59, 93g)) arranged in the elongated planar 6-MR containing an Al-O-(Si-O)$_2$-Al or Al-O-(Si-O)$_3$-Al sequence. The divalent cation in the β-type site exhibits open, approximately planar coordination to three or four oxygens and it is accessible from both sides of the ferrierite cavity, and only from one side poorly accessible in mordenite. The divalent cations are also accessible from one side in the intersection of ZSM-5 channels and the beta zeolite. The γ-type site represents a complex boat-shaped site composed of 5-, 6- and 8-MRs located in the ferrierite cavity, in the mordenite pocket (C site according to Mortier (59, 93g)), in the ZSM-5 sinusoidal channel and the beta cage of the beta zeolite. Two Al atoms of the

Al-O-(Si-O)$_2$-Al sequence can be assumed to be located in the 8-MR. The cation in this site exhibits a close coordination sphere due to its octahedral-like coordination. Note that the exact geometry of the cation in this site is not clear. The cationic sites were not yet completely elucidated in MCM-22. However, it has been suggested that the siting of the Co^{2+} ion in the regular simple 6-MR exhibits planar coordination of the Co^{2+} ion with an open coordination sphere, which is accessible from both sides of the ring (24). These cationic sites were suggested on the basis of the Co^{2+} ion coordination by using Vis spectroscopy of the dehydrated Co-zeolites in analogy with the Ca^{2+} siting in Al-rich mordenite. Nevertheless, they were confirmed by the neutron powder x-ray diffraction experiments on Co- and Ni-ferrierite (9b, 9d, e, 88h) and Cu-mordenite (88h). The Co^{2+} cationic sites can be generalized to accommodate bare divalent cations owing to their similar ionic diameter and the decisive role of the location of the Al-O-(Si-O)$_2$-Al sequence in one ring, as confirmed by the same siting of Ni^{2+} and Co^{2+} in ferrierite and Cu^{2+} in mordenite.

The high flexibility of the T-O-T angle enables optimization of the geometry of the framework rings of the cationic sites to preserve the preferred metal-oxygen distance of the metal ion coordinated to the framework oxygen atoms, as follows from the Co^{2+}-framework oxygen distance of approx. 0.2 nm in different cationic sites of mordenite, ferrierite and ZSM-5 (97). The perturbation of the T-O-T angles and thus of the geometry of the zeolite rings by coordination of the divalent cation is reflected in the characteristic perturbation of the anti-symmetric T-O-T vibration for the α-, β- and γ-type cations as well as in the charge distribution over the cation (97c) obtained from theoretical calculations. As the cations are coordinated to AlO_4 tetrahedra, the preservation of the metal-oxygen distance can result in the perturbation of the framework rings of the cationic sites.

As discussed in Par. 5.2, a wider variability in the maximum relative number of cationic sites was reported for the α–type site (10–40% of sites) and the γ-type site (2–12% of sites) in ZSM-5. Concentration of the β-type site varied between 60–85% of the cationic sites. However, at a high concentration of Al-O-(Si-O)$_2$-Al sequences in one ring, the β-type site represents approx. 60%, the α–type site approx. 30% and the γ-type site less than 10% of the cationic sites for divalent cations without significant variation. The relative concentration of these sites in Al-O-(Si-O)$_2$-Al sequences in one ring in ZSM-5 results from the mechanism of the incorporation of the Al-O-(Si-O)$_2$-Al sequence in one ring into the ZSM-5 framework, see Par. 6.2. Nevertheless, the concentration of the Al-O-(Si-O)$_2$-Al sequence in one ring in the individual cationic sites yields only the maximum possible concentration of bare divalent cations in the zeolite and in the individual sites. At lower M^{2+} loadings, the concentration of M^{2+} ions in the individual sites results from (i) the stabilization energy of the M^{2+} ion in the individual site, (ii) the kinetics of both the ion-exchange procedure and distribution of cations in the dehydrated zeolite, and (iii) competition

with the other metal ions present in the zeolite. This is demonstrated in the significant differences in the distribution of the Co^{2+} ions in the CoH- and CoNa-ferrierites or the dehydrated CoH-, CoNa-, CoCs- and CoBa-mordenites (20, 23a).

It must be stressed that the maximum concentration of bare divalent cations in the zeolite is limited by the concentration of Al-O-(Si-O)$_2$-Al sequences in one ring. Thus, the concentration of Al atoms in the Al-O-(Si-O)$_2$-Al sequences (Al_{2Al}), see Par. 3.1.3, expressed as Si/Al_{2Al} turns out to be a crucial parameter of the zeolite essential for understanding the structure and location of metal-ion species and the general properties of Si-rich zeolites.

8.2.3.2 Metal-oxo and bridged metal-oxo species. Metal-oxo species. The Si-rich zeolites do not have sufficient local negative charge for adequate charge compensation of trivalent cations as bare cations but these cations could be stabilized as metal-oxo formally mono- and divalent species balancing single Al atoms or Al pairs, respectively. Formation of Co^{3+}- or Fe^{3+}-oxo and -peroxo complexes (43a, 98) or hydroxo complexes like $[Fe^{3+}(OH)_2]^+$ was reported (98a, 99). The formal divalent metal-oxo (or hydroxo) complexes would be coordinated, analogous to bare divalent cations, exclusively to the 6-MRs with an Al pair. The formally monovalent species, e.g., $[Cu^{2+}OH]^+$ (3a, 100), $[Fe^{3+}(OH)_2]^+$ (101) or $[Fe^{2+}\ OH)]^+$ and $[Co^{3+}\text{-}O]^+$ (43a, 102) species were proposed; they have to be coordinated to different rings containing single Al atoms or also possibly to one ring containing Al pairs.

Metal-oxo bridged species. The bridged metal-oxo or metal-hydroxo species require the presence of at least two Al atoms in an optimum distance in the zeolite channel. Three types of the formed bridging structures can be suggested. The bridge can be formed from (i) two originally bare divalent cations, (ii) monovalent cations or monovalent complexes, or directly from (iii) the binuclear charged complex. In the case of the bridge ad (i), the distance and geometric arrangement of the cationic sites (the α- and β-type) given by the positions of their rings in the framework and distribution of Al pairs, controls the formation of the bridge (46, 52). In the cases ad (ii) and (iii), the cations could be coordinated to any two Al atoms at the proper distance, located in either one or two rings. In this case, the formation of the bridge coordinated to one ring depends on the population of Al pairs in the ring and the position of the Al atoms in the ring. Formation of bridges coordinated to the Al atoms of two rings is controlled by the siting and distribution of single and unpaired Al atoms.

A considerable amount of effort has been devoted to analysis of the formation of bridged structures between the metal-exchanged cations, i.e., Fe, Co and Cu in MFI, BEA and FER zeolites; nevertheless final consensus has not been achieved. The -O-, -OH-, and -O-O- bridges were proposed as links between two metal cations (84j). For the Cu zeolites, the $[Cu\text{-}OH\text{-}Cu]^{2+}$ (103), $[Cu\text{-}O\text{-}Cu]^{2+}$ (85b, 104), $[Cu^{2+}\text{-}O\text{-}Cu^{+}]^{+}$ (105), $[Cu\text{-}O\text{-}O\text{-}Cu]^{2+}$ or bis(μ-oxo) di-copper

bridged species (106) were suggested. For Co- and Fe-zeolites, the $[Co\text{-}O\text{-}Co]^{2+}$ (83c, 107), dinuclear iron oxo/hydroxo complexes (108) and $[Fe^{2+}\text{-}O\text{-}Fe^{2+}]^{2+}$ structures (86, 109) were proposed. Moreover, the peroxo-bridged binuclear iron (110) and trivalent iron $[HO\text{-}Fe\text{-}O\text{-}Fe\text{-}OH]^{2+}$ complexes (83h) have been suggested.

8.3. Effect of Al Pairs and Single Al Atoms on the Counter Metal Ion Species

The coordination of a bare divalent cation to the ring with Al pair or metal-oxo species, and bridged metal-oxo species to Al pairs and single Al atoms, would basically influence their reducibility, the Lewis acidity and the stability against conversion into a metal oxide. Metal oxo-species and bridged metal-oxo species do not display Lewis acidity. On the other hand, they are readily reducible and the oxidation ability of the peroxo-bridged species is clearly evident. The oxo- and bridged oxo-species are proposed as the reactive intermediates. The redox cycle of these species would depend on the adjacent local negative charge (83e, 90b, 96c, 105).

This implies a decisive role of the Al distribution for the properties of the metal-ion species accommodated in the Si-rich zeolites. Cation bonding to the Al pair or to a single Al atom produces two basically different groups of species with very different properties. In addition, there are numerous small variations inside these groups, determined namely by structural details of the respective sites.

8.3.1. Adsorption Complexes of Divalent Cations

Bare Fe^{2+}, Co^{2+}, Ni^{2+} and Cu^{2+} cations coordinated to an Al pair in the 6-MRs display strong Lewis acidity, resulting in the formation of complexes with a number of bases, e.g., CO, NO, NH_3, pyridine or acetonitrile (101, 111). The differences in the coordinative unsaturation of the metal cations bonded in the different cationic sites and the site accessibility are reflected in the number of coordinated ligands and the stability of the cationic ligand. This could be illustrated by the formation of dinitrosyl complexes at the Co^{2+} ions in the α and β sites and only mononitrosyls at β-type sites in mordenite, ferrierite and ZSM-5 (112). The perturbation of the T-O-T framework bonds due to the coordination of the bare cation is partially relaxed by the adsorbed basic molecule. The strength of the bond with the basic molecule as well as the number of coordinated ligands affects the degree of relaxation of the perturbation of the T-O-T bonds (96b, 97a, 111e, 113).

8.3.2. Redox Behavior of Metal Counter Ion Species

A general feature of bare divalent cations coordinated in the site with an Al pair is their considerable resistance to reduction. The reduction of

bare divalent cations not exhibiting a monovalent state (Co^{2+}, Fe^{2+}) takes place at high temperatures (~900°C) connected with the degradation of the zeolite framework. This stability of a bare divalent cation in a ring with an Al pair could be illustrated for Co^{2+} (114), Cu^{2+} (115), Fe^{2+} (85c), or Ni^{2+} ions (116). On the contrary, metal-oxo species are much easily reduced. Accordingly, the reduction temperature of the metal-ion species and neutral metal oxide species, if it occurs in the zeolite, follows the sequence:

metal-oxo or bridged metal-oxo species < "supported" neutral metal oxide species < bulk metal oxide < bare cation.

9. CATALYTIC ACTIVITY OF H- AND METALLO-ZEOLITES

9.1. H-Zeolites

The location of the protonic sites in the individual rings and channels is governed by the siting of Al atoms in the T sites, zeolite rings and the channels. The location of two Al atoms in the 6-MR (Al pair) evokes two close protonic sites in a one ring and could even form four protons, e.g., at the intersection of the straight and sinusoidal channel in the MFI structure. On the other hand, the Al atoms in mordenite and ferrierite in the T1, T2 and T4 sites place protons in the 10-MR channels, while the Al atoms in T3 sites result in protonic sites accessible through 8-MR in the ferrierite cage or mordenite pocket (T3 site). Both types of Al distributions (Al pairs *vs*. single Al atoms or Al atoms in different channels) in H-zeolites could affect the transition state of the acid-catalyzed transformations of hydrocarbons or other derivatives.

The effect of the distribution of Al atoms between the Al pairs in 6-MR rings and single Al atoms has so far been manifested only in differences in the yields of olefins and aromatics in 1-butene cracking over H-ZSM-5 of similar Si/Al and crystal size, but substantially differing in the concentrations of Al pairs and single Al atoms (81). Higher yields of aromatics and paraffins, which was suggested to originate from enhancement of the bimolecular dimerization and hydrogen transfer reactions at the expense of monomolecular olefin cracking, were attributed to the higher populations of close protons in rings containing Al pairs, while the preferred formation of low olefins was connected with single Al atoms in a ring. However, as far as we know, no additional experimental data are available on the interaction of two protons with the hydrocarbons or other substrates.

The positioning of Al atoms in the framework of ferrierite and mordenite, which controls the presence of the related protons in the channels with different pore opening, could decisively affect the transition state in acid-catalyzed transformations of hydrocarbons or their derivates. The position of an Al atom

and the neighboring framework oxygen atoms within their confined environment would evoke either transition-state-restricted selectivity (well known from shape-selective transformations of hydrocarbons, see, e.g., Ref. (117)) or on the contrary, transition-state-directed selectivity, where the specific spatial geometry of the mutual approach of the reactants at the specific T site in the confined environment enables creation of the most favorable transition state complex. Examples of the latter type of selectivity include, e.g., selective transalkylation of isopropyl benzene or isopropyl toluene to n-propyl benzene or n-propyl toluene induced in the intersecting narrow 10-MR channels of ZSM-5 (118), in contrast to the wide channels of BEA or FAU zeolites (118c, d), where this type of complex is not expected to be formed as transformation of iso- to n-alkylaromatics does not occur. Another example is the carbonylation of methanol or DME in the 8-MR pocket of mordenite (64, 119), where transformation of methanol/DME to hydrocarbons is suppressed. The Al atom specifically at the T3 site (see Fig. 9-1) and the attached O33 atom support an optimum transition state complex (see Fig. 9-2). Siting of the framework Al atoms in the confined environment of the pores has also been shown to influence the relative tendency towards the formation of alkoxides or carbocations in zeolites (120). We could therefore suggest the possibility of affecting the pathway of the other required selective transformations of hydrocarbons by the siting of Al atoms in the specific T sites with suitable

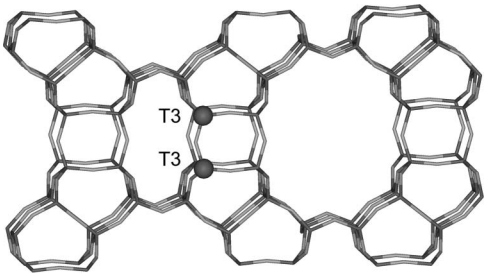

Figure 9-1: Location of T3(Al) sites in mordenite. According to Ref. (1).

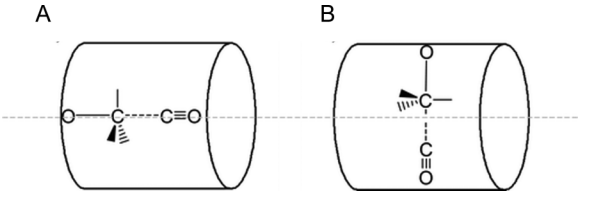

Figure 9-2: Schematic representation of the relative orientation of the $O_{framework}-CH_3$ bond and the channel axis (a) at the T3-O33 position of MOR and (b) any other position in an 8-MR channel. Reprinted with permission from Ref. (123). Copyright 2008 American Chemical Society.

confinement in the pore structure and by the siting of two Al atoms or a single Al atom in 6-MRs of the framework of Si-rich zeolites.

Pérez-Pariente et al. were the first to use a combination of cationic and neutral organic ammines as templates to direct the T(Al) sites of ferrierite into the 10- (T1, T2 and T4 sites) and 8-MR channels in the ferrierite cage (the T3 site), cf. Fig. 5-1, for the purpose of affecting their activity in selective transformation of hydrocarbons (11a, 62b, 121). Location of Al atoms in the T1, T2 and T4 sites, monitored by adsorption of pyridine on SiOHAl groups in the 10-MR channels and/or at the T3 sites of the 8-MR pores of ferrierite not accessible for pyridine was manifested in the isomerization of m-xylene. The isomerization rate was proportional to the concentration of SiOHAl groups in the 10-MR channels, with the low p/o-xylene ratio typical for the reaction occurring in the 10-MR channels. On the other hand, the prevailing concentration of (Al)T3 sites in ferrierite cage and the corresponding SiOHAl groups controlled the rate of selective transformation of 1-butene to isobutene, a molecule of much smaller kinetic diameter compared to xylene. The rate of total transformation of 1-butene was proportional to the total concentration of acid sites regardless of their location in the 10-MR or 8-MR channels. The selective isomerization of 1-butene to isobutene, typically following a monomolecular mechanism (while dimerization yielded an equimolar ratio of $C_3^=$ and $C_5^=$ olefins) (122), occurred to a high extent on ferrierites containing a high population of acid sites at (Al)T3 sites in 8-MR channels. The transition state intermediate for a bi-molecular reaction could not be formed in the 8-MR channels for steric reasons and the selective monomolecular reaction pathway prevailed in these pores with participation of the SiOHAl(T3) sites.

Selective carbonylation of methanol or DME with carbon monoxide to acetic acid or methyl acetate occurring in the 8-MR channels has been suggested to be controlled by the transition state, which was assumed to depend on the location of a proton in the individual pores. The proportionality between the rate of carbonylation and the concentration of acid sites in the 8-MR channels obtained by Roman-Leshkov et al. (11c) in the synthesis of ferrierites with pyridine or a combination of TMA and pyridine, in contrast to those synthesized using large cyclic amines (HMI), demonstrated that the reaction proceeded in 8-MR pores.

The concentration of SiOH(Al)T3 sites in the 8-MR side pockets of mordenite was also proportional to the rate of carbonylation of methanol over H-mordenite (119). Moreover, the activity of H-mordenite appeared to be substantially higher compared to ferrierite, despite the fact that both ferrierite and mordenite exhibited acid sites in 8-MR channels. This is a result of the step involving the attack of a methoxy group by CO molecule, competing with methanol/DME, assumed to be the rate-controlling step of the carbonylation reaction. The ferrierite cage is slightly larger compared to the mordenite

pocket. Moreover, by analyzing methanol carbonylation at different T-O positions of the mordenite 8-MR pocket by quantum chemical calculations, Boronat et al. showed that only the T3-O33 site, and not the T3-O31 site, is responsible for the high carbonylation selectivity (64, 120, 123). The methoxy group at the T3-O33 site with an interacting CO molecule is oriented in the linear position in the direction of the cylindrical side 8-MR pocket, being a highly favorable intermediate in contrast to the unfavorable intermediates of methoxy groups with DME, which are sterically hindered and destabilized. Thus, the location of the T3-O33 site in the side pocket and the pocket geometry itself support the advantageous transition state for the carbonylation of the methoxy group (Fig. 9-2). The carbonylation of methanol/DME represents the first reaction where the reaction transition state has been shown to be controlled by the siting of the Al atoms in the individual framework T sites.

Thus, the effect of the siting of framework Al atoms for the formation of a highly advantageous structure of the reaction intermediate is clearly demonstrated, not only for the location of the Al atoms (and SiOHAl groups) in the pores of different sizes, but also with respect to the local confinement around the individual Al atom given by the local geometry of the pores.

9.2. Metallo-Zeolites

The limited knowledge on the Al siting in the T sites of zeolites and absence of zeolites with controlled siting of Al atoms, together with the fact that the properties of (transition) metal ions depend mainly on the vicinity (visible distance) of Al atoms (see Chapter 2) result in the absence of studies on the effect of particular T(Al) sites or rings coordinating metal ion species on the catalytic performance of metallo-zeolites. On the other hand, the distribution of Al atoms between Al pairs in one ring and single Al atoms (without specifying their T sites) has been shown to affect the structure of the exchanged counter cation species, reflected in their reactivity in various catalytic reactions. Moreover, the ability to synthesize zeolites with controlled Al distribution enabled a detailed study to be carried out on the effect of the Al distribution on the activity of metallo-zeolites.

NO decomposition was the first reaction where the unique high and stable redox activity of the exchanged divalent species in Si-rich pentasil zeolites was revealed, as first reported in 1986 by Iwamoto et al. for Cu-ZSM-5 zeolites (124). Their suggestions related to the presence of two or more cation-exchangeable sites in ZSM-5 zeolites, and the mechanism of NO decomposition proceeding via adsorption of NO molecules on two cooperating Cu^+ ions were already in fact based on the importance of the distribution of Al atoms in the framework for the formation of the Cu^+ active sites.

Here we summarize analysis of the activity of metal (Cu, Co, Fe) Si-rich pentasil zeolites exhibiting quite different distributions of Al atoms

in their framework in order to demonstrate their mutual relationships. Numerous correlations of the structure of metal ion species in Si-rich pentasil zeolites with their activity and selectivity that have been performed have encountered difficulties in the preparation of samples with predominant concentration of one metal structure and straightforward determination of the structure, in spite of the use of a combination of several spectral and diffraction techniques distinguishing the bare metal ion species and several metal-oxo complexes. This general problem of analysis of the activity of metallo-zeolites has recently been outlined for Fe-zeolites by Pirngruber et al. (125). Nevertheless, the analysis of metallo-zeolites with increasing concentrations of metal ion species within one parent zeolite (at a constant distribution of Al atoms) often indicated some trends in the formation of specific metal-ion structures and the related activity. This analysis was based on the assumption that the bare divalent cations predominate at low metal concentration, being accompanied at higher loadings by metal-oxo species and (nano)oxides at the highest metal concentrations in the zeolites (see the discussion below).

Attention is devoted here to the activity of Cu, Co and Fe ions as (i) the bare divalent cations balanced by Al pairs in one ring, (ii) oxo-cations adjacent to single or unpaired Al atoms, and (iii) two cooperating divalent cations in the 4-Al-hyper structures balanced by two rings each with an Al pair.

9.2.1. Effect of Al Pairs, Single and Unpaired Al Atoms, and 4-Al Hyper-Structures

The Al-O-$(Si\text{-}O)_2$-Al sequences in one ring (Al pairs) represents the most important framework Si-Al arrangement in relation to metallo-zeolite catalysts. The 6-MRs (8-MR in MOR) containing Al pairs are essential for the accommodation of bare divalent cations in Si-rich zeolites and a predominant sequence with two close Al atoms in Si-rich zeolites controlling the incorporation of polyvalent cations into the zeolite, as well as for their redox and catalytic behavior. The divalency of bare cations (Cu and Co) in zeolites is highly stabilized, compared to those supported on inorganic carriers, when compensated by two framework negative charges of Al pairs in the ring. Moreover, the rings with Al pairs were reported to be components of the framework 4-Al or 3-Al hyper-structures (46, 96f, 126) (see Fig. 2-4 and for definition Par. 2.2.5).

The Cu^{2+} ions coordinated to 6-MRs containing Al pairs are the most active sites in the $C_{10}H_{22}$-SCR-NO_x reaction over Cu-ZSM-5 (87, 96a). This follows from the superior activity of Cu-ZSM-5 with Cu/Al 0.06–0.5 with predominant Al pairs in the framework compared to Cu-ZSM-5 with the same chemical composition but with predominant single Al atoms, see Fig. 9-3. This complex reaction consists of oxidation of NO to NO_2 and oxidation of a

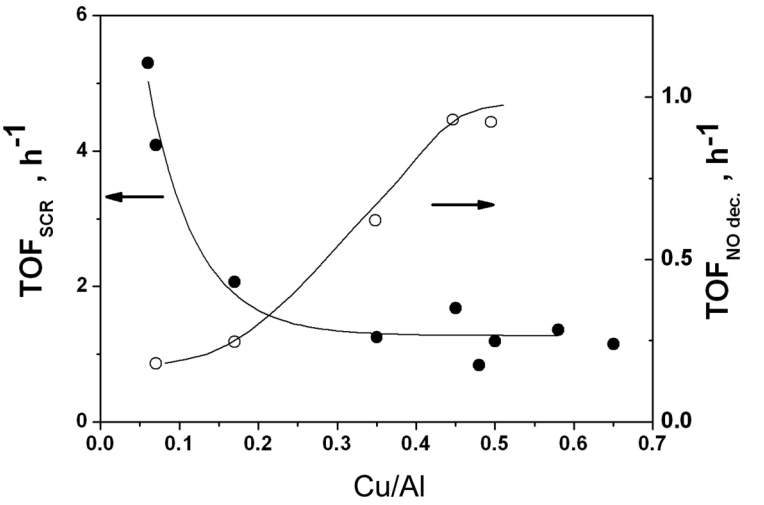

Figure 9-3: Dependence of NO conversion in $C_{10}H_{22}$-SCR-NO and NO decomposition on Cu loading in Cu-ZSM-5. Reaction conditions: $C_{10}H_{22}$-SCR-NO—1000 ppm NO, 450 ppm $C_{10}H_{22}$, 6% O_2, 12% H_2O, 250°C and GHSV 30000 h^{-1}; NO decomposition—4000 ppm NO, 400°C and GHSV 15000 h^{-1}. According to Ref. (96a). with the permission of Elsevier.

hydrocarbon with NO_x. The high activity of Cu^{2+} ions stabilized in the 6-MRs with two Al atoms even in the presence of a large excess of water vapor at low (280°C) temperature is attributed to the strong adsorption of oxygenated hydrocarbon intermediate products on the Cu^{2+} sites protecting them against water adsorption.

The Co^{2+} ions in Co-ZSM-5 containing highly predominant Co ions coordinated to 6-MRs with Al pairs behave as Lewis sites. As strong electron acceptor sites, they activate methane. Methane activation is a crucial step in CH_4-SCR-NO_x, as indicated by the increasing activity of CH_4-SCR-NO_x over Co-ZSM-5 with an increasing degree of the Co ion exchange (52, 127). Similarly to CH_4-SCR-NO_x over Co-zeolites, the bare Co^{2+} ions accommodated in 6-MRs with Al pairs in the beta zeolite have exhibited high activity in C_3H_8-SCR-NO_x. However, as bare Co^{2+} ions are strong Lewis sites, the presence of water vapor in the NO_x stream completely suppresses the activity in both the CH_4- and C_3H_8-SCR-NO_x reactions (43), see Table 9-1.

It should be pointed out that the cooperation of the Co^{2+} Lewis center with another catalytic/sorption center is useful for CH_4-SCR-NO_x (52, 127a, b). This is reflected in the counter-intuitive differences of the effect of the siting of Co^{2+} ions among the α-, β- and γ-type cationic sites in mordenite, ferrierite and ZSM-5. The distances between the distinct cationic sites differ for the individual structural types and the shortest distance between two cations can be obtained for the cations in opposite α-sites in ferrierite and β-sites in ZSM-5.

Table 9-1: CH_4-SCR-NOx and C_3H_8-SCR-NOx in the absence and presence of water over Co-zeolites. According to Refs. (43b, 52).

Paraffin	Zeolite	M/Al_{FR}	C_{NOx} (ppm)	$C_{paraffin}$ (ppm)	C_{H2O} (vol. %)	$Yield_{N2}$ (%)
CH_4	Co-ZSM-5	0.46	900	1200	0	78
					10	0
CH_4	Co-ferrierite	0.42	900	1200	0	92
					10	0
C_3H_8	Co-beta	0.46	1000	1000	0	48
					10	11
C_3H_8	Co-beta*	0.42	1000	1000	0	90
					10	91

*Contains Co-oxo species.

The importance of the Co^{2+}- Co^{2+} distance resulted in the following sequence of the activity of Co^{2+} ions in Co-zeolites in CH_4-SCR-NO_x:

$$\alpha/\mathrm{FER} > \beta/\mathrm{ZSM\text{-}5} > \beta/\mathrm{BEA}^* \approx \alpha/\mathrm{ZSM\text{-}5} >> \beta/\mathrm{FER} \approx \alpha/\mathrm{MOR} >> \beta/\mathrm{MOR}.$$

N_2O decomposition to molecular products is assumed to occur either by recombination of the formed atomic oxygens or by their interaction with another N_2O molecule (108, 128). Bare Fe^{2+} ions located in 6-MRs with Al pairs are undoubtedly responsible for N_2O decomposition over Fe-zeolites (46, 50, 96e, f). These Fe^{2+} ions predominate in Fe-zeolites at low Fe loadings (Fe/Al <0.1) when introduced by a procedure preferring the accommodation of Fe ions in rings with Al pairs and resulting in comparable activity in N_2O decomposition over Fe-BEA and Fe-ZSM-5. However, the most active sites for this reaction resemble the two Fe^{2+} ions located in the 4-Al hyper-structure (for a definition, see Par. 2.2.5). The two Fe^{2+} ions are coordinated each to one β-type 6-MRs with Al pairs on the opposite side of the ferrierite cavity. The optimum distance between the Fe^{2+} ions in the ferrierite 4-Al hyper-structure enables advantageous mutual cooperation of the Fe cations in both the N_2O adsorption and the following process leading to the formation of an oxygen molecule (Fig. 9-4) (46, 96f). This is reflected in the three times higher N_2O decomposition activity (TOF per Fe) over Fe-ferrierite (at Fe/Al <0.1) than in Fe-ZSM-5 and Fe-beta zeolite, and moreover, the higher activity over Fe-ferrierite with predominant concentration of Al pairs compared to that with similar chemical composition, but substantially lower population of Al pairs in the framework.

In contrast to the rings with two Al atoms stabilizing the divalency of the metal ions, cations located in the vicinity of the single Al atoms can be assumed to be readily reducible when their monovalent state is acceptable for a cation. The preferred monovalent state of the Cu ions in zeolites with

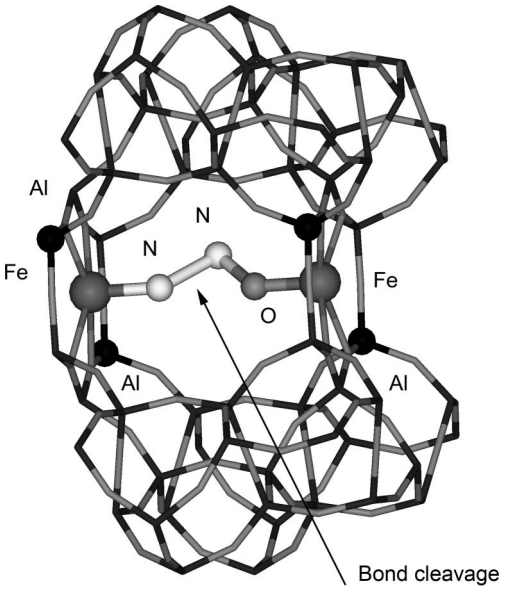

Figure 9-4: Interaction of Fe-beta with N_2O. According to Ref. (96f). with the permission of Elsevier.

a single Al atom facilitating the Cu^{2+}/Cu^{+} redox cycle can be reflected in the much higher activity in NO decomposition of Cu ions in ZSM-5 with predominating single Al atoms compared to the Cu-ZSM-5 with similar Cu/Al/Si chemical composition, but with highly predominant Al pairs, see Fig. 9-3 (3a, 96a).

The negligible activity of Cu^{2+} ions stabilized in the 6-MRs with two Al atoms in the Si-rich zeolite further follows from the low activity of Cu-ZSM-5 with low Cu loadings, where rings with Al pairs are preferentially occupied by Cu^{2+} ions. The Cu^{2+} ions are increasingly exchanged into the vicinity of single Al atoms in the form of monovalent $[Cu^{2+}(H_2O)_5X^{-}]^{+}$ complexes, mainly at higher Cu loadings (3a, 87, 96a). It can be assumed that they are autoreduced to Cu^{+} during the catalyst dehydration. This assumption is in sound agreement with the practically inactive Cu ions in the Al-rich faujasites in NO decomposition (124, 129), in which reduction of Cu^{2+} ions does not occur, as they are balanced by close Al atoms.

Iwamoto et al. (90a) attributed this high activity of Cu-ZSM-5 in NO decomposition to cooperation of the two Cu^{+} ions in "dimeric" Cu^{+}-Cu^{+} species expected to be formed from the Cu^{2+}-O-Cu^{2+} entities. The increased activity of the Cu ions at higher loadings was also intuitively assigned to the exchange of Cu^{2+}-OH, assuming transformation into Cu^{2+}-O species or to Cu^{+}, adjacent to single Al atoms occurring in Si-rich zeolites (in contrast to Al-rich faujasites) (3a). The argument against the occurrence of close Cu ions either

as bare cations bearing oxygen(s) or as bridged Cu-oxo species originates from the low density of Al atoms in the Si-rich zeolites. However, the distances between the Al atoms do not follow from any statistical rules, but from the zeolite structure, the conditions of the zeolite synthesis and the Si/Al composition. Therefore, small distances between the framework rings with single Al atoms could, in principal, be present, but so far the location of these Al atoms was not straightforwardly established. Nevertheless, the assignment of the active sites to the isolated Cu^+ ions adjacent to a single Al atom was supported by the same TOF values per Cu site at increasing Cu concentration at Cu/Al > 0.2 up to "over-exchange" levels, where both the Cu-MFI and Cu-BEA zeolites exhibit naturally different distances between the cations (3a, 130). As the Cu^+ ions at different distances exhibited the same TOF values, the formation of Cu^+-Cu^+ dimeric species seemed not be necessary, and the Cu^+ ions each adjacent to a single Al atom in 6-MR have been suggested as the active sites for NO decomposition. This suggestion is further supported by the TOF per Cu ion over Cu-BEA exhibiting an increasing trend in TOF values up to Si/Al 18 and then constant value for Si/Al up to 40 (130a). This finding can be assumed to indicate that the single Cu ion coordinated to a ring with a single Al atom is an active site in NO decomposition. The reported low activity of Cu-mordenite (131) might stem from the typically low concentration of single Al atoms in mordenite compared to ZSM-5 and the beta zeolites with Si/Al > 12.

In addition to the bare Co^{2+} ions in the 6-MRs with Al pairs, the Si-rich zeolites could also accommodate monovalent Co-oxo species coordinated to unpaired Al atoms in different rings. This follows from the fact that a significant fraction of exchanged Co^{2+} hexaquocomplexes can be transformed to Co-oxo species in some zeolites upon dehydration (43). In contrast to the bare Co^{2+} ions, the Co-oxo species do not represent Lewis centers, which are highly sensitive to water vapor in the reaction stream. The resistance of the active site based on the Co-oxo-species against the presence of water vapor is manifested for C_3H_8-SCR-NO_x over the Co-beta zeolite. While the activity of bare Co^{2+} ions in CoH-BEA is high only in the absence of water in the reactant stream and disappears under conditions close to real NO_x streams (10% water vapor in the presence of 1000 ppm of NO_x), the Co-beta zeolites with Co-oxo species balanced by single Al atoms exhibit high and stable activity. The Co-oxo species in the vicinity of single Al atoms can be formed only in non-dealuminated beta zeolites, where single Al atoms are present, cf. Par. 7.2. The crucial role of single Al atoms for the formation of Co-oxo species has been demonstrated by preparation of the beta zeolite containing prevailingly single Al atoms in the framework. The obtained high concentration of Co-oxo species bonded to rings containing single Al atoms provided the Co-beta catalyst with high activity preserved even in the presence of a large excess of 10% water vapor (43).

9.2.2. *Effect of Metal/Al Content in Zeolites of Non-Established Al Distribution*

Studies analyzing the effect of framework Al distribution between Al pairs and single Al atoms on the limited number of selected catalytic reactions have been discussed in the preceding paragraph. However, numerous studies provide data on the activity of metallo-zeolites with increasing metal content prepared from one parent zeolite of unknown, but fixed distribution of framework Al atoms. Ion exchange from aqueous solutions, if hydrolysis does not occur, indicates that mostly divalent cations adjacent to Al pairs are preferably exchanged, followed by the cation exchange at higher metal loadings next to single Al atoms with formation of various metal-oxo cations. Nevertheless, basically different ion-exchange procedures or even details of protocols or zeolite after-treatments can lead to quite different preparations. Thus, the relationship between metallo-zeolite catalyst performance and Al distribution (as assumed in the published results) can be inferred only in some cases and requires great caution.

Metal-oxo counter species of unusual activities detected in pentasil Si-rich zeolites at M^{2+}/Al loading close or above 0.5 are necessarily related to the Al distribution in the framework, likely to binding via single Al atoms. The di-copper μ-oxo, Cu_2-(μO_2) (132), were suggested as the active sites for a release of O_2 in NO decomposition by the Leuven and Utrecht laboratories on Cu-ZSM-5 of wide Si/Al/Cu composition ranges, on the basis of a combination of an EXAFS experiment and UV-Vis spectroscopy, in analogy with enzymatic structures of Cu-oxo complexes (106, 132, 133). The ability of Cu-ZSM-5 to provide activation of C-H bonds and oxidation of methane to methanol by molecular oxygen at about 150°C (although its desorption without further oxidation represents a problem) was originally attributed to the $Cu_2(\mu\text{-}O_2)$ complexes. However, as the active Cu species represented only a minority of the Cu ions, the $[Cu^{2+}\text{-}O\text{-}Cu^{2+}]^{2+}$ core was assumed as the active site (134). Also Cu-mordenite with Si/Al 8.8, anticipated to exhibit rings with single Al atoms, exhibited Cu-oxo complexes that are even more active in methane oxidation to methanol (135). This implies that Cu ions can be accommodated, amongst other things, in the MFI structure in coordination such that they activate molecular oxygen which then interacts with the stable C-H bonds of methane. Both these Cu structures and their relation to the Al distribution in the zeolite frameworks are unclear, but likely connected with the distribution of single Al atoms in the framework rings. Nevertheless, there is no doubt that the Si-Al arrangement of the framework plays a decisive role for these highly active Cu complexes.

The exchanged Co^{2+} ions in ZSM-5 and the beta zeolite exhibited the highest activity for selective ethane ammoxidation among a spectrum of Co-zeolite structures (Y, MOR, FER, NU) (136). As the two zeolites contained relatively

high Al contents (Si/Al ~ 12), the most populated sites can be expected to be bare Co ions in 6-MRs containing Al pairs. Like the electron acceptor Co^{2+} Lewis sites accommodated in pentasil zeolites activating the C-H bond of methane during CH_4-SCR-NOx, at loadings below Co/Al 0.5 these cations might analogously be represented by the α-, β- and γ-type Co^{2+} ions active in ethane ammoxidation to acetonitrile. However, no data are available on the framework Al distribution and/or the presence of some Co-oxo species for these Co-zeolites. The presence of some Co-oxo species has been indicated at Co/Al loadings ~ 0.5 (136c). Nevertheless, it can be assumed that the distribution of Al atoms in the framework plays also an important role for Co species active in this reaction.

Similar to the Cu^{2+}/Cu^{+} redox couple, the Co^{3+}/Co^{2+} species resemble oxidation of methane by molecular oxygen analogously followed by a difficulty in product desorption. The conversion of methane is not high, but the selectivity for methanol and formaldehyde reaches a value of 50% (137). Thus, also for Co ions, some specific types of Co-oxo species stabilized by two single Al atoms represent optimum arrangement of the active sites. However, their structure has not been elucidated to date.

There are also numerous studies on the activity of Fe^{3+}/Fe^{2+} redox couples in Fe-ZSM-5 zeolites in C_3H_8-SCR-NOx (e.g., Ref. (85c, 138)), NH_3-SCR-NOx (e.g., Ref. (42a) and references therein) and N_2O decomposition (e.g., Ref. (139)), which also indicate the formation of presumably Fe-oxo species which are highly active in these reactions. Both bare Fe^{2+} ions and dinuclear Fe-oxo species were suggested as the highly active sites for NH_3-SCR-NOx. However, owing to the complexity of Fe chemistry itself and to the obvious effect of the distribution of framework Al atoms on the Fe-complexes formed, we do not analyze here the structure vs. activity of Fe species in ZSM-5 (cf. conclusions given in Ref. (125)).

It can be summarized that the results currently available on the distribution of Al atoms in the framework, the potential for its manipulation by the conditions of zeolite hydrothermal synthesis and the decisive effect on the activity of metallo-zeolites, as well as the intuitive assumption on the trends in the influence of Al distribution on the activity of metallo-zeolites with increasing metal content, encourage us to suggest the decisive importance of the distribution of framework Al atoms on the activity of counter cations. The inclusion of the analysis of the distribution of Al atoms in the rings surrounding the cation species would enable one to complete the description of the structure and thereafter to tailor metal ion complexes accommodated in Si-rich zeolites. If in addition a confined local void volume surrounding of the active site (protons or metal ions) is included, then there is a route available for attempting to find a suitable space for the transition state complex for a given reaction within known or even specifically tailored new zeolite structures.

10. CONCLUSIONS

The siting and distribution of Al atoms in the framework emerge as new and decisive parameters of Si-rich zeolites with an impact on the structure and siting of counter ion species and their properties/activity, comparable in importance with the zeolite topology and Al content of the zeolite framework. Variability in the Al siting in Si-rich zeolites follows from the low content of isomorphously substituted Al atoms in the silicate framework and the large number of crystallographic distinct framework T sites in these zeolites.

The siting of Al atoms covers the individual framework T sites, the framework rings and the zeolite channels. The siting of Al atoms in the framework is not random or controlled by simple rules and depends on the zeolite hydrothermal synthesis. Thus, Si-rich zeolites can be prepared with the same topology and chemical composition but different positions of the Al atoms in the framework, as was demonstrated for ZSM-5 and ferrierite. Methods have not yet been developed for control of the siting in the individual T(Al) sites, but the siting of Al atoms in the zeolite rings or in the channels was successfully targeted by the SDA molecules used for the hydrothermal synthesis. ^{27}Al MQ MAS NMR combined with quantum chemical calculations of ^{27}Al isotropic chemical shifts was found to be a promising tool for analysis of the Al atoms in the framework T sites. The use of probe molecules monitored by FTIR spectroscopy can yield the siting of Al atoms in the individual channels. Governing of the catalytic behavior of the zeolite-based catalyst by control of the siting of Al atoms in the framework was demonstrated for mordenite in carbonylation of methanol/DME, but can be suggested as general tool for tuning zeolite activity/selectivity for a range of catalytic reactions.

The distribution of Al atoms in the framework of Si-rich zeolites refers to the distribution of Al atoms in various Al-O-(Si-O)$_n$-Al sequences and geometric (and visible) distances between Al atoms taking into account whether these Al atoms cooperate in binding counter ion species. Al atoms in Al-O-(Si-O)$_2$-Al sequences in one 6-MR and single Al atoms highly predominate in Si-rich zeolites. The distribution of the Al atoms between single Al atoms and Al-O-(Si-O)$_2$-Al sequences in one ring is not random or controlled by simple rules and depends on the conditions of the zeolite synthesis. Procedures were successfully developed for the synthesis of MFI, FER and BEA topologies with a predominance of either Al-O-(Si-O)$_2$-Al sequences in one ring or single Al atoms in a wide range of framework Al contents. Bare Co^{2+} ions in dehydrated zeolites exchanged into a maximum degree, followed by Vis spectroscopy, in combination with other spectroscopic methods (e.g., ^{29}Si MAS NMR), represents a powerful tool for analysis of the distribution of Al atoms in the zeolite framework. The distribution of Al atoms in the framework is an essential parameter controlling the accommodation and structure of metal-ion

species in Si-rich zeolites. The dramatic impact of the framework Al distribution on a number of redox- and Lewis-catalyzed reactions carried out over metallo-zeolites, as well as in acid-catalyzed hydrocarbon transformations over H-zeolites, was clearly demonstrated.

Bare divalent cations, exhibiting Lewis electron acceptor properties, are stabilized by Al-O-(Si-O)$_2$-Al sequences in 6-MRs, while the rings mostly with single Al atoms and unpaired Al atoms in different rings are centers for accommodation of various metal-oxygen and bridged metal-oxo, μ-oxo and -peroxo complexes.

Variability of the siting and distribution of Al atoms in the framework represents a general feature of Si-rich zeolites, resulting in zeolites of the same chemical Si/Al composition, but significantly different siting and distribution of Al atoms and thus, different zeolite properties controlled by these parameters. As both the methods for control of the Al siting and distribution of the Al atoms in the zeolite framework and their monitoring have been successfully developed, this knowledge suggests the possibility of designing a new generation of highly selective zeolite-based catalysts and catalytic processes. This concerns known Si-rich zeolite topologies or even newly discovered topologies with the tuned siting and distribution of Al atoms in their framework.

ACKNOWLEDGMENTS

The authors acknowledge financial support from the Academy of Sciences of the Czech Republic under the Program Nanotechnologies in project #KAN 100400702 and #IAA 400400904, from the EU 7th framework project NEXT GTL #NMP3-LA-2009-229183, and from the Grant Agency of the Czech Republic under the project #P106/11/0624.

REFERENCES

[1] Baerlocker, C.; McCusker, L. B. Database of Zeolite Structures. ETH Zurich: Zurich, 2001. http://www.iza-structure.org/databases (accessed March 19, 2012)

[2] Iwamoto, M.; Yahiro, H.; Mizuno, N.; Zhang, W.X.; Mine, Y.; Furukawa, H.; Kagawa, S. Removal of Nitrogen Monoxide Through a Novel Catalytic Process .2. Infrared Study on Surface-Reaction of Nitrogen Monoxide Adsorbed on Copper Ion-Exchanged ZSM-5 Zeolites. *Journal of Physical Chemistry* **1992**, *96*(23), 9360–9366.

[3] (a) Wichterlova, B.; Dedecek, J.; Sobalik, Z.; Vondrova, A.; Klier, K. On the Cu Site in ZSM-5 Active in Decomposition of NO: Luminescence, FTIR Study, and Redox Properties. *Journal of Catalysis* **1997**, *169*(1), 194–202; (b) Kucherov, A.V.; Slinkin, A.A.; Kondratev, D.A.; Bondarenko, T.N.; Rubinstein, A.M.; Minachev, K.M. Cu-2+-Cation Location and Reactivity in Mordenite and ZSM-5-ESR-Study. *Zeolites* **1985**, *5*(5), 320–324; (c) Kucherov, A.V.; Slinkin, A.A. Introduction of Transition-Metal Ions in Cationic Positions of High-Silica Zeolites by a

Solid-State Reaction - Interaction of Copper-Compounds with H-Mordenite or H-ZSM-5. *Zeolites* **1986**, *6*(3), 175–180.

[4] (a) Sarv, P.; Fernandez, C.; Amoureux, J.P.; Keskinen, K. Distribution of Tetrahedral Aluminium Sites in ZSM-5 Type Zeolites: An Al-27 (Multiquantum) Magic Angle Spinning NMR Study. *Journal of Physical Chemistry* **1996**, *100*(50), 19223–19226; (b) Sklenak, S.; Dedecek, J.; Li, C.B.; Wichterlova, B.; Gabova, V.; Sierka, M.; Sauer, J., Aluminum Siting in Silicon-Rich Zeolite Frameworks: A Combined High-Resolution Al-27 NMR Spectroscopy and Quantum Mechanics/Molecular Mechanics Study of ZSM-5. *Angewandte Chemie-International Edition* **2007**, *46*(38), 7286–7289; (c) van Bokhoven, J.A.; Koningsberger, D.C.; Kunkeler, P.; van Bekkum, H.; Kentgens, A.P.M. Stepwise Dealumination of Zeolite Beta at Specific T-Sites Observed with Al-27 MAS and Al-27 MQ MAS NMR. *Journal of the American Chemical Society* **2000**, *122*(51), 12842–12847; (d) Dedecek, J.; Kaucky, D.; Wichterlova, B. Al Distribution in ZSM-5 Zeolites: An Experimental Study. *Chemical Communications* **2001**, (11), 970–971; (e) Van Bokhoven, J.A.; Lee, T.L.; Drakopoulos, M.; Lamberti, C.; Thiess, S.; Zegenhagen, J. Determining the Aluminium Occupancy on the Active T-Sites in Zeolites Using X-Ray Standing Waves. *Nature Materials* **2008**, *7*(7), 551–555.

[5] (a) Dedecek, J.; Kaucky, D.; Wichterlova, B.; Gonsiorova, O. Co2+ Ions as Probes of Al Distribution in the Framework of Zeolites. ZSM-5 Study. *Physical Chemistry Chemical Physics* **2002**, *4*(21), 5406–5413; (b) Gabova, V.; Dedecek, J.; Cejka, J. Control of Al Distribution in ZSM-5 by Conditions of Zeolite Synthesis. *Chemical Communications* **2003**, (10), 1196–1197; (c) Han, O.H.; Kim, C.S.; Hong, S.B. Direct Evidence for the Nonrandom Nature of Al Substitution in Zeolite ZSM-5: An Investigation by Al-27 MAS and MQ MAS NMR. *Angewandte Chemie-International Edition* **2002**, *41*(3), 469–472; (d) Magusin, P.; Zorin, V.E.; Aerts, A.; Houssin, C.J.Y.; Yakovlev, A.L.; Kirschhock, C.E.A.; Martens, J.A.; van Santen, R.A. Template-Aluminosilicate Structures at the Early Stages of Zeolite ZSM-5 Formation. A Combined Preparative, Solid-State NMR, and Computational Study. *Journal of Physical Chemistry B* **2005**, *109*(48), 22767–22774.

[6] Dedecek, J.; Kaucky, D.; Wichterlova, B. Co2+ Ion Siting in Pentasil-Containing Zeolites, Part 3. Co2+ Ion Sites and Their Occupation in ZSM-5: A VIS Diffuse Reflectance Spectroscopy Study. *Microporous and Mesoporous Materials* **2000**, *35–6*, 483–494.

[7] Dedecek, J.; Lucero, M.J.; Li, C.B.; Gao, F.; Klein, P.; Urbanova, M.; Tvaruzkova, Z.; Sazama, P.; Sklenak, S. Complex Analysis of the Aluminum Siting in the Framework of Silicon-Rich Zeolites. A Case Study on Ferrierites. *Journal of Physical Chemistry C* **2011**, *115*(22), 11056–11064.

[8] Sklenak, S.; Dedecek, J.; Li, C.; Wichterlova, B.; Gabova, V.; Sierka, M.; Sauer, J. Aluminium Siting in the ZSM-5 Framework by Combination of High Resolution Al-27 NMR and DFT/MM Calculations. *Physical Chemistry Chemical Physics* **2009**, *11*(8), 1237–1247.

[9] (a) Dedecek, J.; Capek, L.; Sazama, P.; Sobalik, Z.; Wichterlova, B. Control of Metal Ion Species in Zeolites by Distribution of Aluminium in the Framework: From Structural Analysis to Performance Under Real Conditions of SCR-NOx and NO, N2O Decomposition. *Applied Catalysis a-General* **2011**, *391*(1–2), 244–253; (b) Dalconi, M.C.; Cruciani, G.; Alberti, A.; Ciambelli, P.; Rapacciuolo, M.T. Ni2+ Ion Sites in Hydrated and Dehydrated Forms of Ni-Exchanged Zeolite Ferrierite. *Microporous and Mesoporous Materials* **2000**, *39*(3), 423–430; (c) Dalconi, M.C.; Cruciani, G.; Alberti, A.; Ciambelli, P. Co- and Ni-Exchanged Ferrierite: The Contribution of Synchrotron X-Ray Diffraction Data to Siting of TMIs. *Catalysis Today* **2005**, *110*(3–4), 345–350; (d) Dalconi, M.C.; Alberti,

A.; Cruciani, G.; Ciambelli, P.; Fonda, E. Siting and Coordination of Cobalt in Ferrierite: XRD and EXAFS Studies at Different Co Loadings. *Microporous and Mesoporous Materials* **2003**, *62*(3), 191–200; (e) Dalconi, M.C.; Alberti, A.; Cruciani, G. Cation Migration and Structural Modification of Co-Exchanged Ferrierite Upon Heating: A Time-Resolved X-Ray Powder Diffraction Study. *Journal of Physical Chemistry B* **2003**, *107*(47), 12973–12980.

[10] (a) Bortnovsky, O.; Tokarova, V.; Wichterlova, B.; Dedecek, J.; Sobalik, Z.; Gonsiorova, O.; Balgova, V. Method of Manufacture of Zeolites with Pentasil Structure with Controlled Distribution of Aluminium Atoms in the Skeleton, PCT/CZ2010/000113. 2010; (b) Gabova, V. The effect of the synthesis conditions on the distribution of aluminium in the framework of zeolite ZSM-5. Ph.D. Thesis, Institute of Chemical Technology, J. Heyrovsky Institute of Physical Chemistry, Prague, 2005.

[11] (a) Pinar, A.B.; Marquez-Alvarez, C.; Grande-Casas, M.; Perez-Pariente, J. Template-Controlled Acidity and Catalytic Activity of Ferrierite Crystals. *Journal of Catalysis* **2009**, *263*(2), 258–265; (b) Pinar, A.B.; Wright, P.A.; Gomez-Hortiguela, L.; Perez-Pariente, J. Synthesis of Ferrierite Zeolite with Pyrrolidine as Structure Directing Agent: A Combined X-Ray Diffraction and Computational Study. *Microporous and Mesoporous Materials* **2010**, *129*(1–2), 164–172; (c) Roman-Leshkov, Y.; Moliner, M.; Davis, M.E. Impact of Controlling the Site Distribution of Al Atoms on Catalytic Properties in Ferrierite-Type Zeolites. *Journal of Physical Chemistry C* **2011**, *115*(4), 1096–1102.

[12] (a) Suib, S.L.; Stucky, G.D.; Blattner, R.J. Auger-Spectroscopy Studies of Natural and Synthetic Zeolites .1. Surface and Bulk Compositions. *Journal of Catalysis* **1980**, *65*(1), 174–178; (b) Lin, J.C.; Chao, K.J. Distribution of Silicon-to-Aluminum Ratios in Zeolite ZSM-5. *Journal of the Chemical Society-Faraday Transactions I* **1986**, *82*, 2645–2649.

[13] Groen, J.C.; Moulijn, J.A.; Perez-Ramirez, J. Desilication: On the Controlled Generation of Mesoporosity in MFI Zeolites. *Journal of Materials Chemistry* **2006**, *16*(22), 2121–2131.

[14] van Bokhoven, J.A.; Danilina, N. Aluminum in zeolites: Where is it and what is its structure? In *Zeolites and Catalysis*; Wiley-VCH Verlag GmbH & Co. KGaA: Weinheim, 2010; pp. 283–300.

[15] Loewenstein, W., The Distribution of Aluminum in the Tetrahedra of Silicates ond Aluminates. *American Mineralogist* **1954**, *39*(1–2), 92–96.

[16] (a) Lippmaa, E.; Magi, M.; Samoson, A.; Tarmak, M.; Engelhardt, G. Investigation of the Structure of Zeolites by Solid-State High-Resolution Si-29 NMR-Spectroscopy. *Journal of the American Chemical Society* **1981**, *103*(17), 4992–4996; (b) Engelhardt, G.; Lippmaa, E.; Magi, M. Ordering of Silicon and Aluminum Ions in the Framework of NaX Zeolites - A Solid-State High-Resolution Si-29 NMR-Study. *Journal of the Chemical Society-Chemical Communications* **1981**, (14), 712–713; (c) Klinowski, J.; Ramdas, S.; Thomas, J.M.; Fyfe, C.A.; Hartman, J.S. A Reexamination of Si, Al Ordering in Zeolites NaX and NaY. *Journal of the Chemical Society-Faraday Transactions II* **1982**, *78*, 1025–1050; (d) Melchior, M.T.; Vaughan, D.E.W.; Jacobson, A.J. Characterization of the Silicon Aluminum Distribution In Synthetic Faujasites By High-Resolution Solid-State Si-29 NMR. *Journal of the American Chemical Society* **1982**, *104*(18), 4859–4864; (e) Mackenzie, K.J.D.; Smith, M.E. *Multinuclear Solid State NMR of Inorganic Materials*. Elsevier: 2002; (f) Engelhardt, G.; Michel, A.D. *High-Resolusion Solid State NMR of Siilicates and Zeolites*; John Willey and Sons: New York, 1987.

[17] (a) Thomas, J.M.; Klinowski, J. The Study of Aluminosilicate and Related Catalysts by High-Resolution Solid-State NMR-Spectroscopy. *Advances in Catalysis* **1985**, *33*, 199–374; (b) Fyfe, C.A.; Gobbi, G.C.; Kennedy, G.J. Investigation of the Conversion (Dealumination) of ZSM-5 into Silicalite by High-Resolution Solid-State Si-29 and Al-27 MAS NMR-Spectroscopy. *Journal of Physical Chemistry* **1984**, *88*(15), 3248–3253; (c) Duer, M.J. *Solid-State NMR Spectroscopy: Principles and Applications;* Blackwell Science: Oxford, 2002.

[18] Fyfe, C.A.; Kennedy, G.J.; Kokotailo, G.T.; Deschutter, C.T. Investigation of the Dealumination of High Silica Zeolite A (ZK-4) by Si-29 Magic-Angle-Spinning NMR-Spectroscopy. *Journal of the Chemical Society-Chemical Communications* **1984**, (16), 1093–1094.

[19] Engelhardt, G.; Lohse, U.; Lippmaa, E.; Tarmak, M.; Magi, M. Si-29NMR Investigation of Silicon-Aluminum Ordering in the Aluminosilicate Framework of Faujasite-Type Zeolites. *Zeitschrift Fur Anorganische Und Allgemeine Chemie* **1981**, *482*(11), 49–64.

[20] Dedecek, J.; Wichterlova, B. Co2+ Ion Siting in Pentasil-Containing Zeolites. I. Co2+ Ion Sites and Their Occupation in Mordenite. A Vis-NIR Diffuse Reflectance Spectroscopy Study. *Journal of Physical Chemistry B* **1999**, *103*(9), 1462–1476.

[21] Benco, L.; Bucko, T.; Hafner, J.; Toulhoat, H. Periodic DFT Calculations of the Stability of Al/Si Substitutions and Extra framework Zn2+ Cations in Mordenite and Reaction Pathway for the Dissociation of H-2 and CH4. *Journal of Physical Chemistry B* **2005**, *109*(43), 20361–20369.

[22] Lever, A.B.P., *Inorganic Electronic Spectroscopy*, 2nd ed.; Elsevier: Amsterdam, 1984, p. 864.

[23] (a) Kaucky, D.; Dedecek, J.I.; Wichterlova, B. Co2+ Ion Siting in Pentasil-Containing Zeolites II. Co2+ Ion Sites and Their Occupation in Ferrierite. A VIS Diffuse Reflectance Spectroscopy Study. *Microporous and Mesoporous Materials* **1999**, *31*(1–2), 75–87; (b) Dedecek, J.; Capek, L.; Kaucky, D.; Sobalik, Z.; Wichterlova, B. Siting and Distribution of the Co Ions in Beta Zeolite: A UV-Vis-NIR and FTIR Study. *Journal of Catalysis* **2002**, *211*(1), 198–207.

[24] Dedecek, J.; Cejka, J.; Oberlinger, M.; Ernst, S. Aluminium Distribution in MCM-22. The Effect of Framework Aluminium Content and Synthesis Procedure. In *Impact of Zeolites and Other Porous Materials on the New Technologies at the Beginning of the New Millennium, Pts A and B*, Aiello, R.; Giordano, G.; Testa, F., Eds.; 2002; Vol. 142, Elsevier: Amsterdam, pp. 23–30.

[25] Yu, Z.W.; Zheng, A.M.; Wang, Q.A.; Chen, L.; Xu, J.; Amoureux, J.P.; Deng, F. Insights into the Dealumination of Zeolite HY Revealed by Sensitivity-Enhanced Al-27 DQ-MAS NMR Spectroscopy at High Field. *Angewandte Chemie-International Edition* **2010**, *49*(46), 8657–8661.

[26] (a) Li, S.H.; Zheng, A.M.; Su, Y.C.; Zhang, H.L.; Chen, L.; Yang, J.; Ye, C.H.; Deng, F. Bronsted/Lewis Acid Synergy in Dealuminated HY Zeolite: A Combined Solid-State NMR and Theoretical Calculation Study. *Journal of the American Chemical Society* **2007**, *129*(36), 11161–11171; (b) Li, S.H.; Huang, S.J.; Shen, W.L.; Zhang, H.L.; Fang, H.J.; Zheng, A.M.; Liu, S.B.; Deng, F. Probing the Spatial Proximities Among Acid Sites in Dealuminated H-Y Zeolite by Solid-State NMR Spectroscopy. *Journal of Physical Chemistry C* **2008**, *112*(37), 14486–14494.

[27] (a) Derewinski, M.; Sarv, P.; Mifsud, A. Thermal Stability and Siting of Aluminum in Isostructural ZSM-22 and Theta-1 Zeolites. *Catalysis Today* **2006**, *114*(2–3), 197–204; (b) Sarv, P.; Wichterlova, B.; Cejka, J. Multinuclear MQMAS

NMR Study of NH4/Na-Ferrierites. *Journal of Physical Chemistry B* **1998**, *102*(8), 1372–1378.

[28] (a) Fernandez, C.; Amoureux, J.P. Triple-Quantum MAS-NMR of Quadrupolar Nuclei. *Solid State Nuclear Magnetic Resonance* **1996**, *5*(4), 315–321; (b) Medek, A.; Harwood, J.S.; Frydman, L. Multiple-Quantum Magic-Angle Spinning NMR: A New Method for the Study of Quadrupolar Nuclei in Solids. *Journal of the American Chemical Society* **1995**, *117*(51), 12779–12787.

[29] (a) Kunkeler, P.J.; Zuurdeeg, B.J.; van der Waal, J.C.; van Bokhoven, J.A.; Koningsberger, D.C.; van Bekkum, H. Zeolite Beta: The Relationship Between Calcination Procedure, Aluminum Configuration, and Lewis Acidity. *Journal of Catalysis* **1998**, *180*(2), 234–244; (b) Sklenak, S.; Dedecek, J.; Li, C.B.; Gao, F.; Jansang, B.; Boekfa, B.; Wichterlova, B.; Sauer, J. Aluminum Siting in the ZSM-22 and Theta-1 Zeolites Revisited: A QM/MM Study. *Collection of Czechoslovak Chemical Communications* **2008**, *73*(6–7), 909–920; (c) Dedecek, J.; Sklenak, S.; Li, C.; Wichterlova, B.; Gabova, V.; Brus, J.; Sierka, M.; Sauer, J. Effect of Al-Si-Al and Al-Si-Si-Al Pairs in the ZSM-5 Zeolite Framework on the Al-27 NMR Spectra. A Combined High-Resolution Al-27 NMR and DFT/MM Study. *Journal of Physical Chemistry C* **2009**, *113*(4), 1447–1458; (d) Dedecek, J.; Sklenak, S.; Li, C. B.; Gao, F.; Brus, J.; Zhu, Q.J.; Tatsumi, T. Effect of Al/Si Substitutions and Silanol Nests on the Local Geometry of Si and Al Framework Sites in Silicone-Rich Zeolites: A Combined High Resolution Al-27 and Si-29 NMR and Density Functional Theory/Molecular Mechanics Study. *Journal of Physical Chemistry C* **2009**, *113*(32), 14454–14466.

[30] Lippmaa, E.; Samoson, A.; Magi, M. High-Resolution Al-27 NMR of Aluminosilicates. *Journal of the American Chemical Society* **1986**, *108*(8), 1730–1735.

[31] (a) Kucera, J.; Nachtigall, P. Al-27 NMR Chemical Shifts do Not Correlate with Average T-O-T Angles: Theoretical Study of MCM-58 Zeolite. In *Molecular Sieves: From Basic Research to Industrial Applications, Pts A and B*, Cejka, J.; Zilkova, N.; Nachtigall, P., Eds.; 2005, Vol. 158, pp. 917–924; (b) Kucera, J.; Nachtigall, P. A Simple Correlation Between Average T-O-T Angles and Al-27 NMR Chemical Shifts Does Not Hold in High-Silica Zeolites. *Microporous and Mesoporous Materials* **2005**, *85*(3), 279–283.

[32] (a) Chatterjee, A.; Chandra, A.K. Fe and B Substitution in ZSM-5 Zeolites: A Quantum-Mechanical Study. *Journal of Molecular Catalysis a-Chemical* **1997**, *119*(1–3), 51–56; (b) Schroder, K.P.; Sauer, J.C.; Leslie, M.; Richard, C.; Catlow, A. Siting of Al and Bridging Hydroxyl-Groups in ZSM-5 - A Computer-Simulation Study. *Zeolites* **1992**, *12*(1), 20–23; (c) Derouane, E.G.; Fripiat, J.G. Non-Empirical Quantum Chemical Study of the Siting and Pairing of Aluminum in the MFI Framework. *Zeolites* **1985**, *5*(3), 165–172; (d) Morales, J.; Bonillamarin, M.; Langagne, A. Theoretical-Study on Al Multiple Substitutions in the MFI Zeolite. *International Journal of Quantum Chemistry* **1991**, 659–669; (e) Omalley, P.J.; Dwyer, J. Ab Initio Molecular-Orbital Calculations on the Siting of Aluminum in the Theta-1 Framework - Some General Guidelines Governing the Site Preferences of Aluminum in Zeolites. *Zeolites* **1988**, *8*(4), 317–321; (f) Alvaradoswaisgood, A.E.; Barr, M.K.; Hay, P.J.; Redondo, A. Ab Initio Quantum Chemical Calculations of Aluminum Substitution in Zeolite ZSM-5. *Journal of Physical Chemistry* **1991**, *95*(24), 10031–10036; (g) Lonsinger, S.R.; Chakraborty, A.K.; Theodorou, D.N.; Bell, A.T. The Effects of Local Structural Relaxation on Aluminum Siting within H-ZSM-5. *Catalysis Letters* **1991**, *11*(2), 209–217; (h) Papai, I.; Goursot, A.; Fajula, F.; Weber, J. Density-Functional Calculations on Model Clusters of Zeolite-Beta. *Journal of Physical Chemistry* **1994**, *98*(17), 4654–4659; (i) Blanco, F.; Urbinavillalba, G.; Deagudelo, M.M.R.,

Theoretical Calculations on Zeolites - The Aluminum Substitution in Mordenite, Ferrierite and ZSM-5. *Molecular Simulation* **1995**, *14*(3), 165–176; (j) Grillo, M.E.; Carrazza, J. Computer Simulation Study of Aluminum Incorporation in the Microporous Titanosilicate ETS-10. *Journal of Physical Chemistry B* **1997**, *101*(34), 6749–6752; (k) Grau-Crespo, R.; Peralta, A.G.; Ruiz-Salvador, A.R.; Gomez, A.; Lopez-Cordero, R. A Computer Simulation Study of Distribution, Structure and Acid Strength of Active Sites in H-ZSM-5 Catalyst. *Physical Chemistry Chemical Physics* **2000**, *2*(24), 5716–5722; (l) Zhou, D.H.; Bao, Y.; Yang, M.M.; He, N.; Yang, G. DFT Studies on the Location and Acid Strength of Bronsted Acid Sites in MCM-22 Zeolite. *Journal of Molecular Catalysis a-Chemical* **2006**, *244*(1–2), 11–19.

[33] Sastre, G.; Fornes, V.; Corma, A. On the Preferential Location of Al and Proton Siting in Zeolites: A Computational and Infrared Study. *Journal of Physical Chemistry B* **2002**, *106*(3), 701–708.

[34] (a) Olson, D.H.; Khosrovani, N.; Peters, A.W.; Toby, B.H. Crystal Structure of Dehydrated CsZSM-5 (5.8A1): Evidence for Nonrandom Aluminum Distribution. *Journal of Physical Chemistry B* **2000**, *104*(20), 4844–4848; (b) Heo, N.H.; Kim, C.W.; Kwon, H.J.; Kim, G.H.; Kim, S.H.; Hong, S.B.; Seff, K. Detailed Determination of the Tl+ Positions in Zeolite Tl-ZSM-5. Single-Crystal Structures of Fully Dehydrated Tl-ZSM-5 and H-ZSM-5 (MFI, Si/Al=29). Additional Evidence for a Nonrandom Distribution of Framework Aluminum. *Journal of Physical Chemistry C* **2009**, *113*(46), 19937–19956; (c) Mentzen, B.F. Crystallographic Determination of the Positions of the Monovalent H, Li, Na, K, Rb, and Tl Cations in Fully Dehydrated MFI Type Zeolites. *Journal of Physical Chemistry C* **2007**, *111*(51), 18932–18941; (d) Mentzen, B.F.; Bergeret, G.; Emerich, H.; Weber, H.P. Dehydrated and Cs+-Exchanged MFI Zeolites: Location and Population of Cs+ from In Situ Diffraction Data as a Function of Temperature and Degree of Exchange. *Journal of Physical Chemistry B* **2006**, *110*(1), 97–106.

[35] Galli, E.; Vezzalini, G.; Quartieri, S.; Alberti, A.; Franzini, M. Mutinaite, A New Zeolite from Antarctica: The natural counterpart of ZSM-5. *Zeolites* **1997**, *19*(5–6), 318–322.

[36] Dempsey, E. Calculation of Madelung Potentials for Faujasite-Type Zeolites. I. *Journal of Physical Chemistry* **1969**, *73*(11), 3660–3668.

[37] Melchior, M.T.; Vaughan, D.E.W.; Jarman, R.H.; Jacobson, A.J. The Characterization of Si-Al Ordering in A-Type Zeolite (Zk4) by Si-29 NMR. *Nature* **1982**, *298*(5873), 455–456.

[38] (a) Takaishi, T.; Kato, M.; Itabashi, K. Stability of the Al-O-Si-O-Al Linkage in a Zeolitic Framework. *Journal of Physical Chemistry* **1994**, *98*(22), 5742–5743; (b) Takaishi, T.; Kato, M.; Itabashi, K. Determination of the Ordered Distribution of Aluminum Atoms in a Zeolitic Framework. 2. *Zeolites* **1995**, *15*(1), 21–32.

[39] (a) Muller, M.; Harvey, G.; Prins, R. Comparison of the Dealumination of Zeolites Beta, Mordenite, ZSM-5 and Ferrierite by Thermal Treatment, Leaching with Oxalic Acid and Treatment with SiCl4 by H-1, Si-29 and Al-27 MAS NMR. *Microporous and Mesoporous Materials* **2000**, *34*(2), 135–147; (b) Kiricsi, I.; Flego, C.; Pazzuconi, G.; Parker, W.O.; Millini, R.; Perego, C.; Bellussi, G. Progress Toward Understanding Zeolite-Beta Acidity - An IR and Al-27 NMR Spectroscopic Study. *Journal of Physical Chemistry* **1994**, *98*(17), 4627–4634.

[40] (a) Szostak, R.; Lillerud, K.P.; Stocker, M. Properties of Tschernichite, the Aluminum-Rich Mineral Analog of Zeolite-Beta. *Journal of Catalysis* **1994**, *148*(1), 91–99; (b) Majano, G.; Delmotte, L.; Valtchev, V.; Mintova, S. Al-Rich

Zeolite Beta by Seeding in the Absence of Organic Template. *Chemistry of Materials* **2009**, *21*(18), 4184–4191.

[41] (a) Borade, R.B.; Clearfield, A. Synthesis of Beta Zeolite with High Levels of Tetrahedral Aluminium. *Chemical Communications* **1996**, (5), 625–626; (b) Vaudry, F.; DiRenzo, F.; Espiau, P.; Fajula, F.; Schulz, P. Aluminum-Rich Zeolite Beta. *Zeolites* **1997**, *19*(4), 253–258; (c) Mostowicz, R.; Testa, F.; Crea, F.; Aiello, R.; Fonseca, A.; Nagy, J.B. Synthesis of Zeolite Beta in Presence of Fluorides: Influence of Alkali Cations. *Zeolites* **1997**, *18*(5–6), 308–324.

[42] (a) Brandenberger, S.; Krocher, O.; Tissler, A.; Althoff, R. The State of the Art in Selective Catalytic Reduction of NOx by Ammonia Using Metal-Exchanged Zeolite Catalysts. *Catalysis Reviews-Science and Engineering* **2008**, *50*(4), 492–531; (b) Bortnovsky, O.; Sobalik, Z.; Wichterlova, B.; Bastl, Z. Structure of Al-Lewis Site in Beta Zeolite Active in the Meerwein-Ponndorf-Verley Reduction of Ketone to Alcohol. *Journal of Catalysis* **2002**, *210*(1), 171–182.

[43] (a) Capek, L.; Dedecek, J.; Wichterlova, B. Co-Beta Zeolite Highly Active in Propane-SCR-NOx in the Presence of Water Vapor: Effect of Zeolite Preparation and Al Distribution in the Framework. *Journal of Catalysis* **2004**, *227*(2), 352–366; (b) Capek, L.; Dedecek, J.; Sazama, P.; Wichterlova, B. The Decisive Role of the Distribution of Al in the Framework of Beta Zeolites on the Structure and Activity of Co Ion Species in Propane-SCR-NOx in the Presence of Water Vapour. *Journal of Catalysis* **2010**, *272*(1), 44–54.

[44] (a) Katada, N.; Kanai, T.; Niwa, M. Dealumination of Proton Form Mordenite with High Aluminum Content in Atmosphere. *Microporous and Mesoporous Materials* **2004**, *75*(1–2), 61–67; (b) Koranyi, T.I.; Nagy, J.B. Distribution of Aluminum in Different Periodical Building Units of MOR and BEA Zeolites. *Journal of Physical Chemistry B* **2005**, *109*(33), 15791–15797.

[45] (a) Kato, M.; Itabashi, K.; Matsumoto, A.; Tsutsumi, K. Characteristics of MOR-Framework Zeolites Synthesized in Fluoride-Containing Media and Related Ordered Distribution of Al Atoms in the Framework. *Journal of Physical Chemistry B* **2003**, *107*(8), 1788–1797; (b) Bodart, P.; Nagy, J.B.; Debras, G.; Gabelica, Z.; Jacobs, P.A. Aluminum Siting in Mordenite and Dealumination Mechanism. *Journal of Physical Chemistry* **1986**, *90*(21), 5183–5190; (c) de Macedo, J.L.; Dias, S.C.L.; Dias, J.A. Multiple Adsorption Process Description of Zeolite Mordenite Acidity. *Microporous and Mesoporous Materials* **2004**, *72*(1–3), 119–125; (d) Paixao, V.; Carvalho, A.P.; Rocha, J.; Fernandes, A.; Martins, A. Modification of MOR by Desilication Treatments: Structural, Textural and Acidic Characterization. *Microporous and Mesoporous Materials* **2010**, *131*(1–3), 350–357.

[46] Sklenak, S.; Andrikopoulos, P.C.; Boekfa, B.; Jansang, B.; Novakova, J.; Benco, L.; Bucko, T.; Hafner, J.; Dedecek, J.; Sobalik, Z. N2O Decomposition Over Fe-Zeolites: Structure of the Active Sites and the Origin of the Distinct Reactivity of Fe-ferrierite, Fe-ZSM-5, and Fe-Beta. A Combined Periodic DFT and Multispectral Study. *Journal of Catalysis* **2010**, *272*(2), 262–274.

[47] Garcia, R.; Gomez-Hortiguela, L.; Blasco, T.; Perez-Pariente, J. Layering of Ferrierite Sheets by Using Large Co-Structure Directing Agents: Zeolite Synthesis Using 1-Benzyl-1-Methylpyrrolidinium and Tetraethylammonium. *Microporous and Mesoporous Materials* **2010**, *132*(3), 375–383.

[48] Gil, B.; Mokrzycki, L.; Sulikowski, B.; Olejniczak, Z.; Walas, S. Desilication of ZSM-5 and ZSM-12 Zeolites: Impact on Textural, Acidic and Catalytic Properties. *Catalysis Today* **2010**, *152*(1–4), 24–32.

[49] (a) Vuono, D.; Pasqua, L.; Testa, F.; Aiello, R.; Fonseca, A.; Koranyi, T.I.; Nagy, J.B. Influence of NaOH and KOH on the Synthesis of MCM-22 and MCM-49 Zeolites. *Microporous and Mesoporous Materials* **2006**, *97*(1–3), 78–87; (b) Delitala, C.; Alba, M.D.; Becerro, A.I.; Delpiano, D.; Meloni, D.; Musu, E.; Ferino, I. Synthesis of MCM-22 Zeolites of Different Si/Al Ratio and Their Structural, Morphological and Textural Characterisation. *Microporous and Mesoporous Materials* **2009**, *118*(1–3), 1–10.

[50] Sobalik, Z.; Novakova, J.; Dedecek, J.; Sathu, N.K.; Tabor, E.; Sazama, P.; Stastny, P.; Wichterlova, B. Tailoring of Fe-Ferrierite for N2O Decomposition: On the Decisive Role of Framework Al Distribution for Catalytic Activity of Fe Species in Fe-Ferrierite. *Microporous and Mesoporous Materials* **2011**, *146*(1–3), 172–183.

[51] Kaucky, D.; Sobalik, Z.; Schwarze, M.; Vondrova, A.; Wichterlova, B. Effect of FeH-Zeolite Structure and Al-Lewis Sites on N2O Decomposition and NO/NO2-Assisted Reaction. *Journal of Catalysis* **2006**, *238*(2), 293–300.

[52] Dedecek, J.; Kaucky, D.; Wichterlova, B. Does Density of Cationic Sites Affect Catalytic Activity of Co Zeolites in Selective Catalytic Reduction of NO with Methane? *Topics in Catalysis* **2002**, *18*(3–4), 283–290.

[53] Vaughan, P.A. Crystal Structure of Zeolite Ferrierite. *Acta Crystallographica* **1966**, *21*, 983–990.

[54] (a) Papiz, Z.; Andrews, S.J.; Damas, A.M.; Harding, M.M.; Highcock, R.M. Structure of the Zeolite Theta-1 - Redetermination Using Single-Crystal Synchrotron-Radiation Data. *Acta Crystallographica Section C-Crystal Structure Communications* **1990**, *46*, 172–173; (b) Barri, S.A.I.; Smith, G.W.; White, D.; Young, D. Structure of Theta-1, the 1st Unidimensional Medium-Pore High-Silica Zeolite. *Nature* **1984**, *312*(5994), 533–534; (c) Highcock, R.M.; Smith, G.W.; Wood, D. Structure of the New Zeolite Theta-1 Determined from X-Ray-Powder Data. *Acta Crystallographica Section C-Crystal Structure Communications* **1985**, *41*(OCT), 1391–1394.

[55] Abraham, A.; Lee, S.H.; Shin, C.H.; Hong, S.B.; Prins, R.; van Bokhoven, J.A. Influence of Framework Silicon to Aluminium Ratio on Aluminium Coordination and Distribution in Zeolite Beta Investigated by Al-27 MAS and Al-27 MQ MAS NMR. *Physical Chemistry Chemical Physics* **2004**, *6*(11), 3031–3036.

[56] Kennedy, G.J.; Lawton, S.L.; Fung, A.S.; Rubin, M.K.; Steuernagel, S. Multinuclear MAS NMR Studies of Zeolites MCM-22 and MCM-49. *Catalysis Today* **1999**, *49*(4), 385–399.

[57] Kolodziejski, W.; Zicovichwilson, C.; Corma, A. Al-27 and Si-29 MAS NMR-Study of Zeolite MCM-22. *Journal of Physical Chemistry* **1995**, *99*(18), 7002–7008.

[58] Mortier, W.J., *Extraframework Cationic Positions in Zeolites*; Elsevier: Amsterdam, 1982.

[59] Dedecek, J.; Gabova, V.; Paschkova, V.; P. Klein; Wichterlova, B. *in preparation*.

[60] Schlenker, J.L.; Pluth, J.J.; Smith, J.V. Positions of Cations and Molecules in Zeolites with the Mordenite-Type Framework. 8 Dehydrated Sodium-Exchanged Mordenite. *Materials Research Bulletin* **1979**, *14*(6), 751–758.

[61] (a) Barrer, R.M. *Hydrothermal Chemistry of Zeolites*, Academic Press: London, 1982; (b) Cundy, C.S.; Cox, P.A. The Hydrothermal Synthesis of Zeolites: History and Development from the Earliest Days to the Present Time. *Chemical Reviews* **2003**, *103*(3), 663–701; (c) Cundy, C.S.; Cox, P.A. The Hydrothermal Synthesis of Zeolites: Precursors, Intermediates and Reaction Mechanism. *Microporous and Mesoporous Materials* **2005**, *82*(1–2), 1–78; (d) Tosheva, L.; Valtchev, V.P.

Nanozeolites: Synthesis, Crystallization Mechanism, and Applications. *Chemistry of Materials* **2005**, *17*(10), 2494–2513; (e) Perez-Pariente, J.; Gomer-Hortiguela, L. The Role of Templates in the Synthesis of Zeolites. In *Zeolites: From Model Materials to Industrial Catalysts*, Cejka, J.; Pérez-Pariente, J.; Roth, W.J., Eds.; Transworld Research Network: Trivandrum, 2010; (f) Corma, A.; Davis, M.E. Issues in the Synthesis of Crystalline Molecular Sieves: Towards the Crystallization of Low Framework-Density Structures. *Chemphyschem* **2004**, *5*(3), 304–313; (g) Corma, A.; Garcia, H. Lewis Acids: From Conventional Homogeneous to Green Homogeneous and Heterogeneous Catalysis. *Chemical Reviews* **2003**, *103*(11), 4307–4365; (h) Davis, M.E. Ordered Porous Materials for Emerging Applications. *Nature* **2002**, *417*(6891), 813–821; (i) Schuth, F.; Schmidt, W. Microporous and Mesoporous Materials. *Advanced Materials* **2002**, *14*(9), 629–638.

[62] (a) Pinar, A.B.; Pérez-Pariente, J.; Hortiguela, L.G. Method for Preparation of an Aluminosilicate with Ferrierite Structure from Gels Containing Tetramethyl Ammonium and Benzylmethylpyrrolidine, and Uses Thereof. WO116958, 2008; (b) Marquez-Alvarez, C.; Pinar, A.B.; Garcia, R.; Grande-Casas, M.; Perez-Pariente, J. Influence of Al Distribution and Defects Concentration of Ferrierite Catalysts Synthesized From Na-Free Gels in the Skeletal Isomerization of n-Butene. *Topics in Catalysis* **2009**, *52*(9), 1281–1291.

[63] Carpenter, J.R.; Yeh, S.; Zones, S.I.; Davis, M.E. Further Investigations on Constraint Index Testing of Zeolites that Contain Cages. *Journal of Catalysis* **2010**, *269*(1), 64–70.

[64] Boronat, M.; Martinez-Sanchez, C.; Law, D.; Corma, A. Enzyme-Like Specificity in Zeolites: A Unique Site Position in Mordenite for Selective Carbonylation of Methanol and Dimethyl Ether with CO. *Journal of the American Chemical Society* **2008**, *130*(48), 16316–16323.

[65] Gonsiorova, O. Synthesis and Characterization of ZSM-5 and Beta Zeolites. Evaluation with Respect to the Technological Procedures. Ph.D. Thesis, J. Heyrovsky Institute of Physical Chemistry, Prague, 2007.

[66] Aerts, A.; Kirschhock, C.E.A.; Martens, J.A. Methods for In Situ Spectroscopic Probing of the Synthesis of a Zeolite. *Chemical Society Reviews* **2010**, *39*(12), 4626–4642.

[67] Petrovic, I.; Navrotsky, A.; Davis, M.E.; Zones, S.I. Thermochemical Study of the Stability of Frameworks in High-Silica Zeolites. *Chemistry of Materials* **1993**, *5*(12), 1805–1813.

[68] (a) Chang, C.D.; Bell, A.T. Studies on the Mechanism of ZSM-5 Formation. *Catalysis Letters* **1991**, *8*(5–6), 305–316; (b) de Moor, P.; Beelen, T.P.M.; Komanschek, B.U.; Diat, O.; van Santen, R.A. In Situ Investigation of Si-TPA-MFI Crystallization Using (Ultra-) Small- and Wide-Angle X-Ray Scattering. *Journal of Physical Chemistry B* **1997**, *101*(51), 11077–11086; (c) de Moor, P.; Beelen, T.P.M.; Komanschek, B.U.; Beck, L.W.; Wagner, P.; Davis, M.E.; van Santen, R.A. Imaging the Assembly Process of the Organic-Mediated Synthesis of a Zeolite. *Chemistry-a European Journal* **1999**, *5*(7), 2083–2088.

[69] Flanigen, E.M.; Breck, D.W. In *Growth of zeolite crystals from the gels*, 137th Meeting of the ACS, Division of Inorganic Chemistry, Cleveland, OH, 1960, p. 53-M.

[70] (a) Burkett, S.L.; Davis, M.E. Mechanism of Structure Direction in the Synthesis of Si-ZSM-5 - An Investigation by Intermolecular H-1-SI-29 CP MAS NMR. *Journal of Physical Chemistry* **1994**, *98*(17), 4647–4653; (b) Burkett, S.L.; Davis, M.E. Mechanism of Structure Direction in the Synthesis of Pure-Silica Zeolites. 2. Hydrophobic Hydration and Structural Specificity. *Chemistry of Materials* **1995**,

7(8), 1453–1463; (c) Burkett, S.L.; Davis, M.E. Mechanisms of Structure Direction in the Synthesis of Pure-Silica Zeolites. 1. Synthesis of TPA/Si-ZSM-5. *Chemistry of Materials* **1995**, *7*(5), 920–928.

[71] de Moor, P.; Beelen, T.P.M.; van Santen, R.A.; Beck, L.W.; Davis, M.E. Si-MFI Crystallization Using a "Dimer" and "Trimer" of TPA Studied with Small-Angle X-Ray Scattering. *Journal of Physical Chemistry B* **2000**, *104*(32), 7600–7611.

[72] (a) Kirschhock, C.E.A.; Ravishankar, R.; Van Looveren, L.; Jacobs, P.A.; Martens, J.A. Mechanism of Transformation of Precursors into Nanoslabs in the Early Stages of MFI and MEL Zeolite Formation from TPAOH-TEOS-H2O and TBAOH-TEOS-H2O Mixtures. *Journal of Physical Chemistry B* **1999**, *103*(24), 4972–4978; (b) Kirschhock, C.E.A.; Ravishankar, R.; Verspeurt, F.; Grobet, P.J.; Jacobs, P.A.; Martens, J.A. Identification of Precursor Species in the Formation of MFI Zeolite in the TPAOH-TEOS-H2O System. *Journal of Physical Chemistry B* **1999**, *103*(24), 4965–4971; (c) Kirschhock, C.E.A.; Ravishankar, R.; Jacobs, P.A.; Martens, J.A. Aggregation Mechanism of Nanoslabs with Zeolite MFI-Type Structure. *Journal of Physical Chemistry B* **1999**, *103*(50), 11021–11027; (d) Kirschhock, C.E.A.; Buschmann, V.; Kremer, S.; Ravishankar, R.; Houssin, C.J.Y.; Mojet, B.L.; van Santen, R.A.; Grobet, P.J.; Jacobs, P.A.; Martens, J.A. Zeosil Nanoslabs: Building Blocks in nPr(4)N(+)-Mediated Synthesis of MFI Zeolite. *Angewandte Chemie-International Edition* **2001**, *40*(14), 2637–2640; (e) Kirschhock, C.E.A.; Kremer, S.P.B.; Grobet, P.J.; Jacobs, P.A.; Martens, J.A. New Evidence for Precursor Species in the Formation of MFI Zeolite in the Tetrapropylammonium Hydroxide-Tetraethyl Orthosilicate-Water System. *Journal of Physical Chemistry B* **2002**, *106*(19), 4897–4900; (f) Houssin, C.J.Y.; Kirschhock, C.E.A.; Magusin, P.; Mojet, B.L.; Grobet, P.J.; Jacobs, P.A.; Martens, J.A.; van Santen, R.A. Combined In Situ Si-29 NMR and Small-Angle X-Ray Scattering Study of Precursors in MFI Zeolite Formation from Silicic Acid in TPAOH Solutions. *Physical Chemistry Chemical Physics* **2003**, *5*(16), 3518–3524.

[73] Kirschhock, C.E.A.; Kremer, S.P.B.; Vermant, J.; Van Tendeloo, G.; Jacobs, P.A.; Martens, J.A, Design and Synthesis of Hierarchical Materials from Ordered Zeolitic Building Units. *Chemistry-a European Journal* **2005**, *11*(15), 4306–4313.

[74] Kirschhock, C.E.A.; Ravishankar, R.; Verspeurt, F.; Grobet, P.J.; Jacobs, P.A.; Martens, J.A. Reply to the Comment on "Identification of Precursor Species in the Formation of MFI Zeolite in the TPAOH-TEOS-H2O System". *Journal of Physical Chemistry B* **2002**, *106*(12), 3333–3334.

[75] (a) Pelster, S.A.; Kalamajka, R.; Schrader, W.; Schuth, F. Monitoring the Nucleation of Zeolites by Mass Spectrometry. *Angewandte Chemie-International Edition* **2007**, *46*(13), 2299–2302; (b) Pelster, S.A.; Schuth, F.; Schrader, W.G. Detailed Study on the Use of Electrospray Mass Spectrometry to Investigate Speciation in Concentrated Silicate Solutions. *Analytical Chemistry* **2007**, *79*(15), 6005–6012; (c) Pelster, S.A.; Weimann, B.; Schaack, B.B.; Schrader, W.; Schuth, F. Dynamics of Silicate Species in Solution Studied by Mass Spectrometry with Isotopically Labeled Compounds. *Angewandte Chemie-International Edition* **2007**, *46*(35), 6674–6677; (d) Pelster, S.A.; Schrader, W.; Schuth, F. Monitoring Temporal Evolution of Silicate Species During Hydrolysis and Condensation of Silicates Using Mass Spectrometry. *Journal of the American Chemical Society* **2006**, *128*(13), 4310–4317.

[76] Vankoningsveld, H.; Vanbekkum, H.; Jansen, J.C. On the Location and Disorder of the Tetrapropylammonium (TPA) Ion in Zeolite ZSM-5 with Improved Framework Accuracy. *Acta Crystallographica Section B-Structural Science* **1987**, *43*, 127–132.

[77] (a) Wouters, B.H.; Chen, T.H.; Grobet, P.J. Steaming of Zeolite Y: Formation of Transient Al Species. *Journal of Physical Chemistry B* **2001**, *105*(6), 1135–1139;

(b) Remy, M.J.; Stanica, D.; Poncelet, G.; Feijen, E.J.P.; Grobet, P.J.; Martens, J.A.; Jacobs, P.A. Dealuminated H-Y Zeolites: Relation Between Physicochemical Properties and Catalytic Activity in Heptane and Decane Isomerization. *Journal of Physical Chemistry* **1996**, *100*(30), 12440–12447; (c) Do, T.O.; Nossov, A.; Springuel-Huet, M.A.; Schneider, C.; Bretherton, J.L.; Fyfe, C.A.; Kaliaguine, S. Zeolite Nanoclusters Coated onto the Mesopore Walls of SBA-15. *Journal of the American Chemical Society* **2004**, *126*(44), 14324–14325.

[78] (a) Wichterlova, B.; Tvaruzkova, Z.; Sobalik, Z.; Sarv, P. Determination and Properties of Acid Sites in H-Ferrierite - A Comparison of Ferrierite and MFI Structures. *Microporous and Mesoporous Materials* **1998**, *24*(4–6), 223–233; (b) Sazama, P.; Wichterlova, B.; Dedecek, J.; Tvaruzkova, Z.; Musilova, Z.; Palumbo, L.; Sklenak, S.; Gonsiorova, O. FTIR and Al-27 MAS NMR Analysis of the Effect of Framework Al- and Si-Defects in Micro- and Micro-Mesoporous H-ZSM-5 on Conversion of Methanol to Hydrocarbons. *Microporous and Mesoporous Materials* **2011**, *143*(1), 87–96.

[79] Dedecek, J.; Tvaruzkova, Z.; Urbanova, M.; Wichterlova, B. Structural Parameters Controlling Formation of Framework Al-Lewis Sites in Silicon Rich Zeolites. Multi-spectroscopic Study of ZSM-5, submitted.

[80] Sonnemans, M.H.W.; Denheijer, C.; Crocker, M. Studies on the Acidity of Mordenite and ZSM-5. 2. Loss of Bronsted Acidity by Dehydroxylation and Dealumination. *Journal of Physical Chemistry* **1993**, *97*(2), 440–445.

[81] Sazama, P.; Dedecek, J.; Gabova, V.; Wichterlova, B.; Spoto, G.; Bordiga, S. Effect of Aluminium Distribution in the Framework of ZSM-5 on Hydrocarbon Transformation. Cracking of 1-Butene. *Journal of Catalysis* **2008**, *254*(2), 180–189.

[82] Klier, K., Transition-Metal Ions in Zeolites - The Perfect Surface Sites. *Langmuir* **1988**, *4*(1), 13–25.

[83] (a) Park, J.H.; Park, C.H.; Nam, I.S. Characteristics of Wet and Solid Ion Exchanged Co-Ferrierite Catalysts for the Reduction of NO Using Methane. *Applied Catalysis a-General* **2004**, *277*(1–2), 271–279; (b) Chupin, C.; van Veen, A.C.; Konduru, M.; Despres, J.; Mirodatos, C. Identity and Location of Active Species for NO Reduction by CH4 Over Co-ZSM-5. *Journal of Catalysis* **2006**, *241*(1), 103–114; (c) Indovina, V.; Campa, M.C.; Pietrogiacomi, D. Isolated Co2+ and Co-O-Co (2+) Species in Na-MOR Exchanged with Cobalt to Various Extents: An FTIR Characterization by CO Adsorption of Oxidized and Prereduced Samples. *Journal of Physical Chemistry C* **2008**, *112*(13), 5093–5101; (d) Wichterlova, B.; Dedecek, J.; Sobalik, Z. Cu Coordination in High Silica Zeolites. Effect of the Framework Al Local Siting. In *Catalysis by Microporous Materials*, Beyer, H.K.; Karge, H.G.; Kiricsi, I.; Nagy, J.B., Eds.; Elsevier: Amsterdam, 1995, Vol. 94, pp. 641–648; (e) Sarkany, J.; Ditri, J.L.; Sachtler, W.M.H. Redox Chemistry in Excessively Ion-Exchanged Cu/Na-ZSM-5. *Catalysis Letters* **1992**, *16*(3), 241–249; (f) TorreAbreu, C.; Ribeiro, M.F.; Henriques, C.; Delahay, G. Characterisation of CuMFI Catalysts by Temperature Programmed Desorption of NO and Temperature Programmed Reduction. Effect of the Zeolite Si/Al Ratio and Copper Loading. *Applied Catalysis B-Environmental* **1997**, *12*(2–3), 249–262; (g) Wichtelova, B.; Sobalik, Z.; Dedecek, J. Redox Catalysis Over Metallo-Zeolites - Contribution to Environmental Catalysis. *Applied Catalysis B-Environmental* **2003**, *41*(1–2), 97–114; (h) Voskoboinikov, T.V.; Chen, H.Y.; Sachtler, W.M.H. On the Nature of Active Sites in Fe/ZSM-5 Catalysts for NOx Abatement. *Applied Catalysis B-Environmental* **1998**, *19*(3–4), 279–287; (i) Mauvezin, M.; Delahay, G.; Coq, B.; Kieger, S.; Jumas, J.C.; Olivier-Fourcade, J. Identification of Iron Species in Fe-BEA: Influence of the Exchange Level. *Journal of Physical*

Chemistry B **2001**, *105*(5), 928–935; (j) Jia, J.F.; Pillai, K.S.; Sachtler, W.M.H. One-Step Oxidation of Benzene to Phenol with Nitrous Oxide Over Fe/MFI Catalysts. *Journal of Catalysis* **2004**, *221*(1), 119–126; (k) Ogura, M.; Kage, S.; Shimojo, T.; Oba, J.; Hayashi, M.; Matsukata, M.; Kikuchi, E. Co Cation Effects on Activity and Stability of Isolated Pd(II) Cations in Zeolite Matrices for Selective Catalytic Reduction of Nitric Oxide with Methane. *Journal of Catalysis* **2002**, *211*(1), 75–84.

[84] (a) Schoonheydt, R.A., Transition-Metal Ions in Zeolites - Siting and Energetics of Cu-2+. *Catalysis Reviews-Science and Engineering* **1993**, *35*(1), 129–168; (b) Armor, J.N., The Remarkable Role of Cations in Molecular Sieves. In *Science and Technology in Catalysis 1994*, Izumi, Y.; Arai, H.; Iwamoto, M., Eds.; Elsevier: Amsterdam, 1995, Vol. 92, pp. 51–62; (c) Verberckmoes, A.A.; Weckhuysen, B.M.; Schoonheydt, R.A. Spectroscopy and Coordination Chemistry of Cobalt in Molecular Sieves. *Microporous and Mesoporous Materials* **1998**, *22*(1–3), 165–178; (d) De Vos, D.E.; Dams, M.; Sels, B.F.; Jacobs, P.A. Ordered Mesoporous and Microporous Molecular Sieves Functionalized with Transition Metal Complexes as Catalysts for Selective Organic Transformations. *Chemical Reviews* **2002**, *102*(10), 3615–3640; (e) Delabie, A.; Pierloot, K.; Groothaert, M.H.; Schoonheydt, R.A.; Vanquickenborne, L.G. The Coordination of Cu-II in Zeolites - Structure and Spectroscopic Properties. *European Journal of Inorganic Chemistry* **2002**, (3), 515–530; (f) Kuroda, Y.; Iwamoto, M. Characterization of Cuprous Ion in High Silica Zeolites and Reaction Mechanisms of Catalytic NO Decomposition and Specific N-2 Adsorption. *Topics in Catalysis* **2004**, *28*(1–4), 111–118; (g) Berthomieu, D.; Jardillier, N.; Delahay, G.; Coq, B.; Goursot, A. Experimental and Theoretical Approaches to the Study of TMI-Zeolite (TM = Fe, Co, Cu). *Catalysis Today* **2005**, *110*(3–4), 294–302; (h) Lamberti, C.; Groppo, E.; Spoto, G.; Bordiga, S.; Zecchina, A. Infrared Spectroscopy of Transient Surface Species. In *Advances in Catalysis, Vol 51*, Elsevier: San Diego, 2007, Vol. 51, pp. 1–74; (i) Zecchina, A.; Rivallan, M.; Berlier, G.; Lamberti, C.; Ricchiardi, G. Structure and Nuclearity of Active Sites in Fe-Zeolites: Comparison with Iron Sites in Enzymes and Homogeneous Catalysts. *Physical Chemistry Chemical Physics* **2007**, *9*(27), 3483–3499; (j) Smeets, P.J.; Woertink, J.S.; Sels, B.F.; Solomon, E.I.; Schoonheydt, R.A. Transition-Metal Ions in Zeolites: Coordination and Activation of Oxygen. *Inorganic Chemistry* **2010**, *49*(8), 3573–3583.

[85] (a) Rice, M.J.; Chakraborty, A.K.; Bell, A.T. Site Availability and Competitive Siting of Divalent Metal Cations in ZSM-5. *Journal of Catalysis* **2000**, *194*(2), 278–285; (b) Rice, M.J.; Chakraborty, A.K.; Bell, A.T. Theoretical Studies of the Coordination and Stability of Divalent Cations in ZSM-5. *Journal of Physical Chemistry B* **2000**, *104*(43), 9987–9992; (c) Feng, X.B.; Hall, W.K. FeZSM-5: A Durable SCR Catalyst for NOx Removal from Combustion Streams. *Journal of Catalysis* **1997**, *166*(2), 368–376.

[86] Brandenberger, S.; Krocher, O.; Tissler, A.; Althoff, R. Estimation of the Fractions of Different Nuclear Iron Species in Uniformly Metal-Exchanged Fe-ZSM-5 Samples Based on a Poisson Distribution. *Applied Catalysis a-General* **2010**, *373*(1–2), 168–175.

[87] Capek, L.; Dedecek, J.; Wichterlova, B.; Cider, L.; Jobson, E.; Tokarova, V. Cu-ZSM-5 Zeolite Highly Active in Reduction of NO with Decane - Effect of Zeolite Structural Parameters on the Catalyst Performance. *Applied Catalysis B-Environmental* **2005**, *60*(3–4), 147–153.

[88] (a) Frising, T.; Leflaive, P. Extraframework Cation Distributions in X and Y Faujasite Zeolites: A Review. *Microporous and Mesoporous Materials* **2008**, *114*(1–3), 27–63; (b) Pickering, I.J.; Maddox, P.J.; Thomas, J.M.; Cheetham, A.K. A Neutron Powder Diffraction Analysis of Potassium-Exchanged Ferrierite.

Journal of Catalysis **1989**, *119*(1), 261–265; (c) Schlenker, J.L.; Pluth, J.J.; Smith, J.V. Positions of Cations and Molecules in Zeolites with Mordenite-Type Framework. 7. Dehydrated Cesium Mordenite. *Materials Research Bulletin* **1978**, *13*(9), 901–905; (d) Schlenker, J.L.; Pluth, J.J.; Smith, J.V. Positions of Cations and Molecules in Zeolites with Mordenite-Type Framework. 6. Dehydrated Barium Mordenite. *Materials Research Bulletin* **1978**, *13*(3), 169–174; (e) Schlenker, J.L.; Pluth, J.J.; Smith, J.V. Positions of Cations and Molecules in Zeolites with Mordenite-Type Framework. 5. Dehydrated Rb-Mordenite. *Materials Research Bulletin* **1978**, *13*(1), 77–82; (f) Schlenker, J.L.; Pluth, J.J.; Smith, J.V. Positions of Cations and Molecules in Zeolites with the Mordenite-Type Framework. 10. Dehydrated Calcium Hydrogen Mordenite. *Materials Research Bulletin* **1979**, *14*(8), 961–966; (g) Mortier, W.J.; Pluth, J.J.; Smith, J.V. Positions of Cations and Molecules in Zeolites with Mordenite-Type Framework. 1. Dehydrated Ca-Exchanged Ptilolite. *Materials Research Bulletin* **1975**, *10*(10), 1037–1045; (h) Attfield, M.P.; Weigel, S.J.; Cheetham, A.K. On the Nature of Nonframework Cations in a Zeolitic deNO(x) Catalyst: Cu-Mordenite. *Journal of Catalysis* **1997**, *170*(2), 227–235.

[89] (a) Baes, C.F., Mesmer, R.E. *The Hydrolysis of Cations*; Wiley: New York, 1976; (b) Richens, T.D., *The Chemistry of Aqua Ions*. Wiley-VCH: Weinheim, 1997.

[90] (a) Iwamoto, M.; Yahiro, H.; Tanda, K.; Mizuno, N.; Mine, Y.; Kagawa, S. Removal of Nitrogen Monoxide Through a Novel Catalytic Process. 1. Decomposition on Excessively Copper-Ion Exchanged ZSM-5 Zeolites. *Journal of Physical Chemistry* **1991**, *95*(9), 3727–3730; (b) Dedecek, J.; Wichterlova, B. Siting and Redox Behavior of Cu Ions in CuH-ZSM-5 Zeolites - Cu+ Photoluminescence Study. *Journal of Physical Chemistry* **1994**, *98*(22), 5721–5727.

[91] (a) Marturano, P.; Drozdova, L.; Pirngruber, G.D.; Kogelbauer, A.; Prins, R. The Mechanism of Formation of the Fe Species in Fe/ZSM-5 Prepared by CVD. *Physical Chemistry Chemical Physics* **2001**, *3*(24), 5585–5595; (b) Pieterse, J.A.Z.; Booneveld, S.; van den Brink, R.W. Evaluation of Fe-Zeolite Catalysts Prepared by Different Methods for the Decomposition of N2O. *Applied Catalysis B-Environmental* **2004**, *51*(4), 215–228; (c) Iwasaki, M.; Yamazaki, K.; Banno, K.; Shinjoh, H. Characterization of Fe/ZSM-5 DeNO(x) Catalysts Prepared by Different Methods: Relationships Between Active Fe Sites and NH3-SCR Performance. *Journal of Catalysis* **2008**, *260*(2), 205–216.

[92] Karge, H.G.; Wichterlova, B.; Beyer, H.K. High-Temperature Interaction of Solid Cu Chlorides and Cu Oxides in Mixtures with H-Forms of ZSM-5 and Y-Zeolites. *Journal of the Chemical Society-Faraday Transactions* **1992**, *88*(9), 1345–1351.

[93] Petras, M.; Wichterlova, B. High-Temperature Interaction of Vanadium Pentoxide with H-ZSM-5 Zeolite - ESR and IR Study. *Journal of Physical Chemistry* **1992**, *96*(4), 1805–1809.

[94] Kanazirev, V.; Price, G.L. Activity of Ga, In and Cu Modified MFI Zeolites for Amine Reactions. In *Zeolites and Related Microporous Materials: State of the Art 1994*, Weitkamp, J.; Karge, H.G.; Pfeifer, H.; Holderich, W., Eds.; Elsevier Science Publ B V: Amsterdam, 1994, Vol. 84, pp. 1935–1942.

[95] Wichterlova, B.; Beran, S.; Kubelkova, L.; Novakova, J.; Smieskova, A.; Sebik, R. *Preparation of NiHZSM-5 Catalyst for Isomerization of C_8 Aromatics. Solid-State Incorporation of Nickel*; Elsevier: Amsterdam, 1989, Vol. 46.

[96] (a) Dedecek, J.; Capek, L.; Wichterlova, B. Nature of Active Sites in Decane-SCR-NOx and NO Decomposition Over Cu-ZSM-5 Zeolites. *Applied Catalysis a-General* **2006**, *307*(1), 156–164; (b) Sobalik, Z.; Dedecek, J.; Ikonnikov, I.; Wichterlova, B. State and Coordination of Metal Ions in High Silica

Zeolites Incorporation, Development and Rearrangement During Preparation and Catalysis. *Microporous and Mesoporous Materials* **1998**, *21*(4–6), 525–532; (c) Wichterlova, B.; Sobalik, Z.; Dedecek, J. Cu Ion Siting in High Silica Zeolites. Spectroscopy and Redox Properties. *Catalysis Today* **1997**, *38*(2), 199–203; (d) Dedecek, J.; Wichterlova, B. Role of Hydrated Cu Ion Complexes and Aluminum Distribution in the Framework on the Cu Ion Siting in ZSM-5. *Journal of Physical Chemistry B* **1997**, *101*(49), 10233–10240; (e) Tabor, E.; Zaveta, K.; Sathu, N.K.; Tvaruzkova, Z.; Sobalik, Z. Characterization of Iron Cationic Sites in Ferrierite Using Mossbauer Spectroscopy. *Catalysis Today* **2011**, *169*(1), 16–23; (f) Jisa, K.; Novakova, J.; Schwarze, M.; Vondrova, A.; Sklenak, S.; Sobalik, Z. Role of the Fe-Zeolite Structure and Iron State in the N2O Decomposition: Comparison of Fe-FER, Fe-BEA, and Fe-MFI Catalysts. *Journal of Catalysis* **2009**, *262*(1), 27–34.

[97] (a) Sobalik, Z.; Tvaruzkova, Z.; Wichterlova, B. Monitoring of Skeletal T-O-T Vibrations of Metal Ion Exchanged Zeolites - An Attempt at Quantitative Evaluation. *Microporous and Mesoporous Materials* **1998**, *25*(1–3), 225–228; (b) Groothaert, M.H.; Schoonheydt, R.A.; Delabie, A.; Pierloot, K. Local Site Deformations in Zeolites by the Coordination of Cu(II). In *Catalysis by Unique Metal Ion Structures in Solid Matrices: From Science to Application*, Centi, G.; Wichterlova, B.; Bell, A.T., Eds.; Springer: Dordrecht, 2001, Vol. 13, pp. 205–219; (c) Sponer, J.E.; Sobalik, Z.; Leszczynski, J.; Wichterlova, B. Effect of Metal Coordination on the Charge Distribution Over the Cation Binding Sites of Zeolites. A Combined Experimental and Theoretical Study. *Journal of Physical Chemistry B* **2001**, *105*(35), 8285–8290; (d) Drozdova, L.; Prins, R.; Dedecek, J.; Sobalik, Z.; Wichterlova, B. Bonding of Co Ions in ZSM-5, Ferrierite, and Mordenite: An X-Ray Absorption, UV-Vis, and IR Study. *Journal of Physical Chemistry B* **2002**, *106*(9), 2240–2248; (e) Mentzen, B.F.; Bergeret, G. Crystallographic Determination of the Positions of the Copper Cations in Zeolite MFI. *Journal of Physical Chemistry C* **2007**, *111*(34), 12512–12516.

[98] (a) Garten, R.L.; Delgass, W.N.; Boudart, M. A Mossbauer Spectroscopic Study of Reversible Oxidation of Ferrous Ions in Y zeolite. *Journal of Catalysis* **1970**, *18*(1), 90–107; (b) Smeets, P.J.; Meng, Q.G.; Corthals, S.; Leeman, H.; Schoonheydt, R.A. Co-ZSM-5 Catalysts in the Decomposition of N2O and the SCR of NO with CH4: Influence of Preparation Method and Cobalt Loading. *Applied Catalysis B-Environmental* **2008**, *84*(3–4), 505–513.

[99] Lobree, L.J.; Hwang, I.C.; Reimer, J.A.; Bell, A.T. Investigations of the State of Fe in H-ZSM-5. *Journal of Catalysis* **1999**, *186*(2), 242–253.

[100] Delabie, A.; Pierloot, K.; Groothaert, M.H.; Weckhuysen, B.M.; Schoonheydt, R.A. The Siting of Cu(II) in Mordenite: A Theoretical Spectroscopic Study. *Physical Chemistry Chemical Physics* **2002**, *4*(1), 134–145.

[101] Fellah, M.F., CO and NO Adsorptions on Different Iron Sites of Fe-ZSM-5 Clusters: A Density Functional Theory Study. *Journal of Physical Chemistry C* **2011**, *115*(5), 1940–1951.

[102] (a) Gil, B.; Janas, J.; Wloch, E.; Olejniczak, Z.; Datka, J.; Sulikowski, B. The Influence of the Initial Acidity of HFER on the Status of Co Species and Catalytic Performance of CoFER and InCoFER in CH4-SCR-NO. *Catalysis Today* **2008**, *137*(2–4), 174–178; (b) Gora-Marek, K.; Datka, J. The Transformation of Formaldehyde on CoZSM-5 Zeolites. *Catalysis Today* **2008**, *137*(2–4), 466–470; (c) Gora-Marek, K.; Gil, B.; Datka, J. Quantitative IR Studies of the Concentration of Co2+ and Co3+ Sites in Zeolites CoZSM-5 and CoFER. *Applied Catalysis a-General* **2009**, *353*(1), 117–122.

[103] Sayle, D.C.; Catlow, C.R.A.; Gale, J.D.; Perrin, M.A.; Nortier, P. Active Site Configurations Within the NO Decomposition Catalyst, Cu-ZSM-5; The Role of Framework Aluminium. *Journal of Materials Chemistry* **1997**, *7*(8), 1635–1639.

[104] (a) Da Costa, P.; Moden, B.; Meitzner, G.D.; Lee, D.K.; Iglesia, E. Spectroscopic and Chemical Characterization of Active and Inactive Cu Species in NO Decomposition Catalysts Based on Cu-ZSM5. *Physical Chemistry Chemical Physics* **2002**, *4*(18), 4590–4601; (b) Ene, A.B.; Bauer, M.; Archipov, T.; Roduner, E. Adsorption of Oxygen on Copper in Cu/HZSM5 Zeolites. *Physical Chemistry Chemical Physics* **2010**, *12*(24), 6520–6531.

[105] Bulanek, R.; Wichterlova, B.; Sobalik, Z.; Tichy, J. Reducibility and Oxidation Activity of Cu Ions in Zeolites - Effect of Cu Ion Coordination and Zeolite Framework Composition. *Applied Catalysis B-Environmental* **2001**, *31*(1), 13–25.

[106] Groothaert, M.H.; Lievens, K.; van Bokhoven, J.A.; Battiston, A.A.; Weckhuysen, B.M.; Pierloot, K.; Schoonheydt, R.A. Bis(mu-oxo)dicopper as Key Intermediate in the Catalytic Decomposition of Nitric Oxide. *Chemphyschem* **2003**, *4*(6), 626–630.

[107] Li, W.; Yu, S.Y.; Meitzner, G.D.; Iglesia, E. Structure and Properties of Cobalt-Exchanged H-ZSM5 Catalysts for Dehydrogenation and Dehydrocyclization of Alkanes. *Journal of Physical Chemistry B* **2001**, *105*(6), 1176–1184.

[108] Dubkov, K.A.; Ovanesyan, N.S.; Shteinman, A.A.; Starokon, E.V.; Panov, G.I. Evolution of Iron States and Formation of Alpha-Sites Upon Activation of FeZSM-5 Zeolites. *Journal of Catalysis* **2002**, *207*(2), 341–352.

[109] Marturano, P.; Drozdova, L.; Kogelbauer, A.; Prins, R. Fe/ZSM-5 Prepared by Sublimation of FeCl3: The Structure of the Fe Species as Determined by IR, Al-27 MAS NMR, and EXAFS Spectroscopy. *Journal of Catalysis* **2000**, *192*(1), 236–247.

[110] Gao, Z.X.; Kim, H.S.; Sun, Q.; Stair, P.C.; Sachtler, W.M.H. UV-Raman Characterization of Iron Peroxo Adsorbates on Fe/MFI Catalyst with High Activity for NOx Reduction. *Journal of Physical Chemistry B* **2001**, *105*(26), 6186–6190.

[111] (a) Sobalik, Z.; Dedecek, J.; Kaucky, D.; Wichterlova, B.; Drozdova, L.; Prins, R. Structure, distribution, and properties of Co ions in ferrierite revealed by FTIR, UV-Vis, and EXAFS. *Journal of Catalysis* **2000**, *194*(2), 330–342; (b) Mihaylov, M.; Ivanova, E.; Drenchev, N.; Hadjiivanov, K. Coordination Chemistry of Fe2+ Ions in Fe,H-ZSM-5 Zeolite as Revealed by the IR Spectra of Adsorbed CO and NO. *Journal of Physical Chemistry C* **2010**, *114*(2), 1004–1014; (c) Ivanova, E.; Mihaylov, M.; Hadjiivanov, K.; Blasin-Aube, V.; Marie, O.; Plesniar, A.; Daturi, M. Evidencing Three Distinct Fe-II Sites in Fe-FER Zeolites by Using CO and NO as Complementary IR Probes. *Applied Catalysis B-Environmental* **2010**, *93*(3–4), 325–338; (d) Benco, L.; Bucko, T.; Grybos, R.; Hafner, J.; Sobalik, Z.; Dedecek, J.; Sklenak, S.; Hrusak, J. Multiple Adsorption of NO on Fe2+ Cations in the Alpha- and Beta-Positions of Ferrierite: An Experimental and Density Functional Study. *Journal of Physical Chemistry C* **2007**, *111*(26), 9393–9402; (e) Sobalik, Z.; Tvaruzkova, Z.; Wichterlova, B. Skeletal T-O-T Vibrations as a Tool for Characterization of Divalent Cation Complexation in Ferrierite. *Journal of Physical Chemistry B* **1998**, *102*(7), 1077–1085; (f) Benco, L.; Bucko, T.; Grybos, R.; Hafner, J.; Sobalik, Z.; Dedecek, J.; Hrusak, J. Adsorption of NO in Fe2+-Exchanged Ferrierite. A Density Functional Theory Study. *Journal of Physical Chemistry C* **2007**, *111*(2), 586–595.

[112] Georgieva, I.; Benco, L.; Tunega, D.; Trendafilova, N.; Hafner, J.; Lischka, H. Multiple Adsorption of NO on Cobalt-Exchanged Chabazite, Mordenite, and

Ferrierite Zeolites: A Periodic Density Functional Theory Study. *Journal of Chemical Physics* **2009**, *131*(5).

[113] (a) McMillan, S.A.; Snurr, R.Q.; Broadbelt, L.J. Interaction of Divalent Metal Cations with Ferrierite: Insights from Density Functional Theory. *Microporous and Mesoporous Materials* **2004**, *68*(1–3), 45–53; (b) Wichterlova, B.; Dedecek, J.; Sobalik, Z. Redox Catalysis over Molecular Sieves. Structure and Function of Active Sites. In *12th International Zeolite Conference, Baltimore 1998*, Treacy, M.M.J.; Marcus, B.K.; Bisher, M.E.; Higgins, J.B., Eds.; Materials Research Society: Warrendale, Pennsylvania, 1998; Vol. II, pp. 941–973.

[114] Resini, C.; Montanari, T.; Nappi, L.; Bagnasco, G.; Turco, M.; Busca, G.; Bregani, F.; Notaro, M.; Rocchini, G. Selective Catalytic Reduction of NOx by Methane over Co-H-MFI and Co-H-FER Zeolite Catalysts: Characterisation and Catalytic Activity. *Journal of Catalysis* **2003**, *214*(2), 179–190.

[115] Kuroda, Y.; Mori, T.; Yoshikawa, Y.; Kittaka, S.; Kumashiro, R.; Nagao, M. What are the Important Factors Determining the State of Copper Ion on Various Supports? Analysis Using Spectroscopic Methods and Adsorption Calorimetry. *Physical Chemistry Chemical Physics* **1999**, *1*(16), 3807–3816.

[116] Mirodatos, C.; Dalmon, J.A.; Garbowski, E.D.; Barthomeuf, D. Reduction of Nickel in Mordenite and Silica Catalysts - Influence of Support and Pretreatment. *Zeolites* **1982**, *2*(2), 125–130.

[117] (a) Csicsery, S.M., Shape-Selective Catalysis in Zeolites. *Zeolites* **1984**, *4*(3), 202–213; (b) Chang, C.D., Methanol-to-Gasoline Process - Reaction-Mechanism. *ACS Symposium Series* **1988**, *368*, 596–614.

[118] (a) Ivanova, I.I.; Brunel, D.; Nagy, J.B.; Daelen, G.; Derouane, E.G. An In-Situ C-13-NMR Study of the Mechanism of Cumene-n-Propylbenzene Isomerization Over H-ZSM-11. In *Heterogeneous Catalysis and Fine Chemicals III*, Guisnet, M.; Barbier, J.; Barrault, J.; Bouchoule, C.; Duprez, D.; Perot, G.; Montassier, C., Eds.; Elsevier Science Publ B V: Amsterdam, 1993; Vol. 78, pp. 587–594; (b) Ivanova, I.I.; Brunel, D.; Nagy, J.B.; Derouane, E.G. An In-Situ C-13 MAS NMR-Study of Benzene Isopropylation Over H-ZSM-11 - Cumene Formation and Side-Reactions. *Journal of Molecular Catalysis a-Chemical* **1995**, *95*(3), 243–258; (c) Wichterlova, B.; Cejka, J. Mechanism of N-Propyltoluene Formation in C3 Alkylation of Toluene - The Effect of Zeolite Structural Type. *Journal of Catalysis* **1994**, *146*(2), 523–529; (d) Wichterlova, B.; Cejka, J.; Zilkova, N., Selective Synthesis of Cumene and p-Cymene Over Al and Fe Silicates with Large and Medium Pore Structures. *Microporous Materials* **1996**, *6*(5–6), 405–414.

[119] Bhan, A.; Allian, A.D.; Sunley, G.J.; Law, D.J.; Iglesia, E. Specificity of Sites Within Eight-Membered Ring Zeolite Channels for Carbonylation of Methyls to Acetyls. *Journal of the American Chemical Society* **2007**, *129*(16), 4919–4924.

[120] Boronat, M.; Viruela, P.M.; Corma, A. Reaction Intermediates in Acid Catalysis by Zeolites: Prediction of the Relative Tendency to Form Alkoxides or Carbocations as a Function of Hydrocarbon Nature and Active Site Structure. *Journal of the American Chemical Society* **2004**, *126*(10), 3300–3309.

[121] Gomez-Hortiguela, L.; Pinar, A.B.; Cora, F.; Perez-Pariente, J. Dopant-Siting Selectivity in Nanoporous Catalysts: Control of Proton Accessibility in Zeolite Catalysts Through the Rational Use of Templates. *Chemical Communications* **2010**, *46*(12), 2073–2075.

[122] Cejka, J.; Wichterlova, B.; Sarv, P. Extent of Monomolecular and Bimolecular Mechanism in n-Butene Skeletal Isomerization to Isobutene Over Molecular Sieves. *Applied Catalysis a-General* **1999**, *179*(1–2), 217–222.

[123] Boronat, M.; Martinez, C.; Corma, A. Mechanistic Differences Between Methanol and Dimethyl Ether Carbonylation in Side Pockets and Large Channels of Mordenite. *Physical Chemistry Chemical Physics* **2011**, *13*(7), 2603–2612.

[124] Iwamoto, M.; Furukawa, H.; Mine, Y.; Uemura, F.; Mikuriya, S.I.; Kagawa, S. Copper(II) Ion-Exchanged ZSM-5 Zeolites as Highly-Active Catalysts for Direct and Continuous Decomposition of Nitrogen Monoxide. *Journal of the Chemical Society-Chemical Communications* **1986**, (16), 1272–1273.

[125] Pirngruber, G.D.; Roy, P.K.; Prins, R. On Determining the Nuclearity of Iron Sites in Fe-ZSM-5 - A Critical Evaluation. *Physical Chemistry Chemical Physics* **2006**, *8*(34), 3939–3950.

[126] Sobalik, Z.; Novakova, J.; Dedecek, J.; Sathu, N.K.; Tabor, E.; Sazama, P.; Stastny, P.; Wichterlova, B. Tailoring of Fe-ferrierite for N2O Decomposition: On the Decisive Role of Framework Al Distribution for Catalytic Activity of Fe Species in Fe-ferrierite. *Microporous Mesoporous Materials* **2011**, *146* (1–3), 172–183.

[127] (a) Kaucky, D.; Vondrova, A.; Dedecek, J.; Wichterlova, B. Activity of Co Ion Sites in ZSM-5, Ferrierite, and Mordenite in Selective Catalytic Reduction of NO with Methane. *Journal of Catalysis* **2000**, *194*(2), 318–329; (b) Kaucky, D.; Dedecek, J.; Vondrova, A.; Sobalik, Z.; Wichterlova, B. Siting and Reactivity of the Co Ions in Ferrierite in Selective Catalytic Reduction of NO with CH4. *Collection of Czechoslovak Chemical Communications* **1998**, *63*(11), 1781–1792; (c) Aylor, A.W.; Lobree, L.J.; Reimer, J.A.; Bell, A.T. An Infrared Study of NO Reduction by CH4 Over Co-ZSM-5. In *11th International Congress on Catalysis - 40th Anniversary, Pts A and B*, Hightower, J.W.; Delgass, W.N.; Iglesia, E.; Bell, A.T., Eds.; Elsevier Science Publ B V: Amsterdam, 1996, Vol. 101, pp. 661–670.

[128] Panov, G.I.; Sobolev, V.I.; Kharitonov, A.S., The Role of Iron in N2O Decomposition on ZSM-5 Zeolite and Reactivity of the Surface Oxygen Formed. *Journal of Molecular Catalysis* **1990**, *61*(1), 85–97.

[129] Iwamoto, M.; Yokoo, S.; Sakai, K.; Kagawa, S., Catalytic Decomposition of Nitric-Oxide Over Copper(II)-Exchanged Y-Type Zeolites. *Journal of the Chemical Society-Faraday Transactions I* **1981**, *77*, 1629–1638.

[130] (a) Dedecek, J.; Bortnovsky, O.; Vondrova, A.; Wichterlova, B. Catalytic Activity of Cu-Beta Zeolite in NO Decomposition: Effect of Copper and Aluminium Distribution. *Journal of Catalysis* **2001**, *200*(1), 160–170; (b) Wichterlova, B.; Dedecek, J.; Vondrova, A. Identification of Cu Sites in ZSM-5 Active in NO Decomposition. *Journal of Physical Chemistry* **1995**, *99*(4), 1065–1067.

[131] (a) Lee, C.Y.; Choi, K.Y.; Ha, B.H., Catalytic Decomposition of Nitric-Oxide on Copper Zeolites. *Applied Catalysis B-Environmental* **1994**, *5*(1–2), 7–21; (b) Dedecek, J. Siting of Cu+ ions in pentasil-ring zeolites. Ph.D. Thesis, Academy of Sciences of the Czech Republic, Prague, 1995; (c) Wichterlova, B.; Sobalik, Z.; Vondrova, A. Differences in the Structure of Copper Active Sites for Decomposition and Selective Reduction of Nitric Oxide with Hydrocarbons and Ammonia. *Catalysis Today* **1996**, *29*(1–4), 149–153.

[132] Groothaert, M.H.; van Bokhoven, J.A.; Battiston, A.A.; Weckhuysen, B.M.; Schoonheydt, R.A. Bis(mu-oxo)dicopper in Cu-ZSM-5 and its Role in the Decomposition of NO: A Combined in Situ XAFS, UV-Vis-Near-IR, and Kinetic Study. *Journal of the American Chemical Society* **2003**, *125*(25), 7629–7640.

[133] Groothaert, M.H.; Lievens, K.; Leeman, H.; Weckhuysen, B.M.; Schoonheydt, R.A. An Operando Optical Fiber UV-vis Spectroscopic Study of the Catalytic Decomposition of NO and N2O Over Cu-ZSM-5. *Journal of Catalysis* **2003**, *220*(2), 500–512.

[134] Woertink, J.S.; Smeets, P.J.; Groothaert, M.H.; Vance, M.A.; Sels, B.F.; Schoonheydt, R.A.; Solomon, E.I. A Cu2O (2+) Core in Cu-ZSM-5, the Active Site in the Oxidation of Methane to Methanol. *Proceedings of the National Academy of Sciences of the United States of America* **2009**, *106*(45), 18908–18913.

[135] Groothaert, M.H.; Smeets, P.J.; Sels, B.F.; Jacobs, P.A.; Schoonheydt, R.A. Selective Oxidation of Methane by the Bis(mu-oxo)dicopper Core Stabilized on ZSM-5 and Mordenite Zeolites. *Journal of the American Chemical Society* **2005**, *127*(5), 1394–1395.

[136] (a) Li, Y.J.; Armor, J.N. A Reaction Pathway for the Ammoxidation of Ethane and Ethylene Over Co-ZSM-5 Catalyst. *Journal of Catalysis* **1998**, *176*(2), 495–502; (b) Li, Y.J.; Armor, J.N. Ammoxidation of ethane to Acetonitrile Over Metal-Zeolite Catalysts. *Journal of Catalysis* **1998**, *173*(2), 511–518; (c) Sobalik, Z.; Belhekar, A.A.; Tvaruzkova, Z.; Wichterlova, B. Metal Ligand Complexes in CoH-BEA Relevant to Ethane Ammoxidation to Acetonitrile: An FTIR Study. *Applied Catalysis a-General* **1999**, *188*(1–2), 175–186.

[137] Beznis, N.V.; Weckhuysen, B.M.; Bitter, J.H. Partial Oxidation of Methane Over Co-ZSM-5: Tuning the Oxygenate Selectivity by Altering the Preparation Route. *Catalysis Letters* **2010**, *136*(1–2), 52–56.

[138] (a) Chen, H.Y.; Sachtler, W.M.H. Activity and Durability of Fe/ZSM-5 Catalysts for Lean Burn NOx Reduction in the Presence of Water Vapor. *Catalysis Today* **1998**, *42*(1–2), 73–83; (b) Schwidder, M.; Kumar, M.S.; Bruckner, A.; Grunert, W. Active Sites for NO Reduction Over Fe-ZSM-5 Catalysts. *Chemical Communications* **2005**, (6), 805–807; (c) Kumar, M.S.; Schwidder, M.; Grunert, W.; Bruckner, A. On the Nature of Different Iron Sites and Their Catalytic Role in Fe-ZSM-5 DeNO(x) Catalysts: New Insights by a Combined EPR and UV/VIS Spectroscopic Approach. *Journal of Catalysis* **2004**, *227*(2), 384–397.

[139] (a) Hensen, E.J.M.; Zhu, Q.; Hendrix, M.; Overweg, A.R.; Kooyman, P.J.; Sychev, M.V.; van Santen, R.A. Effect of High-Temperature Treatment on Fe/ZSM-5 Prepared by Chemical Vapor Deposition of FeCl3I. Physicochemical Characterization. *Journal of Catalysis* **2004**, *221*(2), 560–574; (b) Pirngruber, G.D.; Roy, P.K.; Prins, R. The Role of Autoreduction and of Oxygen Mobility in N2O Decomposition Over Fe-ZSM-5. *Journal of Catalysis* **2007**, *246*(1), 147–157.